Birgit Ploier

Engineering of Sterol Synthesis in Yeast

Diplomarbeit

zur Erlangung des akademischen Grades eines

Diplom-Ingenieurs

der Studienrichtung Biotechnologie

eingereicht an der

Technischen Universität Graz

Univ.-Prof. Dipl.-Ing. Dr.techn. Helmut Schwab

Ass.-Prof. Dipl.-Ing. Dr.techn. Harald Pichler

Institut für Molekulare Biotechnologie

Technische Universität Graz

2010

The outcome of any serious research
can only be to make two questions grow
where only one grew before.
Thorstein Bunde Veblen (1857-1929)

DANKSAGUNG

Ich widme diese Arbeit meinen Eltern, die mir durch ihre mannigfaltige, uneingeschränkte Unterstützung die Erfüllung meiner Träume ermöglichen und mich in Phasen der Ernüchterung liebevoll auffangen.

Während der Erarbeitung dieser Diplomarbeit haben mich viele Menschen unterstützt und begleitet.

Ich möchte zuerst Herrn Univ.- Prof. Dr. Helmut Schwab danken, dass ich diese Arbeit unter seiner Betreuung durchführen durfte.

Herr Ass.-Prof. Dr. Harald Pichler hat durch seinen Enthusiasmus, sein unermüdliches Engagement und seine Fähigkeit, sein enormes Wissen in absorbierbaren Mengen weiterzugeben, nicht nur meine Wahl für diesen Studienzweig mitgeprägt sondern auch meine Leidenschaft für die Forschung geweckt, wofür ich ihm herzlich danken möchte. Er ist nicht nur für mich und meine Arbeit, sondern für sein ganzes Umfeld Herz und Motor.

Frau Priv.-Doz. Dr. Regina Leber hat mich mit viel Geduld in die Welt von *Saccharomyces cerevisiae* eingeführt. Durch ihre herzliche und motivierende Art, mit der sie mich bei den ersten Gehversuchen in der komplexen Lipidforschung begleitet hat, konnte ich viel lernen.

Auch bei Frau Dr. Barbara Petschacher möchte ich mich für die gute Zusammenarbeit bedanken.

Herr Ao. Univ.-Prof. Dr. Erich Leitner hat meine Arbeit durch die Vermessung der GC/MS Proben sehr unterstützt, wofür ich auch ihm und seiner Laborgruppe ein herzliches Dankeschön aussprechen möchte.

Die Anlaufzeit dieses Projekts wäre um einiges schwieriger gewesen, wenn wir die Gerätschaften zur Lipidanalytik während der ersten Monate dieser Arbeit nicht am Institut für Biochemie nutzen hätten können. An dieser Stelle möchte ich mich bei Herrn Univ.-Prof. Dr. Günther Daum für die Unterstützung bedanken. Am Institut für Biochemie durfte ich auch Frau Univ.-Doz. Dr. Karin Athenstaedt beim Dissektieren von Tetraden über die Schulter schauen. Diese Technik wäre mir ohne ihre große und allzeit bereite Hilfe noch viel länger als Mysterium erschienen.

Die Zeit meiner Diplomarbeit wäre ohne die lieben Menschen dieser Laborgruppe wohl ganz anders verlaufen. Ich möchte mich bei Peter Augustin, Anita Emmerstorfer, Michael Felber, Gerald Richter, Corinna Odar, Christine Winkler und Tamara Wriessnegger herzlich bedanken. Sie alle haben mich auf vielfältige Weise unterstützt und auch bereichert. Das freundschaftliche und motivierende Klima innerhalb dieser Gruppe schafft eine konstruktive und animierende Atmosphäre, die mir ein optimales Umfeld für das Gelingen dieser Arbeit bot.

Mein Dank gilt auch vielen hier namentlich nicht Genannten, von denen ich Kraft, Impulse, Unterstützung und Teilhabe an ihrem Wissen gewonnen habe, all den gegenwärtigen und ehemaligen Lehrern und Anregern, die mich mit zu dem gemacht haben was ich bin und vielleicht einmal sein werde.

Abschließend möchte ich dem Austrian Centre of Industrial Biotechnology (ACIB) und DSM für die finanzielle Unterstützung der Arbeit und die Bereitstellung der Räumlichkeiten und notwendigen Hilfsmittel und Geräte danken.

EIDESSTATTLICHE ERKLÄRUNG

Ich erkläre an Eides statt, dass ich die vorliegende Arbeit selbstständig verfasst, andere als die angegebenen Quellen/Hilfsmittel nicht benutzt und die den benutzten Quellen wörtlich und inhaltlich entnommenen Stellen als solche kenntlich gemacht habe.

Graz, am _____ _____

Unterschrift

STATUTORY DECLARATION

I declare that I have authored this thesis independently, that I have not used other than the declared sources / resources, and that I have explicitly marked all material which has been quoted either literally or by content from the used sources.

Graz, _____ _____

signature

Kurzfassung

Saccharomyces cerevisiae, Ergosterol Biosynthese, Sterolester, Lipidpartikel, Sterol-Acyltransferasen

Die Biosynthese von Ergosterol ist ein sehr komplexer biochemischer Prozess, in dem zumindest 28 beteiligte Enzyme aus Acetyl-CoA Bausteinen das Endprodukt Ergosterol bilden. Die Reaktionsabfolge wird üblicherweise in den Prä-Squalen Weg und den Post-Squalen Weg eingeteilt. Hefesterole kommen in zwei Formen vor, freie Sterole und Sterolester. Unter guten Wachstumsbedingungen produziert Saccharomyces cerevisiae mehr Sterole als zur Membranbildung gebraucht werden. Überschüssige Sterole werden durch die beiden Acyltransferasen Are1p und Are2p verestert, sodaß bis zu 90% des zellulären Gesamtsterolanteils als Ester vorliegen. Gemeinsam mit Triglyceriden werden Sterolester in organell-ähnlichen Strukturen gespeichert, die man als Lipidpartikel bezeichnet. Durch die Veresterung wird eine inerter Sterol-pool erzeugt, da Sterolester nicht mehr für weitere Umwandlungen im Sterolbiosyntheseweg zur Verfügung stehen.
Durch Engineering des Ergosterolbiosynthesewegs und der Sterol-Veresterung können nicht-physiologische Sterolstrukturen angereichert werden, die von industrieller Bedeutung sind.

Abstract

Saccharomyces cerevisiae, ergosterol biosynthesis, steryl esters, lipid particles, sterol acyltransferases

Ergosterol biosynthesis is one of the most complex biochemical pathways known. It can be divided into the pre-squalene pathway and the post-squalene pathway. Twenty eight enzymes, mainly located in the endoplasmic reticulum, are involved until several units of acetyl-CoA are successfully converted to the final product ergosterol. Sterols of yeast exist as two major forms, free sterols and steryl esters. When the amount of free sterols exceeds the levels required for membrane formation, sterols are esterified by the two acyltransferases Are1p and Are2p. In yeast, steryl esters can constitute up to 90% of the total cellular sterol content. Along with triglycerides, they are stored in organelle-like structures, so-called lipid droplets or lipid particles, forming an inert sterol pool which is not available for further conversions in the ergosterol biosynthetic pathway.
Engineering of both the ergosterol biosynthesis and the sterol esterification pathways leads to the formation of increased pools of well-defined, non-physiological sterol structures of industrial interest.

TABLE OF CONTENTS

LIST OF ABBREVIATIONS

aa	aminoacid
ab	antibody
ACAT	acylCoA:Cholesteroltransferase
amp	ampicillin
bidest	bidestillated
bp	base pairs
BP	Birgit Ploier strains
CoA	coenzyme A
DC	disruptioncassette
DG	diglycerides
DMSO	dimethylsulfoxid
dNTP	dideoxynucleotidtriphosphate
DTT	dithiothreitol
ER	endoplasmic reticulum
ERG	ergosterol related gene
EtOH	ethanol
Fig	figure
FS	free sterols
G418	geneticin 418 sulfate
GC/MS	gas chromatography/ mass spectroscopy
HAP	heme activator protein
his	histidin
HMG-CoA	(*3S*)-3-hydroxy-3-methylglutaryl-CoA
Incub	incubation
kan	kanamycin
LB	Luria-Bertani Broth (Lennox)
leu	leucin
LiAc	lithium acetate
LV	Leervektor (reference vector without insert but with selective marker)
Mat	mating type
MeOH	methanol
min	minutes
Mut	mutant
No	number
OD	optical density
OD-U	OD- Units
ON	over night
ONC	over night culture
p	page
PBS	phosphate buffered saline
PCR	polymerase chain reaction
PEG	polyethylenglycol
Pfu	pyrococcus furiosus
PH	Pichler Harald – *S. cerevisiae* strain collection

PL	phospholipids
Prep gel	preparative agarose gel
rpm	rotations per minute
RT	roomtemperature
s	seconds
SAM	S-adenosylmethionine
SD	synthetic defined
SDS- PAGE	sodium dodecyl sulfate Polyacrylamide gel electrophoresis
SE	sterylester
ss	singlestrand
T	temperature
TG	triglycerides
TLC	thin layer chromatography
Trafo	transformation
Tris	tris(hydroxymethyl)-aminomethan
trp	tryptophan
ura	uracil
WB	Western Blot
WT	wild-type
YPD	yeast extractpeptone dextrose
Zym	zymolyase

1 INTRODUCTION

1.1 Abstract of Sterol Cell Biology in Yeast

Sterols are essential compounds of all eukaryotic cells and serve as structural and signalling biomolecules. As constituents of cellular membranes they affect membrane fluidity and permeability and it has been shown that cells are not viable without sterols (Daum, 1998). The final product of the sterol biosynthesis in fungi, such as *Saccharomyces cerevisiae*, is ergosterol (Figure 1).The parent structure, cyclopentanoperhydrophenanthrene, is common to all sterols. The double bond between C-7,8 in the ring and C-22 in the side chain as the presence of a methyl group at C-24 differs from the animal sterol cholesterol. The hydroxyl group at C-3 is the only hydrophilic component allowing directed integration into membranes.

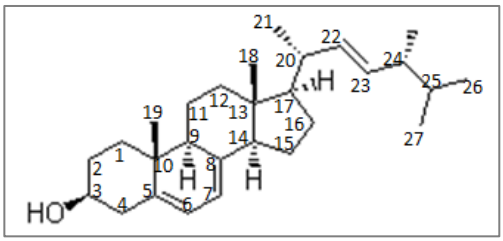

Figure 1: Chemical structure of ergosterol with consecutive numbering of the C- atoms

1.1.1 Ergosterol Biosynthesis

Ergosterol is synthesized in one of the most complex biochemical pathways known with nearly thirty different biochemical reactions. Most of the enzymes involved are located in the ER membrane, with the exception of Erg1p, Erg6p and Erg7p, which are mainly localized at lipid particles (Athenstaedt, 1999; Leber, 1994; Leber, 1998).

The ergosterol biosynthesis can be divided into the pre-squalene pathway and the post-squalene pathway. The former is common to the biosynthesis of all sterols in fungi, plants and animals (Figure 2). The first sterol lanosterol, several intermediates and the end product

ergosterol are formed in the post-squalene pathway (Figure 4). Both reaction pathways are well known, and basically all enzymes of the sterolbiosynthesis are identified and their functions have been evaluated. However, the detailed regulation mechanisms are not yet completely understood.

The pre-squalene pathway

The synthesis of squalene does not depend on oxygen making it possible under aerobic and anaerobic culture conditions. The biosynthesis is initiated by the condensation of two acetyl-CoA molecules under the catalytic influence of acetoacetyl-CoA thiolase (Erg10p) to form acetoacetyl-CoA which condenses with another acetyl-CoA molecule to form (*3S*)-3-hydroxy-3-methylglutaryl-CoA (HMG-CoA) which is subsequently reduced to mevalonate by hydroxymethylglutaryl-CoA reductase 1 and 2. These two isoenzymes seem to be functionally redundant, each containing several transmembrane and catalytic domains. This step is one of the most important and well known control points of sterol synthesis because HMG-CoA reductase shows feedback inhibition by ergosterol (Bard, 1981). Overexpression of a truncated version of this key enzyme, HMG-CoA reductase (HMG1p), leads to an increase in the early sterols (Polakowski, 1999).

Phosphate groups are transferred to mevalonate yielding phosphomevalonate which is further phosphorylated to mevalonate-5-pyrophosphate which is then decarboxylated leading to isopentenyl pyrophosphate. This segment, from acetoacetyl-CoA to isopentenyl pyrophosphate is also known as mevalonate pathway. Isopentenyl pyrophosphate is not only the precursor for subsequent building of squalene but also for isoprenoids. After isomerisation to dimethylallyl pyrophosphate the head-to-tail condensation reaction of isopentenyl pyrophosphate and dimethylallyl pyrophosphate yields geranyl pyrophosphate. This reaction is catalyzed by Erg20p. The same enzyme facilitates formation of farnesyl pyrophosphate by adding two isopentenyl pyrophosphate units to dimethylallyl pyrophosphate. Erg9p (squalene synthase) finally catalyzes the coupling of two molecules farnesylpyrophosphate to squalene (Figure 2).

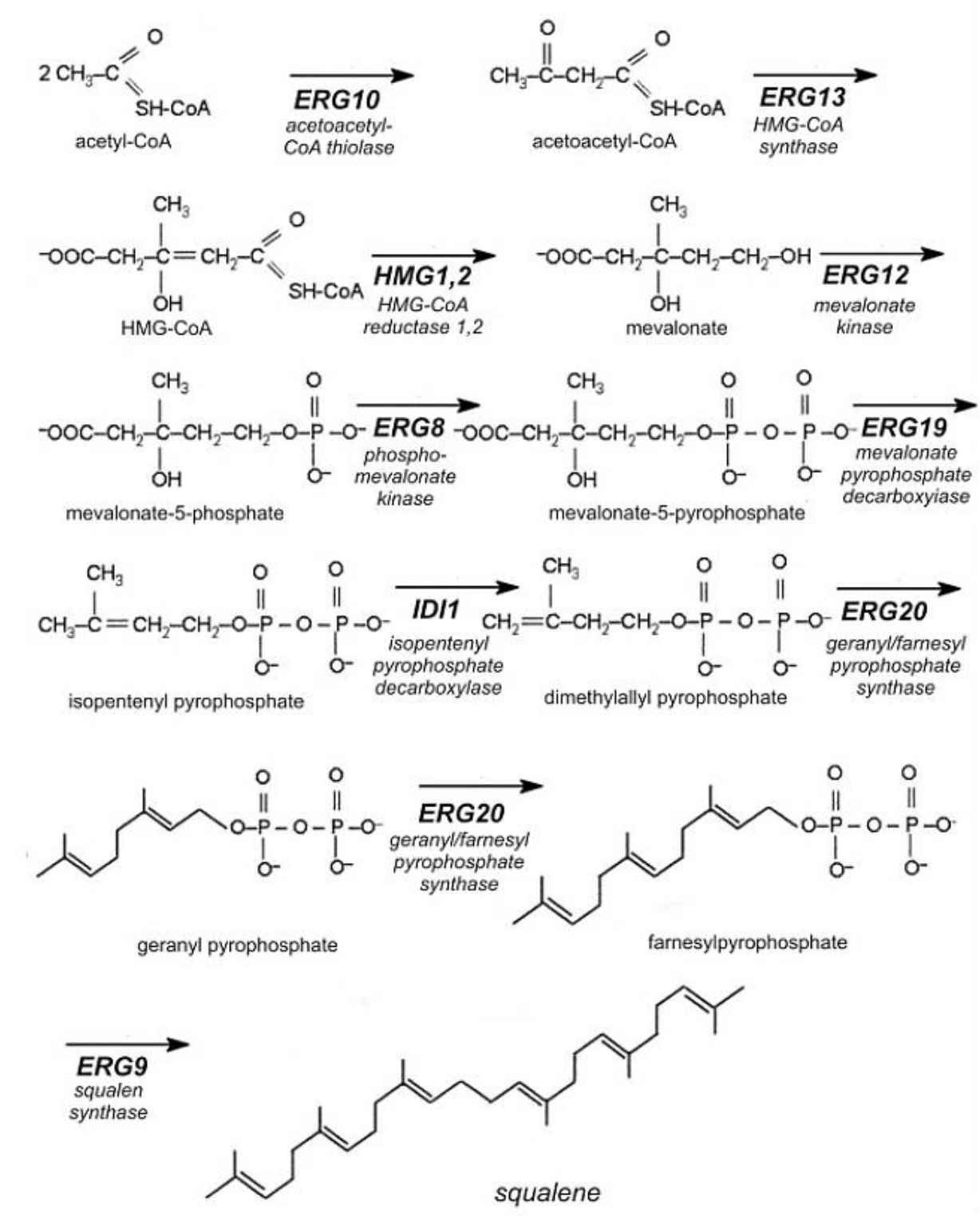

Figure 2: The presqualene pathway, according to Maczek, 2009, and Pichler, 2005

The post squalene pathway

Some steps in the post squalene pathway depend on the presence of oxygen making the ergosterol synthesis just possible under aerobic conditions. The reaction steps until the precursor zymosterol are conserved in all eukaryotic cells, and it could be shown that deletion of genes before this step leads to sterolauxotrophy, whereas cells with deletions of later *ERG* genes are still viable. The biochemical reactions of the post squalene pathway take place in the endoplasmic reticulum and in lipid particles as shown in Figure 3, which gives an overview of the distribution of those enzymes between the ER and the lipid particles and shows the route of transport of the sterol intermediates.

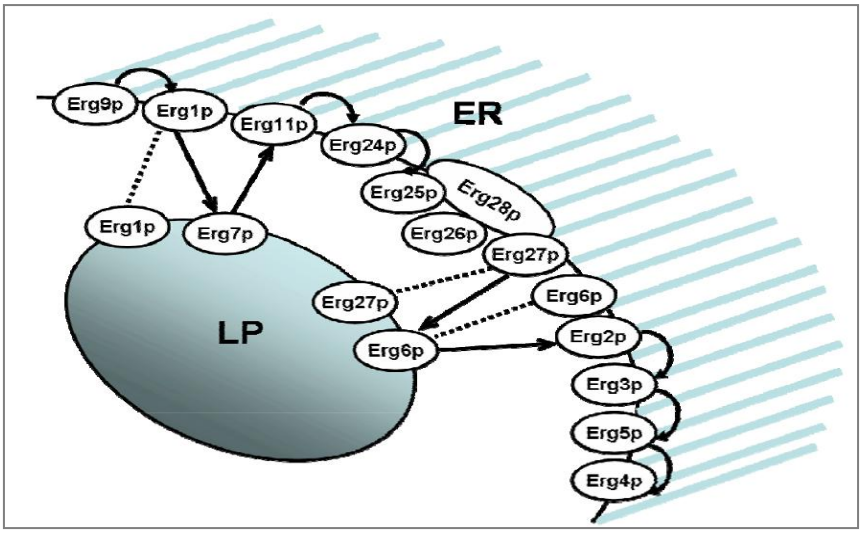

Figure 3: Distribution of *ERG*-genes of the post-squalene pathway between lipid particles (LP) and endolplasmic reticulum (ER) (Maczek, 2009)

The post-squalene pathway starts with the epoxidation of squalene by squalene epoxidase (Erg1p). The next step is the formation of lanosterol by Erg7p (lanosterol synthase) forming the typical sterol structure in a number of cyclisation events, which are one of the most complex biochemical reactions known. Demethylation and the introduction of a new double bond yields 4,4-dimethylcholesta-8,14,24-trienol. This new double bond is subsequently saturated by Erg24p (C-14 sterol reductase) in the next step. The next *ERG* genes until *ERG28* seem to function as an Erg-complex which is localized in the ER. The removal of two methylgroups in four reactions mediated by Erg25p (C-4 methyl sterol oxidase) and Erg26p (C-3 sterol dehydrogenase) yields zymosterone, which is reduced by Erg27p (3-keto sterol reductase) to zymosterol. The further transformation of zymosterol is unique for yeast and other fungi. Fecosterol is the outcome of methylation of zymosterol by Erg6p (C-24 sterol methyl transferase) at C-24. The next reaction, a shift of a double bond to the C-7 position, is

catalyzed by Erg2p (C-8 sterol isomerase). Then a double bond at the C-5 position, which is conserved in all sterols, is introduced by Erg3p (C-5 sterol desaturase). The last steps of the pathway are introducing and removing double bonds in the side chain. Erg5p (C-22 sterol desaturase) introduces one at the C-22 position, whereas Erg4p (C-24(28) sterol reductase) removes it at the C-24 position yielding the end product, ergosterol. Figure 4 shows the summary of the post-squalene pathway with all enzymes involved.

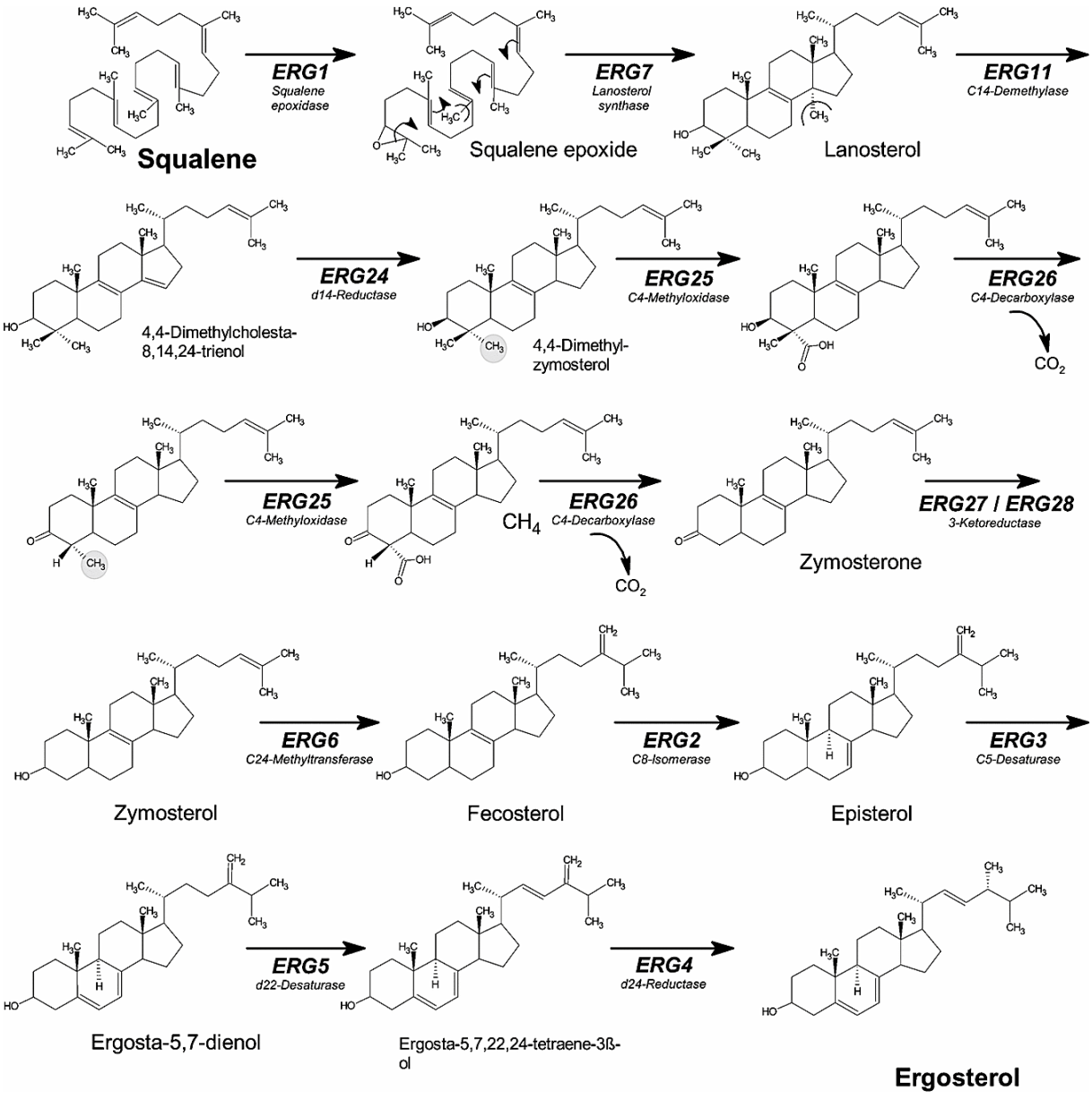

Figure 4: The post-squalene pathway (Veen, M., 2005)

1.1.2 Sterol esterification and hydrolysis

Yeast cells usually produce much more sterols than can be embedded into membranes without losing favourable membrane properties. Two mechanisms operate to maintain sterol homeostasis: esterification of free sterols and their reciprocal hydrolysis (Chang, 2006).

An excess of sterols is esterified and stored together with triacylglycerols, which are synthesized by the two enzymes Dga1p and Lro1p, as so-called neutral lipids in lipid particles (lipid droplets). These are small spherical organelles with an approximate diameter of 400 nm. They have got a highly hydrophobic core of mainly triacylglycerols, surrounded by shells consisting of steryl esters covered by a phospholipid monolayer with only a few proteins embedded (Czabany, 2008; Leber, 1994).

As only free sterols are used as substrate in the ergosterol biosynthesis pathway and as membrane building blocks, this creation of an inert sterol pool is a cell internal protective mechanism and functions as storage for components needed for membrane formation (Athenstaedt, 1999). It has to be noted that lipid particles do not only serve as storage pool but fulfil many other functions in lipid metabolism (Zinser, 1993).

Steryl esters of *S. cerevisiae* are synthesized by acyl-CoA:cholesterol acyl transferase (**A**CAT) **r**elated **e**nzymes, namely, Are1p and Are2p (Yang, 1996). They are both localized to the ER and carry multiple transmembrane domains. Even though these two enzymes share 49% identity with each other it was shown that they have slightly different substrate specificities. Are2p is responsible for the main part of esterification, accounting for approximately 70% of the total activity, and has a very strong preference for the end product ergosterol, whereas Are1p esterifies mainly precursors with a slight preference for lanosterol and all other ergosterol precursors. The esterification takes place at the hydroxyl group (see Figure 1) at the C3-atom with C16:1 as preferred fatty acid, followed by C18:1. Steryl esters mainly accumulate during stationary phase and the early stage of sporulation (Bailey, 1975).

are1are2 double knockout strains are viable but do not contain any detectable amounts of steryl esters. Thus, it is regarded as a fact that those two enzymes are the only ones with sterol acylation activity in yeast (Zweytick, 2000). However, the presence or absence of steryl esters has an enormous impact on the cellular sterol profile (Czabany, 2008).

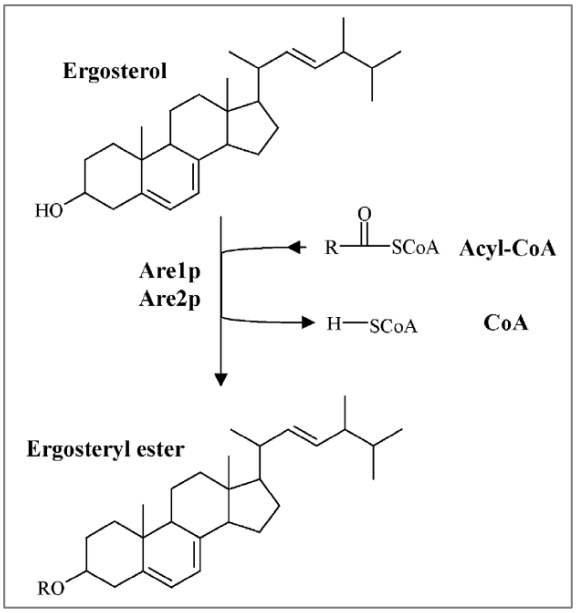

Figure 5: Steryl ester formation in yeast (Müllner and Daum, 2004)

The storage of neutral lipids would be useless without the possibility to mobilize them in case of starvation or during growth when many sterols are needed for the formation of new membranes (Leber, 1995). In *S. cerevisiae*, three steryl ester hydrolases have been identified so far, Yeh1p, Yeh2p, and Tgl1p. The highest activity was attributed to Yeh2p (Müllner, 2005). The mobilization of steryl esters by the above hydrolases recycles sterol intermediates, mainly zymosterol, fecosterol, lanosterol and episterol, which are the four most abundant esterified sterols, to the sterol biosynthetic pathway. Consequently, the cycle of esterification of free sterols and hydrolysis of steryl esters contributes to a balanced cellular level of free ergosterol (Wagner, 2008).

1.2 Project specification

This master thesis was part of a project running for two years in cooperation with DSM Nutritional Products Ltd with the stated aim to obtain high amounts of cholesta-5,7,24-trienol. This is a precursor of 25-hydroxy vitamin D3, an intermediate in the metabolism of vitamin D3. The latter is an important prohormone involved in the regulation of calcium levels and bone augmentation.

Yeast cells acquire the capacity of high-level production of cholesta-5,7,24-trienol upon upregulation of steryl synthesis by overexpression of a truncated version of HMG-CoA reductase and by deletion of the two genes *ERG5* and *ERG6*. Another important factor is to use a yeast strain with a wild type *HAP1* background. *HAP1* stands for heme activator protein and codes for a regulatory transcription factor. A defect of *HAP1*, caused by an insertional mutation of a *Ty1* transposon, decreases the expression of many ergosterol related genes. For example, the promotor region of *HMG1* is recognized in transcriptional activation by Hap1p. (Tamura, 2004).

Excessive cholesta-5,7,24-trienol is acylated and stored in lipid droplets, which is a good source for extraction. With the described genetic setup, yeast does not only produce high amounts of the desired cholesta-5,7,24-trienol but also very high amounts of zymosterol and some cholesta-7,24-dienol indicating that the reactions leading to the vitamin D3 precursor are incomplete, limiting the yield severely.

Two possible reasons for the over-accumulation of zymosterol have been identified and tested experimentally: Erg2p and Erg3p might be the limiting activities for the conversion of zymosterol, because of their potentially higher substrate specificities for ergosta-sterols. Secondly, zymosterol may be the preferred substrate of the two acyltransferases Are1p and Are2p. However, neither the overexpression of *ERG2* and *ERG3* nor the overexpression of the three steryl ester hydrolases *YEH1*, *YEH2* and *TGL1* and inactivation of Are1p solved the problem (Martin Lehmann and Hans-Peter Hohmann, personal communication). All attempts ended without significant change of the zymosterol to cholesta-5,7,24-trienol ratio in total sterols.

We hypothesized that the deletion of *ERG6* may lead to the decomposition of the Erg25p/Erg26p/Erg27p/Erg28p/Erg6p/Erg2p/Erg3p “complex” in which all these Erg-proteins closely interact, as described by Mo et al. (2004), see Figure 6. Therefore, we suggested that inactivation rather than deletion of *ERG6* may maintain this complex so that Erg2p and Erg3p

can more efficiently convert zymosterol in to cholesta-5,7,24-trienol and suppress formation of zymosterol esters.

The intended deliverables of this project are

- A yeast strain with the described genetic requirements to produce high amounts of cholesta-5,7,24-trienol, *erg5erg6*
- A yeast strain devoid of Are1p and Are2p
- A combination of those two strains to create an *erg5erg6are1are2* quadruple mutant
- A screening system for different sterol selectivities of acyltransferases derived from different organisms or by engineering of Are1/2p.

Finally:

- A yeast strain with improved conversion of zymosterol to cholesta-5,7,24-trienol, and therefore relatively higher enrichment of the latter sterol.

1.3 Targets of this Master thesis

The first aim of this Master thesis was to confirm that the wild-type yeast strain CEN.PK2 harbours a fully functional *HAP1* gene. Subsequently, the two double knockout strains *erg5erg6* and *are1are2* in haploid yeast strains with opposite mating types were to be constructed. After PCR verification and characterization of their sterol patterns, these two double knockout strains should be mated, the heterozygous diploid sporulated and the ascospores dissected to obtain a haploid quadruple mutant *erg5erg6are1are2* strain. The quadruple mutant would be employed to test acyltransferases of other organisms for their substrate specificity.

Furthermore, seven *ERG6* mutants were created by site specific mutagenesis to inactivate rather than delete *ERG6* to presafe a functional Erg-protein complex as described by Mo et al. (2004).

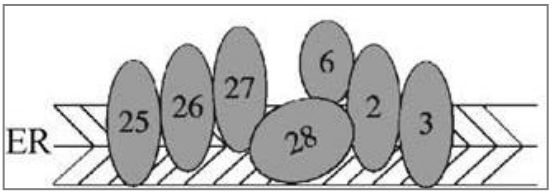

Figure 6: Model in which Erg28p anchors Erg27p and Erg6p as part of an „erg-complex“ (Mo, 2004)

2 MATERIALS

2.1 Strains

Table 1: Yeast strains used in this work

Strain	Genotype	Source
CEN.PK2-1C	MATa; ura3-52; trp1-289; leu2-3_112; his3Δ1; MAL2-8^{C}; SUC2	EUROSCARF
CEN.PK2- 1D	MATα; ura3-52; trp1-289; leu2-3_112; his3Δ1; MAL2-8^{C}; SUC2	EUROSCARF
CEN.PK2	MATa/ MATα; ura3-52/ ura3-52; trp1-289/ trp1-289; leu2-3_112/ leu2-3_112; his3Δ1/ his3Δ1; MAL2-8^{C}/ MAL2-8^{C}; SUC2/ SUC2	EUROSCARF
BY4741	MATa; his3Δ1; leu2Δ0; met15Δ0; ura3Δ0	Prof. Daum
SC0458	ATC1562; MATα; pARC304S is lost; pARC300D in trp1 locus, ura-/trp-	DSM NP
BP1_erg5	MATα; ura3-52; trp1-289; his3Δ1; MAL2-8^{C}; SUC2 *erg5*::*LEU2*	this work
BP2_erg5erg6	MATα; ura3-52; his3Δ1; MAL2-8^{C}; SUC2 *erg5*::*LEU2; erg6::TRP1*	this work
BP3_are2	MATa; ura3-52; trp1-289; leu2-3_112; his3Δ1; MAL2-8^{C}; SUC2; are2::loxP-kanMX-loxP	this work
BP4_are1are2	MATa; ura3-52; trp1-289; leu2-3_112; MAL2-8^{C}; SUC2; are2::loxP-kanMX-loxP; are1::HIS3	this work
BP5_erg5erg6are1are2	MATa/ MATα; ura3-52/ ura3-52; trp1-28/ *erg6::TRP1*; leu2-3_112/ *erg5*::*LEU2;* are1::HIS3/ his3Δ1; MAL2-8^{C}/ MAL2-8^{C}; SUC2/ SUC2; are2::loxP-kanMX-loxP	this work

Table 2*: E. coli* strains used in this work

Strain	Genotype	Source
Top10F'	F´{lacI^{q} Tn10 (Tet^{R})} mcrA Δ(mrr-hsdRMS-mcrBC) Φ80lacZΔM15 ΔlacX74 recA1 araD139 Δ(ara-leu)7697 galU galK rpsL endA1 nupG	Invitrogen
BL21 Gold	E. coli B F– ompT hsdS(rB– mB–) dcm+ Tetr gal endA Hte	Stratagene

2.2 Plasmids

Table 3: Plasmids used in this work

Plasmid	Major Features	Source
pRS315	LEU2 - f1 ori (NaeI) - T7 promoter - lacZ'/MCS - T3 promoter - pMB1 ori - bla -CEN6 - ARSH4	Regina Leber
pFA6a-TRP1	TRP1-pBR322 ori-T7 promoter- lacZ'/MCS- ampR-CEN6	Harald Pichler
pRS313	HIS3 - f1 ori (NaeI) - T7 promoter - lacZ'/MCS - T3 promoter - pMB1 ori - bla - CEN6 - ARSH4.	Regina Leber
pUG6	ampR- loxP- kanMX- TEF2 promoter	Harald Pichler
pFL44-ERG6	oriColE1-bla-ERG6-URA3-2µ	DSM NP Ltd.
pFL44L	oriColE1-bla-URA3-2µ	DSM NP Ltd.

2.3 Primers

Table 4: Primers to check for *Ty1* insertion in *HAP1*

Primername	Sequence	Tm [°C]
HAP1-1	5'- CCCGGATCCCCCTGCCATTCCAATCTTAGATGAACAGAA -3'	67.3
HAP1-2	5'- CCCGGATCCACTCTTATTAACCAATGTCGTGCGGGTCAA -3'	67.4

Table 5: Primers for site specific mutagenesis of ERG6

Primername	Sequence	Tm [°C]
E6_4FW	5'-GATTTAGTTCTCGCCGTTGCTTGTGCTGTTGCGGGCCCAGCAAGA-3'	71.6
E6_4RV	5'-TCTTGCTGGGCCCGCAACAGCACAAGCAACGGCGAGAACTAAATC-3'	71.6
erg6D152Nfw	5‘-GTCATCGGTCTAAACAATAACAATTACCAAATTGCCAAGGCAA-3‘	63.6
erg6D152Nrv	5‘-TTGCCTTGGCAATTTGGTAATTGTTATTGTTTAGACCGATGAC-3‘	63.6
erg6D152Afw	5‘-CATCGGTCTAAACAATAACGCTTACCAAATTGCCAAGGC-3‘	64.2
erg6D152Arv	5‘-GCCTTGGCAATTTGGTAAGCGTTATTGTTTAGACCGATG-3‘	64.2
E6_2GFW	5‘-GAGGCGATTTAGTTCTCGACGTTATTTGTGGTGTTATGGGCCCAGCAAG-3‘	68.3
E6_2GRV	5‘-CTTGCTGGGCCCATAACACCACAAATAACGTCGAGACTAAATCGCCTC-3‘	68.3
E6_G2FW	5'-CGACGTTGGTTGTTGTGTTGGGGGCCC-3'	67.4
E6_G2RV	5'-GGGCCCCCAACACAACAACCAACGTCG-3'	67.4
E6_G3FW	5'-CGACGTTGGTTGTGGTGTTTGGGGCCCAGC-3'	69.5
E6_G3RV	5'-GCTGGGCCCCAAACACCACAACCAACGTCG-3'	69.5
E6_DFW	5'-AGGCGATTTAGTTCTCGCCGTTGGTTGTGGTGTTG-3'	66.8
E6_DRV	5'-CAACACCACAACCAACGGCGAGAACTAAATCGCCT-3'	66.8
E6_D2FW	5'-GAGGCGATTTAGTTCTCGACGTTATTTGTGGTGTT-3'	64.2
E6_D2RV	5‘-AACACCACAAATAACGTCGAGAACTAAATCGCCTC-3'	64.2
E6_G1FW	5'-ATTTAGTTCTCGACGTTTGTTGTGGTGTTGGGGGC-3'	65.6
E6_G1RV	5'-GCCCCCAACACCACAACAAACGTCGAGAACTAAAT-3'	65.6

Table 6: Primers for the creation of disruption cassettes

Primer	Sequence	Tm [°C]
E6Trp1	5'-CATAATTTAAAAAAACAAGAATAAAATAATAATATAGTAGGCAGCATAAGATGTCTGTTATTAATTTCACAGG -3'	63.0
E6Trp2	5'ATAGGTATATATCGTGCGCTTTATTTGAATCTTATTGATCTAGTGAATTTCTATTTCTTAGCATTTTTGACG -3'	64.9
E5Leu1	5'- AAAACATCACATTTTGCTATTCCAATAGACAATAAATACCTTTTAACAAAATGTCTGCCCCTAAGAAGATC -3'	66.0
E5Leu2	5'--TAATGAAGTAAATATGATTTATTGTCTGGACAAAGTTCTGTTTTTCCCCATTAAGCAAGGATTTTCTTAACTTC -3'	65.8
A1His1	5'-GTGGTTGTTCAGCACGGCTTGCAGCAAGAGCGCCAAAACAGATTGCAAGAACAGAGCAGAAAGCCCTAG-3'	72.4
A1His2	5'-ATTGTATATCTATCAAGGGCTTGCGAGGGACACACGTGGTATGGTGGCAGTCTACATAAGAACACCTTTGGTGGAG-3'	70.7
Are1Hfw	5'CAGGTGGTTGTTCAGCACGGCTTGCAGCAAGAGCGCCAAAACAGATTGCAAGAATGACAGAGCAGAAAGCCCTAGTAAAGCG-3'	72.7
Are2Hrv	5'-CCCTATTGTATATCTATCAAGGGCTTGCGAGGGACACACGTGGTATGGTGGCAGTCTACATAAGAACACCTTTGGTGGAGGGAACATCG-3'	71.3
A1upFW	5'-GTGGTGCCAACTCCTCAGGAC-3'	60.2
A1upRV	5'-CTGCAAGCCGTGCTGAACAAC-3'	59.7
A1downFW	5'-GTGTCCCTCGCAAGCCCTTG-3'	61.2
A1downRV	5'-CCTTGGATTGCGGGGTCATGG-3'	61.0
FW_A2lox	5'-CAGACACATTACGTTAGCAAAAGCAACAATAACAAACACAACCCAGCTGAAGCTTCGTACGC-3'	68.8
RV_A2lox	5'-CTATAAAGATTTAATAGCTCCACAGAACAGTTGCAGGATGCCGCATAGGCCACTAGTGGATCTG-3'	68.6

Table 7: Primers for verification by Colony PCR

Primername	Sequence	Tm [°C]
K1E5	5'-GGTTTCCCTCGTTTAAGTCTGCG-3'	58.1
K2E5	5'-ATCAGCCTTCTTGGAGGCTTCC-3'	59.3
K2exE5	5'-CAAAACGCCAACCCTTAATGAAG-3'	55.0
K1E6	5'-CTGCTCCACTTCGTCTCAATGG-3'	57.8
K2E6	5'-CTTGCCACGACTCATCTCCATG-3'	57.9
K2inE6	5'-GCCACGTCGACATGGAACAT-3'	58.0
K2exE6	5'-GCCTGCTAGCAATGAACGTGCTA-3'	59.8
K1A1	5'-CCATCAAATACCCGGCCGTGG-3'	60.9
K2A1	5'-CGGAATGCTTGGCCAGAGCA-3'	60.8
K2exA1	5'-ACCTAGGAGCTCTTTGCCCC-3'	59.1
KA2up	5'-GCGGAGTTAACATTTAACGGC-3'	54.6
Klox	5'-TGGGGATGTATGGGCTAAATG-3'	54.6
KA2rev	5'-CTCTGTATTGCCTTCGGTAGC-3'	55.3
KA2down	5'-CTTCGCCGATACGAGACCG-3'	57.8

2.4 Instruments and Devices

Table 8: List of instruments and devices used in this work

Instrument/ Device/Enzyme	Supplier
Automatic TLC sampler	CAMAG
Centrifuges	Centrifuge 5810R, Eppendorf, Germany Centrifuge 5415R Eppendorf, Germany
Dispensette	Brand GmbH, Germany
Electrophoresis gel chambers	PowerPac™ Basic + Sub-Cell GT, Biorad, USA
Electrotransformation	MicroPulser™, BIO-RAD, USA Electroporation Cuvettes (2mm gap) Molecular BioProducts Inc., USA
Eppendorf tubes	Greiner bio-one International AG
Falcon tubes	Greiner bio-one International AG
G:Box HR	Syngene, UK
GC caps	VWR International, GmbH
GC vials	VWR International, GmbH
GC Zange	VWR International, GmbH
GC/MS	Agilent Technologies, Austria
Glas bottles	Schott/ Duran, Ilmabor TGI
Glass beads	Carl Roth GmbH + Co KG
Incubator (30°C and 37°C)	Binder GmbH
Kolben	Simax
Laminar flow chamber BSB4A	Gelaire Flow Laboratories,
Microscope DM LB2	Leica Microsystems GmbH
Mixing of small volumes	Vortex-Genie 2, Scientific Industries Inc, USA
NuPAGE®SDS Gels: 4-12% Bis-Tris Gel 1mm x 15 wells	Invitrogen- Life Technologies Corp.
PCR machines	GeneAmp® PCR System 2700, Applied Biosystems, USA
PCR tubes	Greiner bio-one International AG
Petridishes	Greiner bio-one International AG
Photometer	BioPhotometer, Eppendorf, Germany
Pipette tips	Greiner bio-one International AG
Pipettes	Pipetman P20N Gilson Inc., USA Pipetman P200N Gilson Inc., USA Pipetman P1000N Gilson Inc., USA Eppendorf research 0.5-10 µL, Eppendorf, Germany
Pyrex® tubes	Pyrex, Incorp.
Scanner	HP scanjet 4370
Shaker	HT MiltronII, Infors AG, Swiss Certomat® BS-1, Sartorius, Germany

Tetrade dissection microscope	Nikon/ SINGER
Thermixer	Thermomixer comfort, Eppendorf, Germany
TLC chambers	CAMAG
TLC scanner	CAMAG
TLC silica plates: aluminium sheets 20 x 20 cm, silica gel 60	Merck GmbH.
Transferpettor (200-1000 µL; 10-50 µL)	Brand GmbH, Germany
UV-cuvettes	Greiner bio-one International AG
Vibrax	Vibrax VXR basic, IKA GmbH& Co KG. Germany
Western Blot membrane: nitrocellulose blotting membrane	Sartorius AG

2.5 Reagents

Table 9: List of reagents used in this work

Reagent	**Supplier**
Acetic acid	Carl Roth GmbH + Co KG
Agar	BD Bacto- Becton, Dickinson and Company
Agarose	Biozym Scientific GmbH
Chloroform	Carl Roth GmbH + Co KG
Cholesterol	Sigma- Aldrich Corp.
dATP	Fermentas- Thermo Fisher Scientific Inc.
dCTP	Fermentas- Thermo Fisher Scientific Inc.
Deionised water	Fresenius Kabi Austria GmbH
dGTP	Fermentas- Thermo Fisher Scientific Inc.
Diethylether	Carl Roth GmbH + Co KG
DpnI	Fermentas- Thermo Fisher Scientific Inc.
DreamTaq buffer	Fermentas- Thermo Fisher Scientific Inc.
DreamTaq DNA polymerase	Fermentas- Thermo Fisher Scientific Inc.
DTT	Carl Roth GmbH + Co KG
dTTP	Fermentas- Thermo Fisher Scientific Inc.
Easy DNA Kit	Invitrogen- Life Technologies Corp.
EDTA	Carl Roth GmbH + Co KG
Ethanol	Australco Handels GmbH
Ethylacetate	Carl Roth GmbH + Co KG
Gene Jet Plasmid Miniprep Kit	Fermentas- Thermo Fisher Scientific Inc.
Gene Ruler DNA Ladder Mix	Fermentas- Thermo Fisher Scientific Inc.
Geneticinsulfate	Gibco/ Invitrogen- Life Technologies Corp.
Glucose Monohydrate	Carl Roth GmbH + Co KG
Glycerol	Carl Roth GmbH + Co KG
HCl	Carl Roth GmbH + Co KG

L-Adenine	Carl Roth GmbH + Co KG
L-Histidine	Carl Roth GmbH + Co KG
Lithiumacetate	Fluka/ Sigma- Aldrich Corp.
L-Leucine	Carl Roth GmbH + Co KG
L-Lysine	Carl Roth GmbH + Co KG
Loading Dye (6x)	Fermentas- Thermo Fisher Scientific Inc.
L-Tyrosine	Carl Roth GmbH + Co KG
L-Uracil	Fluka/ Sigma- Aldrich Corp.
Lyticase (from A. luteus)	Sigma- Aldrich Corp.
Magnesiumchloride	Carl Roth GmbH + Co KG
Manganesechloride	Carl Roth GmbH + Co KG
Mass Ruler DNA Ladder Mix	Fermentas- Thermo Fisher Scientific Inc.
Maxima Hot Start Green PCR Mastermix	Fermentas- Thermo Fisher Scientific Inc.
Methanol	Carl Roth GmbH + Co KG
n-heptane	Carl Roth GmbH + Co KG
N'O'-bis(trimethylsilyl)-trifluoracetamid	Sigma- Aldrich Corp.
Nitrogen base without amino acids	Difco- Becton, Dickinson and Company
NuPAGE Antioxidant	Invitrogen- Life Technologies Corporation
PageRuler Prestained Protein Ladder	Fermentas- Thermo Fisher Scientific Inc.
PEG 4000	Sigma- Aldrich Corp.
Petrolether	Carl Roth GmbH + Co KG
PfuUltra buffer 10x	Promega Corp.
PfuUltra DNA polymerase	Promega Corp.
Phusion DNA polymerase	Finnzymes- Thermo Fisher Scientific Inc.
Phusion HF buffer	Finnzymes- Thermo Fisher Scientific Inc.
Ponceau S	Amersham Life Science
Potassiumacetate	Carl Roth GmbH + Co KG
Potassiumchloride	Carl Roth GmbH + Co KG
Potassiumhydroxide	Carl Roth GmbH + Co KG
Primary antibody- Rabbit anti Erg6p	Ao.Univ-Prof. Dr. Günther Daum
Pyridine	Carl Roth GmbH + Co KG
Pyrogallol	Carl Roth GmbH + Co KG
Quick Change Mutagenesis Kit	Invitrogen- Life Technologies Corp.
RNaseA	Fermentas- Thermo Fisher Scientific Inc.
Secondary antibody- Goat anti rabbit IgG, horseradish peroxidase conjugated	Sigma- Aldrich Corp.
Single stranded carrier DNA (fish sperm)	Roche Diagnostics, GmbH
Skim milk powder (Eiweiß 90)	DM Drogerie Markt GmbH
Sodiumchloride	Carl Roth GmbH + Co KG
Sodiumcitrate	Carl Roth GmbH + Co KG
Sodiumhydroxide	Carl Roth GmbH + Co KG
Sorbitol	Carl Roth GmbH + Co KG

Spectra Broad Range Protein Standard	Invitrogen- Life Technologies Corp.
Sulfuric acid	Carl Roth GmbH + Co KG
SuperSignal West Pico Chemiluminescent Substrate Kit	Pierce
Trichloroacetic acid	Carl Roth GmbH + Co KG
Tris	Carl Roth GmbH + Co KG
Tryptophan	Carl Roth GmbH + Co KG
Tween20	Carl Roth GmbH + Co KG
Wizard- Gel Slice and PCR Product Preparation	Promega
Yeast extract	Carl Roth GmbH + Co KG
Zymolyase (from A. luteus)	Seikagaku Biobusiness, Corp.
β-Mercaptoethanol	Carl Roth GmbH + Co KG

2.6 Media and Buffers

Table 10: Cultivation media used in this work; the agar is omitted for liquid media

Medium	Compostion
LB	10 g/L tryptone, 5 g/L yeast extract, 5 g/L NaCl, 20 g/L agar
LB- amp	LB + 1 mL ampicillin stock solution (1000x)/1L
SD all dropout mix	3 g Adenine, 3 g Lysin, 3 g Tyrosin, 3 g Histidin, 3 g Leucin, 3 g Uracil Tryptophan was added after autoclaving of the media: 4 mL of 250 stock (10 g/L) sterile filtrated 0.2 µm f.c. 40 mg/ L
SD all	6.7 g/L Bacto- yeast nitrogen base without amino acids (0.67%), 20 g/L Glucose (2%), 20 g/L Agar (2%), 2 g/L SD all dropout powder mix (0.2%)
SD-his	Like SD all but without histidine in the dropout powder mix
SD-his-leu-trp	Like SD all but without histidine, leucine and tryptophane in the dropout powder mix
SD-leu	Like SD all but without leucine in the dropout powder mix
SD-trp	Like SD all but without the amino acid tryptophane
SD-ura	Like SD all but without uracil in the dropout powder mix
SOC	20 g/L bacto tryptone, 0.58 g/L NaCl, 5 g/L bacto yeast extract, 2 g/L $MgCl_2$, 0.16 g/L KCl, 2.46 g/L $MgSO_4$, 3.46 g/L dextrose
Sporulation medium	1 g potassium acetate, 0.25 g Yeast extract, 0.1 g glucose in 100 mL distilled H_2O
YPD	10 g/L Yeast extract (1%), 20 g/L Peptone (2%) , 20 g/L Glucose (2%), 20 g/L Agar (2%)
YPD+G418	YPD medium+ 200 mg/L geneticin sulphate
YPD+Nystatin	YPD medium+ Nystatin (5 µg/mL f.c.)

Table 11: Buffers used in this work

Buffer/ solution	Composition
Protein sample buffer (2x)	100 mM Tris/HCl pH 8.8, 4 mM EDTA, 4% SDS, 20% glycerol, 0.002% bromophenol blue
Ponceau S	0.1% Ponceau S in 5% acetic acid
MOPS NuPAGe®Running buffer (1x)	50 mL MOPS NuPAGe® Running buffer (20x), 950 mL bidest H_2O
EDTA stock solution (0.5 M)	93.05 g EDTA disodium salt, dissolved in 400 mL bidest H_2O ; pH adjusted to about 8, solution toped up to a final volume of 500 mL
TAE buffer (50x)- stock solution for electrophoresis	242 g Tris base dissolved in 750 mL deionized water; addition of 57.1 ml glacial acid acid and 100 mL of 0.5 M EDTA (pH 8.0) solution adjusted to a final volume of 1 L
TAE Buffer (1x) for electrophoresis	200 mL of TAE (50x), 9.8 L bidest H_2O
TBS (10x)	30.3 g Tris (0.25 M), 87.6 g NaCl (1.5 M), pH adjusted with 1 M HCl to pH 7.5, to 1 L with ddH_2O
TBST	999.5 mL 1x TBS, 0.5 mL Tween 20
TBST milk	5 g dry milk powder dissolved in 100 mL TBST
Transfer buffer (20x)	14.5 g Tris (24 M), 72 g Glycin (1920 mM), to 500 mL ddH_2O
Transfer buffer (1x)	50 mL 20x transfer buffer, 100 mL methanol to 1 L with ddH_2O
Transformation mix	90 mL 45% PEG4000, 10 mL 1 M LiAc, 1 mL 1 M TrisHCl, pH 7.5, 0.2 mL 0.5 M EDTA subject vortex mixing
Tris-HCl (100 mM, pH 7)	12.1 g Tris diluted in ddH_2O pH adjusted with 1 M HCl
Ampicillin stock (1000x)	100 mg/ mL dissolved in ddH_2O; steril filtered 0.2 µm

3 METHODS

3.1 PCR mediated Gene Disruption: creation of disruption cassettes

In general, disruption cassettes were amplified by PCR using primers composed of approximately 40 bp at the 5'- end that correspond to the up- or downstream region of the gene which is meant to be deleted and 20 bp at the 3'- end that anneal to the selectable marker gene which is meant to be introduced (Longtine, 1998; Lorenz, 1995). In case of the deletion of *ARE1*, longer homologous fragments were necessary because of the *his3Δ1* allele of the CEN.PK2 wild-type strain. This allele is a 187 bp internal deletion of the *HIS3* gene, which is of a size of 663 bp. It was therefore difficult to integrate a *HIS3* disruption cassette at the intended position without conversion of the *his3Δ1* allele (Daniel, 2005). PCR amplification of the selectable marker gene from a standard vector yielded a linear fragment consisting of the entire marker flanked by short regions homologous to the target sequence. After transformation, these constructs integrate by homologous recombination. To ensure that the whole gene was knocked out, the homologous upstream and downstream regions directly flanked the coding sequence to be deleted. The disruption cassettes were transformed into *Saccharomyces cerevisiae* using one of the methods described on page 35 and homologous recombinants were identified by auxotrophy or resistance markers. Four auxotrophy markers, *leu2*, *trp1*, *his3* and *ura3* are available in the wild-type strain CEN.PK2. The *ERG5*, *ERG6, ARE1* and *ARE2* genes were replaced by *LEU2*, *TRP1*, *HIS3* and the *loxP-kanMX-loxP* disruption cassettes, respectively, as described by Güldener et al. (1996). The Cre-loxP recombination system was applied to retain a selective marker, *ura3,* for potential further manipulations. Yeast transformants become resistant to the aminoglycoside antibiotic G418 when expressing the *E. coli kan*^{r} gene (Webster, 1983). PCRs were performed with Phusion DNA polymerase and a two-step cycling protocol to allow the 3'-section of the primers, homologous to the marker genes, to anneal, before increasing the annealing temperature to the optimum for the whole primer.

3.1.1 Disruption of *ERG5* with *LEU2*

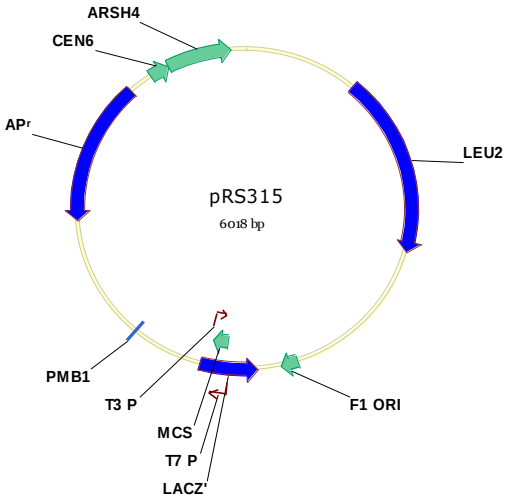

Figure 7: VNTI map of pRS315

10 µL	Phusion HF buffer (5x)
5 µL	dNTP Mix (2mM each)
2.5 µL	primer E5leu1
2.5 µL	primer E5leu2
1 µL	template pRS315 (10 ng)
28.5 µL	H_2O bidest
0.5 µL	Phusion DNA Polymerase
50 µL	total volume

PCR cycling conditions:

98°C/30 s- (98°C/7 s- 50°C/30 s-72°C/2 min) x 10- 72°C/7 min- 4°C/∞

subsequently followed by

98°C/30 s- (98°C/7 s- 60°C/30 s-72°C/2 min) x 25- 72°C/7 min- 4°C/∞

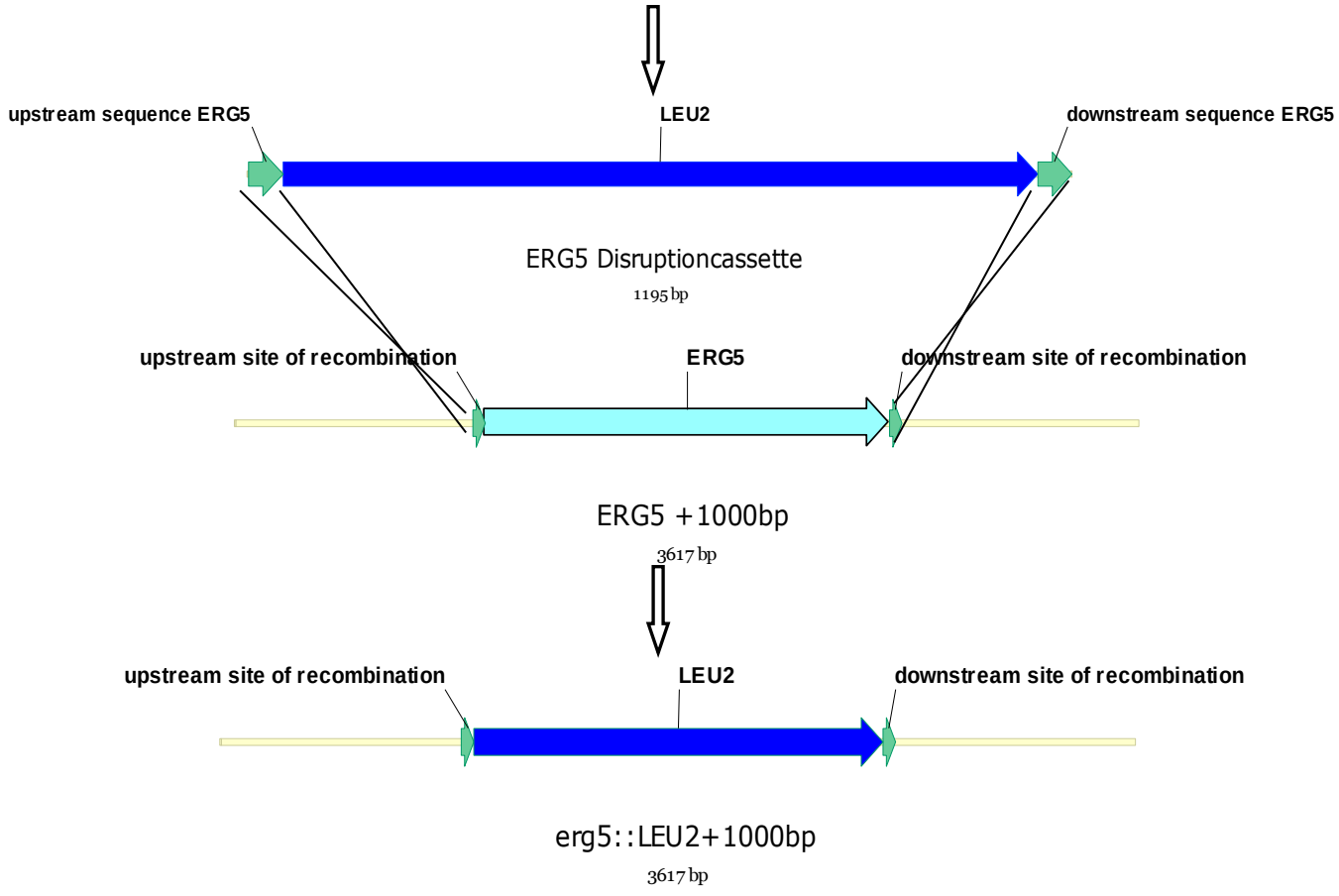

Figure 8: Generation of *erg5::LEU2* disruption cassette and strain

3.1.2 Disruption of *ERG6* with *TRP1*

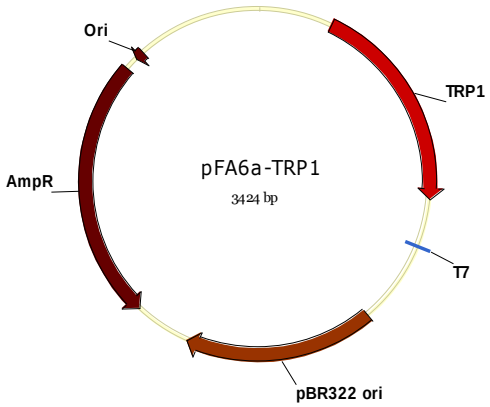

Figure 9: VNTI map of pFA6a-TRP1

10 µL	Phusion HF buffer (5x)
5 µL	dNTP Mix (2mM each)
2.5 µL	primer E6Trp1
2.5 µL	primer E6Trp2
1 µL	template pFA6a- TRP1(10 ng)
28.5 µL	H_2O bidest
0.5 µL	Phusion DNA Polymerase
50 µL	total volume

PCR cycling conditions:

98°C/30 s- (98°C/7 s- 55°C/30 s-72°C/1 min) x 10- 72°C/7 min- 4°C/∞

subsequently followed by

98°C/30 s- (98°C/7 s- 65°C/30 s-72°C/1 min) x 25- 72°C/7 min- 4°C/∞

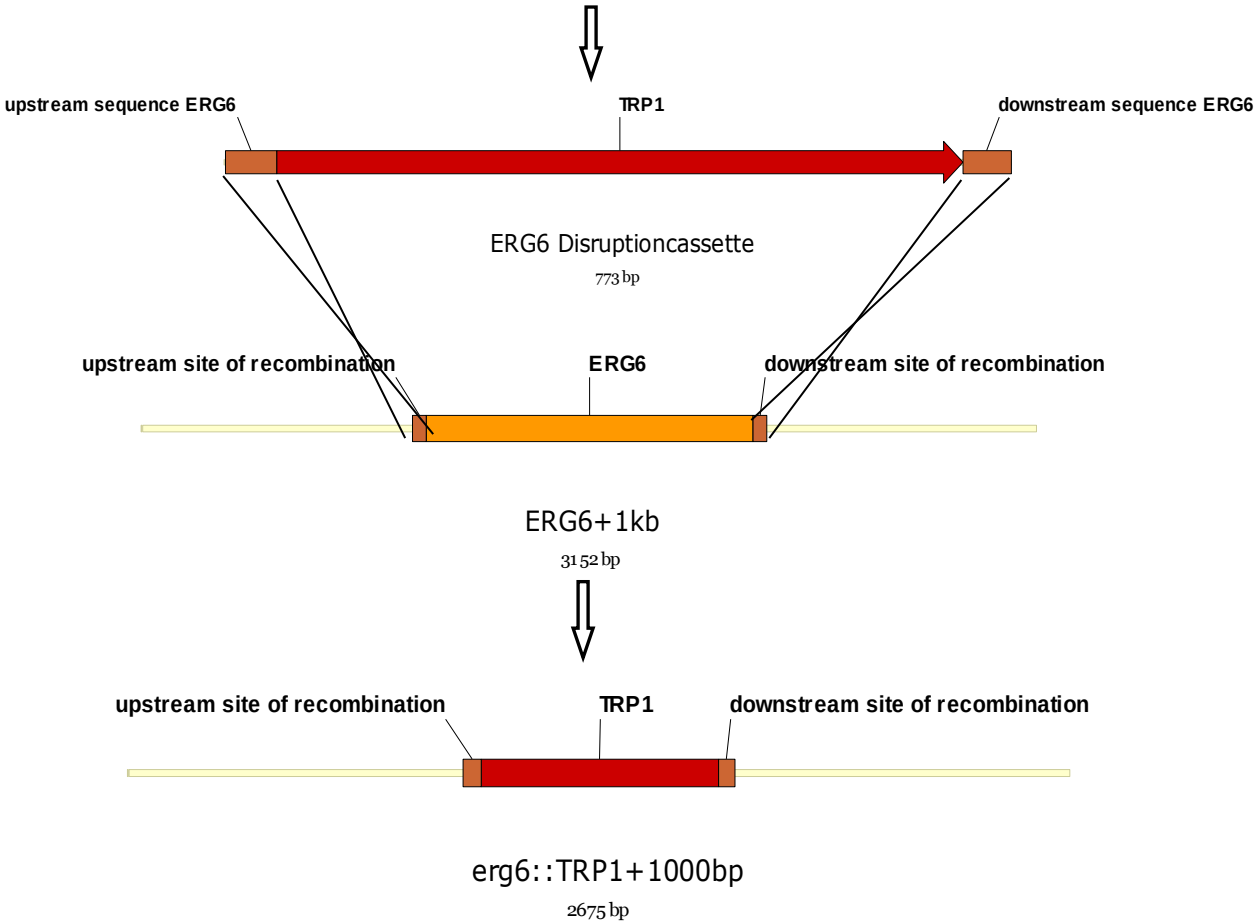

Figure 10: Generation of *erg6::TRP1* disruption cassette and strain

3.1.3 Disruption of *ARE1* with *HIS3*

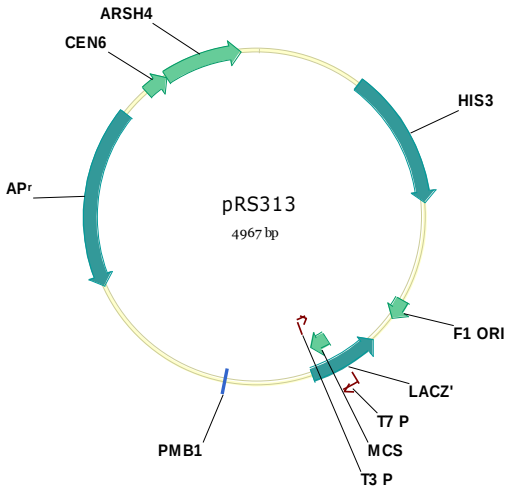

Figure 11: VNTI map of pRS313

10 µL	Phusion HF buffer (5x)
5 µL	dNTP Mix (2mM each)
2.5 µL	primer Are1Hfw
2.5 µL	primer Are2Hrv
1 µL	template pRS313(10 ng)
28.5 µL	H_2O bidest.
0.5 µL	Phusion DNA Polymerase
50 µL	total volume

PCR cycling conditions:

98°C/30 s- (98°C/7 s- 60°C/30 s-72°C/1 min) x 10- 72°C/7 min- 4°C/∞

subsequently followed by

98°C/30 s- (98°C/7 s- 65°C/30 s-72°C/1 min) x 25- 72°C/7 min- 4°C/∞

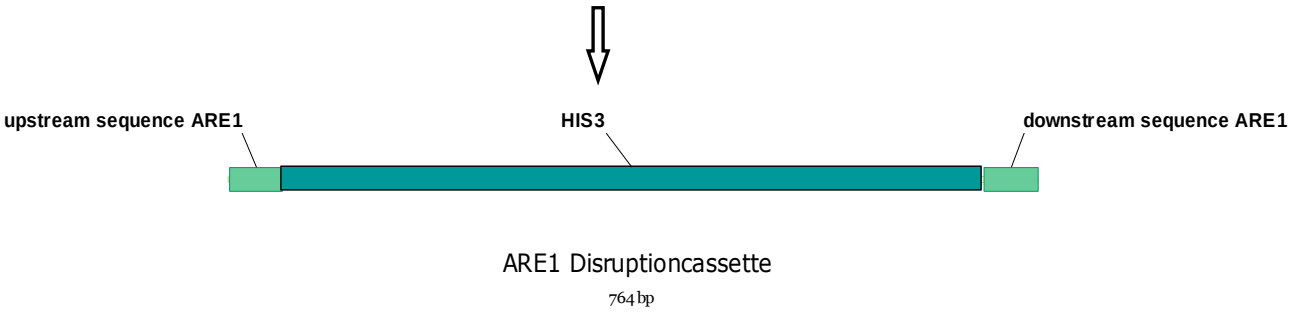

Figure 12: First generated *ARE1* disruption cassette

Colony PCR (with primers K1A1 and K2A1) and sequencing of the fragment between upstream and downstream primers (K1A1 and K2exA1) of the *ARE1* gene proved all transformants wrong, even though they grew on selective SD- his plates. The most obvious assumption was that this disruption cassette integrated at a wrong place because of internal gene conversion of *his3Δ1* (Daniel, 2005). To avoid this problem, longer upstream and downstream fragments were attached to the disruption cassettes.

Creation of longer up- and downstream fragments:

Colony PCR of a *Saccharomyces cerevisiae* wild-type strain under following conditions

3 µL	pellet *S. cerevisiae*
31.5 µL	H_20 bidest.
5 µL	HF buffer (10x)
5 µL	dNTP mix (2 mM each)
2.5 µL	A1upFW
2.5 µL	A1upRV
0.5 µL	Phusion DNA Polymerase
50 µL	total volume

3 µL	pellet *S. cerevisiae*
31.5 µL	H_20 bidest.
5 µL	HF buffer (10x)
5 µL	dNTP mix (2 mM each)
2.5 µL	A1downFW
2.5 µL	A1downRV
0.5 µL	Phusion DNA Polymerase
50 µL	total volume

PCR cycling conditions:

98°C/30 s- (98°C/7 s- 55°C/30 s-72°C/40 s) x 35- 72°C/7 min- 4°C/∞

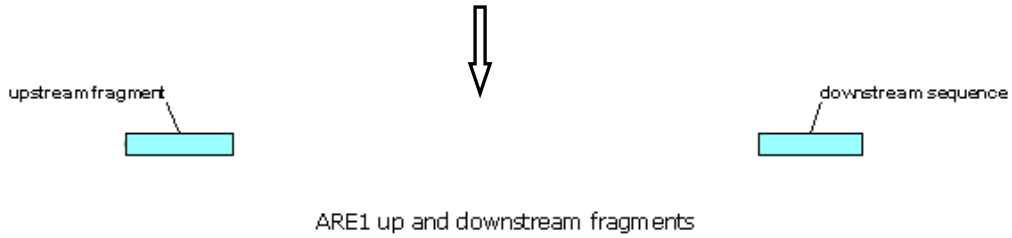

Figure 13: Generation of up- and downstream fragments of *ARE1*

Creation of the *ARE1* disruption cassette with longer homologous 3' and 5' fragments:

26.5 µL	H_2O bidest.
10 µL	HF buffer (5x)
5 µL	dNTP mix (2mM each)
1 µL	up fragment (10 ng)
1 µL	ARE1 DK (10 ng)
1 µL	down fragment (10 ng)
2.5 µL	primer A1upFW
2.5 µL	primer A1downRV
0.5 µL	Phusion DNA polymerase
50 µL	total volume

PCR cycling conditions:

98°C/30 s- (98°C/7 s- 55°C/30 s-72°C/40 s) x 35- 72°C/7 min- 4°C/∞

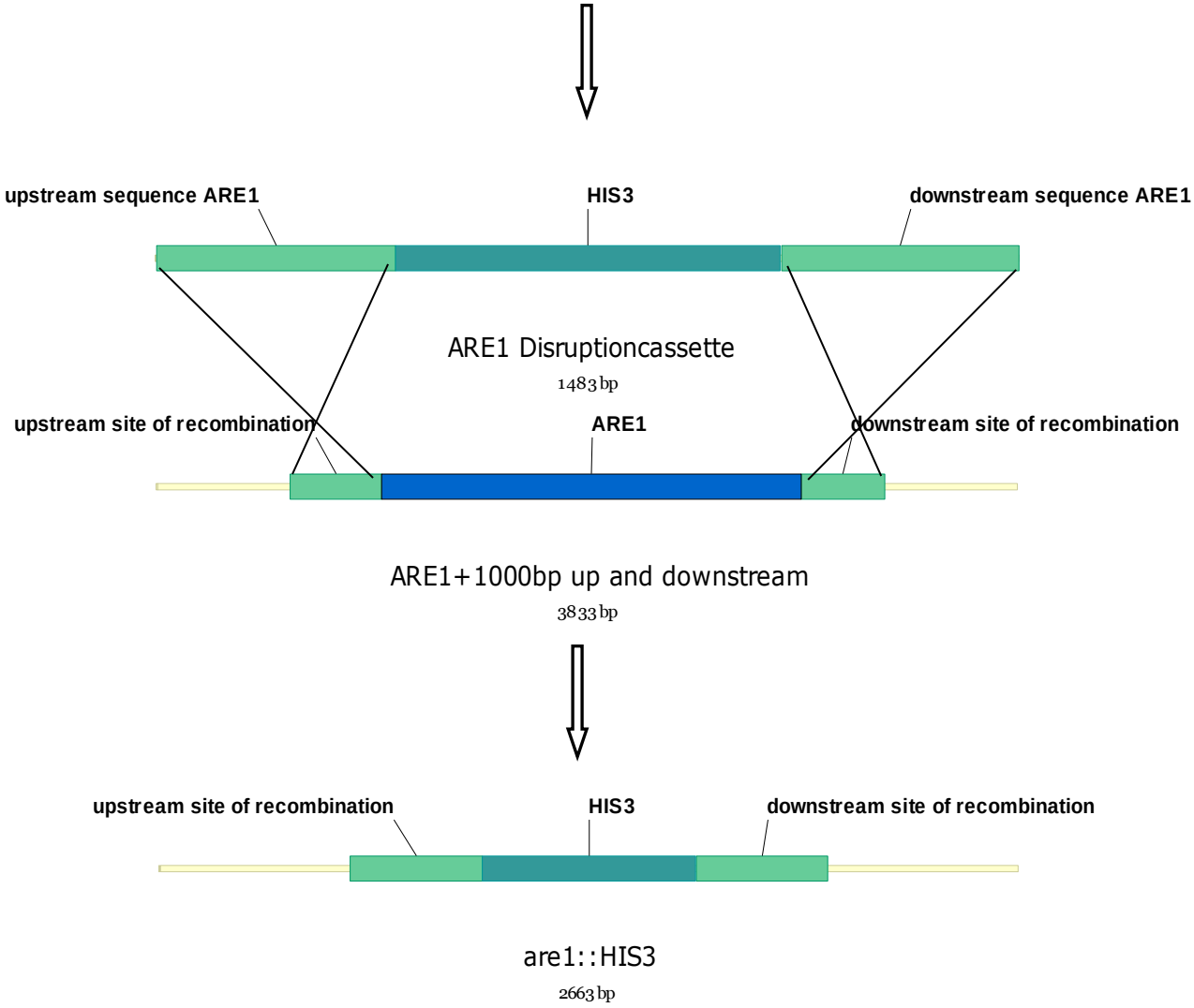

Figure 14: Generation of *are1::HIS3* disruption cassettes and strain

3.1.4 Disruption of *ARE2* with a *loxP-kanMX-loxP* disruption cassette

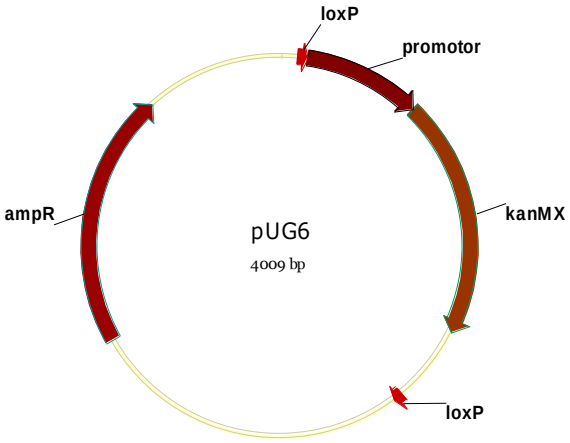

Figure 15: VNTI map of pUG6

10 µL	Phusion HF buffer (5x)
5 µL	dNTP Mix (2mM each)
2.5 µL	primer FW-A2lox
2.5 µL	primer RV-A2lox
1 µL	template pUG6(10 ng)
28.5 µL	H_2O bidest.
0.5 µL	Phusion DNA Polymerase
50 µL	total volume

PCR cycling conditions:

98°C/30 s- (98°C/7 s- 63°C/30 s-72°C/2.5 min) x 35- 72°C/7 min- 4°C/∞

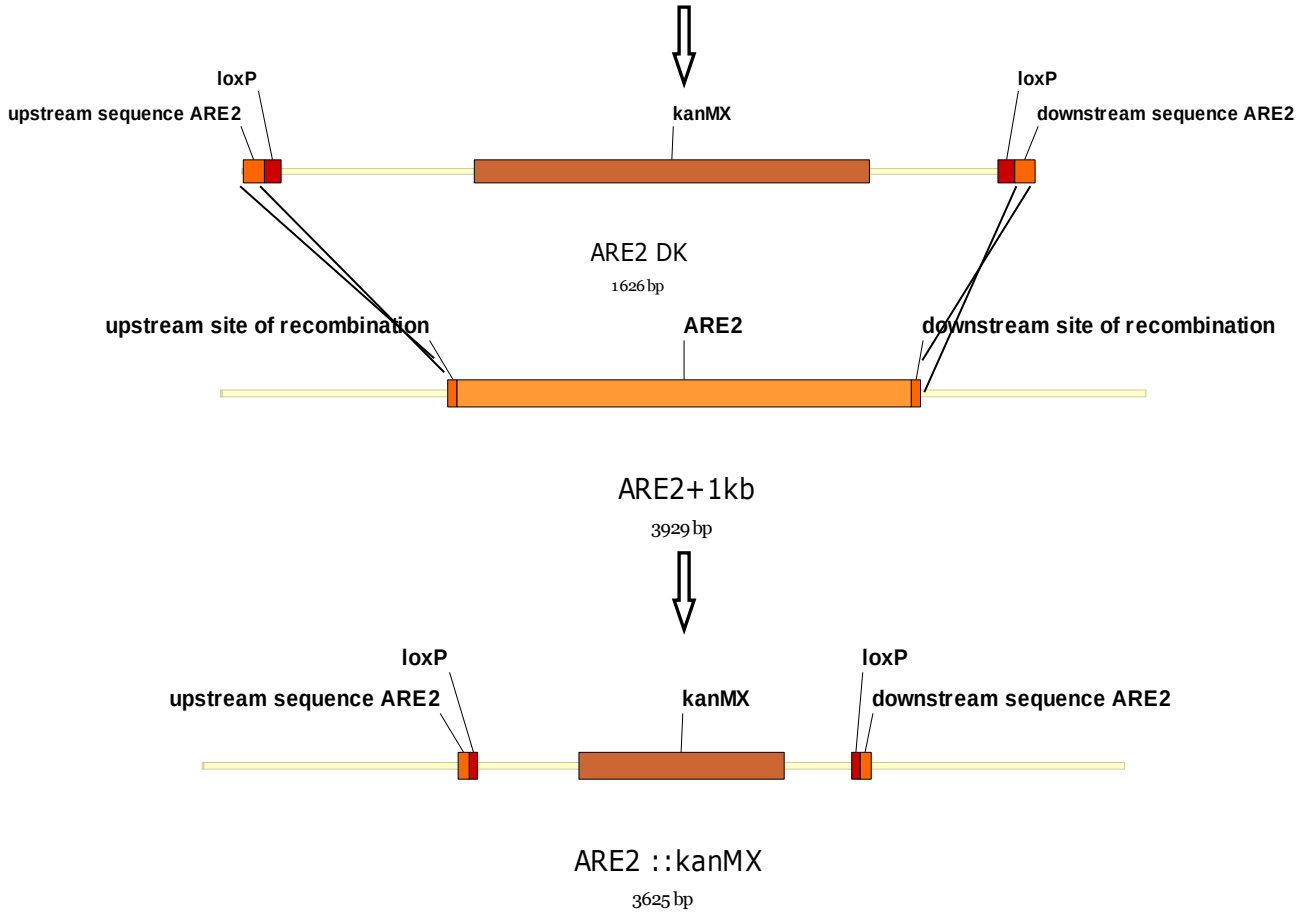

Figure 16: Generation of are2: loxp-kanMX-loxP disruption cassettes and strain

3.2 Transformation of Yeast

During this work two different transformation procedures were used. Both of them are based on the treatment of cells with lithium acetate (LiAc), followed by incubation with DNA in PEG solution. I made the best experiences for the transformation of disruption cassettes with the following procedure, a roundup of the protocol described by Adams, 1997.

50 mL of YPD were inoculated to an OD of 0.1 with a fresh ONC and incubated at 30°C between three and five hours. The culture was then harvested in a sterile 50 mL centrifuge tube at 2500 rpm for 5 min. The pellet was washed with 25 mL of sterile, ice-cold H_2O, centrifuged as before and, after discarding the water, resuspended in 1 mL of 100 mM LiAc and transferred to a sterile 1.5 mL microfuge tube. The cells were harvested at top speed for 5 s and the LiAc was removed with micropipette. Then the pellet was resuspended in 400 µL of 100 mM LiAc, which yielded sufficient material for 10 transformations. The transformation mix was added in the following order to 50 µL of this LiAc competent cell suspension:

240 µL PEG 50% w/v

36 µL 1 M LiOAc

5 µL single stranded carrier DNA (10 mg/mL)

500- 1000 ng of disruption cassette DNA

After snapping each tube until the pellet was completely resuspended, the mixture was incubated for 30 min at 30°C before being heat shocked at 42°C for 25 min. The cells were collected by centrifugation at 3000 rpm for 15 s, before the transformation mix was removed with a micropipette. Subsequently, the cells were resuspended in 1 mL of YPD and incubated for 1 h at 30°C. Regeneration was followed by centrifugation at top speed for 10 s and the supernatant was discarded. Regenerated cells were resuspended in 100 µL of sterile H_2O and plated onto selective media which were then incubated for three to seven days at 30°C. Single colonies of transformants were tested by colony PCR.

The transformation of plasmids worked quite well by a quick and easy protocol described by Elble (1992).

25 mL of YPD were inoculated with cells from a fresh plate and incubated for 5 h at 30°C and 140 rpm. For every transformation event, 1 mL of culture was spin at 3000 x g for 10 s. After discarding the supernatant, the pellet was carefully resuspended in 10 µL of carrier DNA (10 mg/mL), 1 µg transforming DNA and 500 µL of transformation-mix (consisting of 90 mL

sterile 45% PEG 4000, 10 mL of 1 M lithium acetate, 1 mL of 1 M Tris-HCl, pH 7.5, and 0.2 mL of 0.5 M EDTA, pH 8). The transformation mixture was incubated at room temperature overnight on the benchtop. After collecting the cells by centrifugation at 3000 x g for 10 s and discarding the supernatant, the pellet was resuspended in 200 µL of YPD and incubated for 2 h at 30°C. The whole volume was plated onto selective media.

3.3 Colony PCR

To test transformants for correct integration of the disruption cassettes a single colony of 1 mm in diameter was resuspended in 50 µL of zymolyase (2.5 mg/mL ~ 50 U) or 50 µL of lyticase (1.25 mg/mL ~75 U) in a PCR reaction tube and incubated for 15 min at 37°C. After harvesting the cells at 5000 rpm for 1 min the supernatant was discarded and the pellet heated for 5 min at 92°C to inactivate DNases. The pellet was resuspended in a prepared PCR Master-Mix before starting the PCR under the following conditions:

When using "DreamTaq DNA polymerase":

~ 3 µL	Pellet of *S. cerevisiae*
31.75 µL	deion. H_2O
5 µL	Dream Taq Buffer (10x)
5 µL	dNTP mix of 2 mM each
2.5 µL	primer fw of 10 µM
2.5 µL	primer rv of 10 µM
0.25 µL	DreamTaq DNA polymerase of 5 U/µL
50 µL	total volume

Cycling conditions:

95°C/3 min-{95°C/30 s-(Tm primer-5°C/30 s)-(72°C/1 min per kbp)} x40 -72°C/10 min -4°C/∞

When using "Maxima Hot Start Green PCR Master Mix":

~ 3 µL	Pellet of *S. cerevisiae*
19 µL	deion. H_2O
25 µL	Maxima Taq Mastermix
2.5 µL	primer fw of 10 µM
2.5 µL	primer rv of 10 µM
52 µL	total volume

Cycling conditions:

95°C/4 min-{95°C/30 s-(Tm primer-5°C/30 s)-(72°C/1 min per kbp)} x40 -72°C/10 min -4°C/∞

3.4 Gel electrophoresis

The separation and purification of DNA fragments by agarose gel-electrophoresis was performed according to standard protocols. One % agarose gels in TAE buffer were run at 90 V for about 80 min for preparative gels and 120 V for 45 min for analytical gels. The sizes of DNA fragments were assessed by comparison to the standard “GeneRuler DNA Ladder Mix”, and the concentrations were estimated based on the “MassRuler DNA Ladder Mix” standard, both by Fermentas.

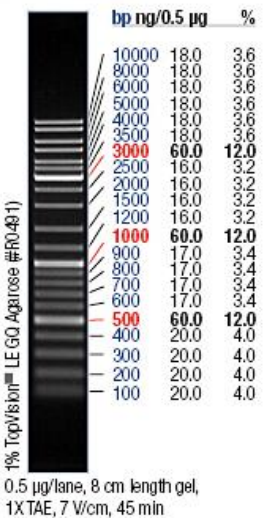

Figure 17: GeneRuler™ DNA Ladder Mix

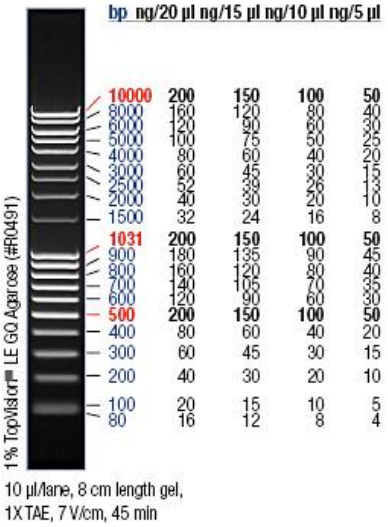

Figure 18: MassRuler ™ DNA Ladder Mix

3.5 Preparation of plasmids, PCR products, and DNA fragments

All plasmids were isolated with Fermentas “GeneJet Plasmid Miniprep Kit” according to the supplier’s manual and finally eluted with 25 µl ddH_20. DNA fragments and PCR products were purified over standard DNA agarose gels and extracted with “Wizard SV Gel Slice and PCR Product Preparation” by Promega, as described in the manual.

3.6 Sequencing

All disruption cassettes and all plasmids carrying an*ERG6* mutation were sequenced by LGC Genomics GmbH (Berlin, Germany), in very high quality. For best sequencing results, 10 µL of a plasmid preparation were mixed with 4 µL of a 5 µM sequencing primer. For sequencing of disruption cassettes, 4 µL of a 5 µM sequencing primer were added to 10 µL of a 40 ng/µL solution of sequencing template.

3.7 Mating type determination

Yeast cells can either be haploid, with mating types *MATa* or *MATα*, or diploid *MATa*/*α*. Haploid cells with different mating types are able to mate with each other, yielding a diploid strain which cannot mate any more. To cross two strains to combine their genetic features, one needs yeast strains with different mating types. Therefore it is important to have a method of mating type determination.

Two tester strains, PH5 (*MATahis1*) and PH6 (*MATαhis1*) were incubated in 5 mL of YPD over night at 30°C. Three mL each of these cultures were harvested at 2500 rpm for 5 min and the pellets were resuspended in 500 µL of sterile water. 300 µL of this suspensions were plated onto SD-his plates until completely dry. The strains to be tested for mating type were streaked onto these tester plates and incubated over night at 30°C for mating to take place. The tester strains themselves cannot grow on SD-his plates. Strains that mate with PH5 are *MATα*, and, therefore, resulting diploids that grow on selective SD-his plates. Strains that mate and form diploids with PH6 on SD- his are *MATa*.

3.8 Mating, Sporulation, and Tetrad Dissection

Mating of two haploid yeast strains with compatible mating types (a and α) was done by smearing dabs of the size of a coin of “a” and “α” strains together on a YPD plate and incubating them over night at 30°C. On the next day, colonies taken from the middle of these dabs were tested for combined auxotrophy markers deriving from each haploid strain.

Starvation of diploid cells for nitrogen and carbon sources induces meiosis und spore formation. This process is induced in cells grown in sporulation media for several days until spores are detected by microscopy. Two mL of a diploid ONC were spin at 2500 x g for 5 min and the pellet was washed with two mL of sterile water. After discarding the supernatant, the pellet was resuspended in two mL of sporulation medium. The first spores were usually observed after three days. For tetrad dissection sporulation was carried out for at least five days.

The dissection of ascospores, a bundle of four haploid daughter cells, was performed according to the following protocol. Depending on cell density, 200-1000 µL of sporulation culture were centrifuged for one min at 13,000 x g. After removing the supernatant with a micropipette, the pellet was resuspended in 125 µL of sterile water. For partial digestion of the membrane sac surrounding the ascospores, 15 µL of zymolyase solution (5 mg/100 µL)

were added and the mixture was incubated at room temperature for one to four min. After suitable incubation time, 25 µL of the digested spores were transferred into 75 µL of ice cold, sterile water and put on ice. For dissection, 20 µL of this suspension were applied to an appropriate YPD agar plate as a single line in the centre.

3.9 Ion Analysis

Wild-type CEN.PK2 and *erg5erg6* double knockout strains were analysed for their Cu, Fe, Mg, Mn and Zn ion content at the Institute for Analytical Chemistry by Dr. Helmar Wiltsche, Graz University of Technology.

The cells were grown for about 16 h in YPD medium or 24 h in SD-all medium. Three OD_{600}-units were harvested in 50 mL falcon tubes at 2500 rpm for 5 min and washed twice with deionized water before the samples were given to Dr. Wiltsche, who prepared the samples as follows.

Pulping:

0.1 – 0.2 g of each sample were dissolved in 3 mL of subboiled HNO_3, 1 mL of 30% H_2O_2 (Merck suprapur) and 2 mL of MilliQ deionized water. Microwave supported pressure pulping (Anton Paar Multiwave 3000; HF-hollow ware) was done with maximum pressure at 40 bar and 1200 W for 15 min. The samples were then transferred and filled up to 30 mL with deionized MilliQ water.

The technical data of ICP-OES analysis:

Spectro Ciros Vision EOP at 1300W in a Scott Spray Chamber equipped with a Crossflow Nebulizer and sample uptake at 0.9 ml/min.

Sc was used as internal standard and calibration was performed at 0, 5, 10, 20, 50, 100 and 500 µg/L of each analyte.

3.10 Lipid extraction

Lipids were extracted by the method of Folch (1957).

To get equal amounts of each strain, 250 OD_{600} units of early stationary cultures were harvested in Pyrex glass tubes. The cell pellets were resuspended in 4 mL $CHCl_3$:MeOH (2:1, v/v) and agitated in the presence of glass beads and for one hour at room temperature on a Vibrax at full speed to extract the total lipids. After sedimenting the glass beads at 1500 rpm for 3 min the crude lipid extract was transferred to a new Pyrex tube. Proteins and non-polar substances were removed by sequentially washing the organic phase with 2 mL of 0.034% $MgCl_2$, 2 mL of 2 N KCl: MeOH (4:1, v/v) and 1.5 mL of $CHCl_3$:MeOH:H_2O (3:48:47, per vol.). Each washing step consisted of 2 min of vortexing and subsequent centrifugation to separate the phases. The upper, aqueous phases were always discarded. The lipid extracts were dried under a stream of nitrogen and finally dissolved in 50 µL of $CHCl_3$:MeOH (2:1, v/v). These lipid extracts were used for TLC analysis or stored at -20°C immediately.

3.11 Thin Layer Chromatography

To analyze the ratio between free sterols and steryl esters, a two step separation on Silica TLC plates was carried out. Therefore, lipid extracts were automatically spotted onto 20 x 10 cm silica plates. In parallel, the first solvent mixture, petrol ether/diethyl ether/acetic acid (49:49:2 per vol.) was prepared. After equilibration of the TLC chamber for about 30 min, TLC plates were developed until reaching one third of the plate's height. After drying the TLC plates completely, the same plates developed in a second, pre-equilibrated chamber using petrolether/diethyl ether (49:1, v/v) as a solvent mixture until the solvent front reached the top of the plate. Free sterols and steryl esters were quantified relatively using a TLC scanner, at 275 nm. Bands of free sterols, steryl esters, triglycerides and squalene were visualized by by charring. TLC plates were dipped into a solution of 0.4 g $MnCl_2$, 60 mL H_2O, 60 mL methanol and 4 mL H_2SO_4 conc. for 10 seconds and then heated at 105°C for 40 min.

3.12 GC/MS

For GC/MS samples were prepared by harvesting 15 OD_{600} units of ONC in Pyrex glass tubes. The culture medium was discarded, and the pellets were suspended in 0.6 mL methanol, 0.4 mL pyrogallol (0.5% dissolved in methanol) and 0.4 mL 60% KOH each. After addition of 5 µL of 2 mg/mL internal cholesterol standard, the pellets were vigorously vortexed and heated

for two h on a sandbath at 90°C. After cooling to room temperature, saponified lipids were extracted three times with 1 mL of n-heptane. For good extraction efficiency, the samples were vortexed for one minute. The phases were separated by centrifugation at 1500 rpm for 3 min. The upper phases were collected in a new pyrex tube, while the lower phases were re-extracted. The combined upper phases of each sample were dried under a stream of nitrogen. The extracted sterols were dissolved in 10 µL of pyridine and derivatized with 10 µL of N'O'-bis(trimethylsilyl)-trifluoracetamid to improve volatility. Then, the samples were diluted in 50 µL ethylacetate and subsequently analysed by Prof. Dr. Erich Leitner at the Institute of Analytical Chemistry and Food Chemistry, Graz University of Technology. The technical data of GC-MS analysis are described in Table 12.

Table 12: Technical data of GC/MS analysis

GLC	HP 5890 Series II Plus with Electronic Pressure Control and 6890 automated liquid sampler (ALS)
Injector	Split/splitless 270°C, mode: splitless, purge on: 2 min
Injection volume	1 µl
Column	HP 5-MS (Crosslinked 5% Phenyl Methyl Siloxane), 30 m x 0.25 mm i.d. x 0.25 µm film thickness
Carrier	Helium, 5.0
Flow	0.9 ml, linear velocity 35.4 cm/s, constant flow
Oven	100°C (1 min), range of 10°C/min to 250°C (0 min) and range of 3°C/min to 300°C (0 min)
Detector	selective Detector HP 5972 MSD
Ionization	EI, 70 eV
Mode	Scan, scan range: 100-550 amu, 2.58 scans/s
EM Voltage	Tune Voltage
Tune	Auto Tune

3.13 Protein Analysis: Cell disruption, SDS-PAGE and Western Blot

The double knockout strain *erg5erg6* as well as all *erg6* point mutants were analysed by Western Blot to determine whether Erg6p was expressed or not. The first step of protein analysis was to break the yeast cells and precipitate the proteins by a method described first by Volland et al. (1993), modified by Schimmoeller et al. (1995), and finally adapted to own specific needs.

For this purpose, four OD units of an overnight culture of each sample were harvested. The pellets were resuspended in 300 µL of 1.85 M NaOH/7.5% (v/w) β-mercaptoethanol and incubated for ten min on ice. Upon addition of 300 µL of 50% TCA, the samples were mixed thoroughly and incubated for additional 30 min on ice. Protein was pelleted at 10,000 rpm for five min and the supernatant was removed with a micropipette. For neutralization of the TCA, the pellet was washed once with 1 mL of ice cold water and then resuspended in a mixture of

66 µL of NuPage sample buffer 1x,

33 µL of TrisBase 1 M and

2 µL of β- Mercaptoethanol

per pellet.

The proteins were denatured for five min at 95°C prior to loading 5 to 10 µL on a NuPAGE SDS Gel (4-12% Bis-Tris Gel), following standard protocols.

For Western Blot analysis the blotting sandwich was built up as shown in Figure 19.

Transfer was performed for up to 1 h with a current of 400 mA as the limiting variable.

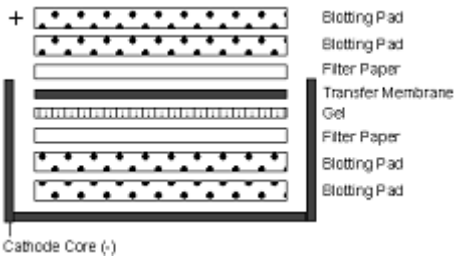

Figure 19: Scheme for Western Blot assembly, (copyright by Invitrogen)

The membranes were stained with Ponceau S solution, a sodium salt of a diazo dye that reversibly stains protein bands to check if protein transfer from the gel to the membrane worked out. After taking an image, the Ponceau S stain was washed away with water before blocking the membrane with TBST-milk over night at 4°C. This step was followed by rinsing

the membrane with 1xTBST before applying a 1:30,000 working solution of the primary antibody, anti-Erg6p produced in rabbit, on the membrane and incubating over night at room temperature and moderate shaking. After washing the membrane three times for five min with 1xTBST, the secondary antibody (Goat anti rabbit IgG, horseradish peroxidase conjugated) was applied at 1:5000 dilution for one h at room temperature and moderate shaking. After repeating the washing steps three times for five min with 1xTBST, the detection was done with the SuperSignal West Pico Chemiluminescent Substrate Kit from Pierce. The two substrate components, peroxide solution and enhancer solution, were mixed in a 1:1 ratio. This working solution was protected from sunlight and used immediately after preparation. For one membrane, 5 mL of the working solution were applied with a micropipette directly onto the membrane and incubated for one to eight minutes. During incubation, chemiluminescence signals were detected with the G:Box Bioimager.

3.14 Isolation of genomic DNA

In the course of this work two methods for the isolation of genomic DNA were used. The first was according to the manual “Large Scale Isolation of DNA from Yeast Cells” of the Invitrogen “Easy DNA Kit” yielding high concentrations of genomic DNA, the other was the so-called “Bust n’ Grab” method (Harju, 2004). For this purpose, 1.5 ml of an overnight culture were transferred into a microfuge tube and pelleted at 13,000 x g for five min. The pellet was resuspended in 200 µL of lysis buffer (2% Triton X-100,1% SDS, 100 mM NaCl, 10 mM Tris-HCl, pH 8.0, 1 mM EDTA, pH 8.0) and then placed in a -80°C freezer until completely frozen. The mixture was quickly thawed in a thermomixer at 95°C. This procedure was repeated twice before vortexing the sample for 30 s. After adding 200 µL of chloroform, the tubes were vortexed for 2 min and centrifuged for three min at room temperature and maximum speed. For DNA precipitation, the upper aqueous phase was transferred to a microcentrifuge tube containing 400 µl of ice-cold 100% ethanol which was then mixed by inversion. To increase the yield, samples were incubated at -20°C for five to ten min and centrifuged for five min at maximum speed. The supernatant was removed with a micropipette and the pellet was dried in an incubator at 37°C before dissolving it in 20 µL of TE buffer (10 mM Tris-HCl, 1 mM EDTA, pH 8).

3.15 Site Directed Mutagenesis

Site Directed Mutagenesis of the *ERG6* gene was done according to the manual of the Stratagene QuikChange Site Directed Mutagenesis Kit. In brief, the plasmid containing the gene with the target site of mutation, pFL44-*ERG6* (Figure 20) was amplified with primers containing the desired mutation(s) resulting in mutated nicked circular strands. The amplifications were performed with "PfuTurbo" DNA polymerase. The parental, methylated strands were then digested by *Dpn* I, an endonuclease with the target sequence 5'-Gm^{6}ATC-3', which is specific for methylated DNA. DNA isolated from almost all *E. coli* strains, like BL21 Gold, is dam methylated and therefore susceptible to *Dpn* I digestion. The PCR products were transformed to electrocompetent *E. coli* (Top10F') cells. Supercoiled plasmids carrying the mutated gene were isolated from *E. coli*, sequenced and transformed into the *erg5erg6* double knockout strain to investigate the effects of site directed mutagenesis by GC/MS of sterols and Western blotting against Erg6p.

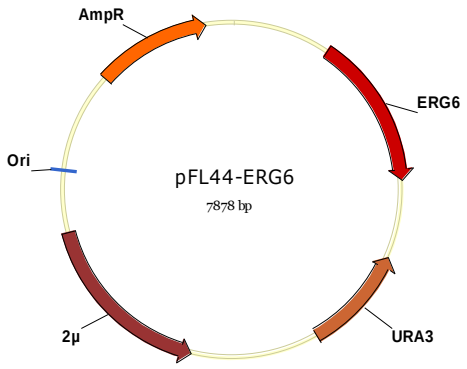

Figure 20: Template for the site directed mutagenesis of *ERG6*: pFL44-ERG6

All PCRs were first done separately for the forward and the reverse primers for primer expansion:

5 µL	PfuUltra Buffer 10x
10 ng	template: pFL44-ERG6
5 µL	dNTP- Mix (2mM each)
36.5 µL	ddH_2O
1.5 µL	primer fw or rv of 10 µM
1 µL	PfuUltra DNA polymerase
50 µL	total volume

PCR cycling conditions:

95°C/1 min- (95°C/50 s- 60°C/50 s- 72°C/8 min) x 4 – 72°C/7 min- 4°C/∞

After this first step, both PCR reactions were pooled in a 1:1 ratio by mixing 25 µL of each reaction for the standard mutagenesis PCR using the same cycling conditions for further 18 cycles.

Dpn I digestion was started by adding 1 µL of 10 u/µL Dpn I to each PCR reaction and incubation for one h at 37°C. An additional microliter of Dpn I was added and incubation was extended for another h. The enzyme was inactivated at 80°C for 20 min before transforming 2 µL into electrocompetent TOP10F' *E. coli* cells and selecting positive transformants on ampicillin plates. Single colonies were streaked out on new plates to isolate the plasmids with the Fermentas GeneJet Plasmid Miniprep Kit.

3.16 Electrocompetent *E. coli* Cells

30 mL of LB media were inoculated with the chosen *E. coli* strain and incubated over night at 37°C and 220 rpm. The following day, the main culture of 500 mL of LB media was inoculated with 5 mL of the overnight culture and incubated at 37°C until reaching an OD between 0.7 and 0.9, which usually took between two and four h. After transferring the culture to chilled 500 mL centrifuge bottles, it was cooled on ice for 30 min before harvesting the cells at 2,000 x g and 4°C for 15 min. The supernatant was discarded and the pellet was carefully resuspended in pre-chilled 500 mL ddH_2O. The suspension was centrifuged as before and the supernatant was discarded. Then, the cell pellet was resuspended in 35 mL of pre-chilled, sterile 10% glycerol and centrifuged at 4,000 x g and 4°C for 15 min. After discarding the supernatant, the pellet was resuspended in 1 mL ice-cold, sterile 10% glycerol before aliquoting the electrocompetent cells to 80 µL into sterile Eppendorf tubes. The cells were frozen in liquid N_2 and stored at -80°C until needed.

3.17 Electroporation of *E. coli* cells

The transformation of plasmids into electrocompetent E. coli cells TOP10F' followed a standard procedure. 50 µL of electrocompetent cells, prepared as described above, were thawed on ice. After adding 2 µL of a plasmid preparation and transferring the mixture to chilled transformation cuvettes, they were incubated on ice for ten minutes before pulsing them in the electroporator. Immediately after the electro-pulse, 1 mL of SOC medium was added and the cells were regenerated at 37°C for one h at 650 rpm before plating them on selective media.

4 RESULTS

Only final and representative results will be shown in this section. All experimental raw data are available on the attached CD and experimental problems as well as necessary repetition of experiments are discussed.

4.1 ANALYSIS OF THE CEN.PK2 STRAIN FOR ITS *HAP1* STATUS

As already explained in the introduction, we wanted to work with a yeast strain with a wild-type like situation at the *HAP1* locus. To ensure that our strain background does not have a defect at *HAP1* e.g. a transposon insertion, we analysed this ORF.

Therefore genomic DNA was prepared of the diploid wild-type strain CEN.PK2, two isogenic haploid wild-type strains with opposite mating types, CEN.PK2-IC and CEN.PK2-ID, as well as of SC0458, a strain we received from DSM NP and BY4741, a wild-type yeast strain which is known to carry a *Ty1* insertion in *HAP1* and which served as a reference strain. Genomic DNA was used as template to amplify the DNA fragment between two primers annealing up- and downstream of *HAP1,* HAP1-1 and HAP1-2, respectively. Isolation of genomic DNA turned out to be the essential step in the analysis, because the expected fragment of BY4741 was obviously too big to be amplified by standard colony PCR protocol which failed twice.

As can be seen in Figure 21, there is a clear difference in the size of the resulting PCR fragments between the strain BY4741 which yielded a fragment larger than 10,000 bp and all other strains which just gave a 4500 bp fragment. This difference corresponds to the size of the *Ty1* transposon which is about 6000 bp. Thus the wild-type yeast strain we used for further experiment, CEN.PK2 does not have the typical *Ty1* insertion and hence carries a fully functional *HAP1* gene.

PCR reaction mix:

10 µL	Phusion HF buffer (5x)
5 µL	dNTP Mix (2mM each)
2.5 µL	primer HAP1-1
2.5 µL	primer HAP1-2
1 µL	template genomic DNA (1:10)
28.5 µL	H_2O bidest.
0.5 µL	Phusion DNA Polymerase
50 µL	total volume

PCR cycling conditions:

98°C/30 s-(98°C/7 s-63°C/30 s-72°C/10 min) x 35- 72°C/7 min- 4°C/∞

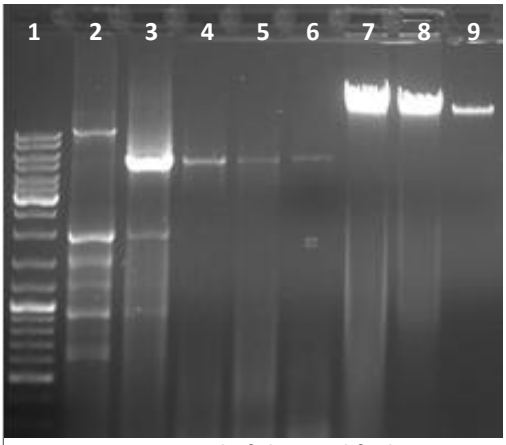

Figure 21: Agarose gel of the amplified *HAP1* gene of the strains CEN.PK2, SC0458 and BY4741

Table 13: Lane description of Figure 21

Sample ID	Description	Volume [µL]	Visible bands [bp]
1	Gene Ruler DNA Ladder Mix	5	-
2	BY4741	10	10400
3	CEN.PK2	10	4500
4	CEN.PK2-IC	10	4500
5	CEN.PK2-ID	10	4500
6	SC0458	10	4500
7	Genomic DNA CEN. PK2	10	-
8	Genomic DNA BY4741	10	-
9	Genomic DNA SC0458	10	-

4.2 STRAIN CONSTRUCTION

All strain constructions followed the same route, starting with the amplification of the corresponding disruption cassette, followed by purification on an agarose gel, and by the extraction of the DNA which was then transformed into yeast. Several transformants were streaked on selective media and tested by Colony PCR and GC/MS or TLC.

4.2.1 Construction of the *erg5* knockout strain

The creation of the *ERG5* disruption cassette was done according to the method described in chapter 3.1.1 using a DNA polymerase with proofreading function to avoid unwanted mutations. The amplified disruption cassette was separated on an agarose gel (Figure 22). The additional bands which can be seen on the gel are unspecific products originating from the low annealing temperature at 55°C. To avoid unspecific bands when generating disruption cassettes, a two- step PCR was applied for all other disruption cassettes later on. The DNA fragments were excised and the DNA was extracted with the WIZARD SV Gel and PCR Clean-Up System by Promega. For yeast transformations, a DNA concentration between 500 and 1000 ng is necessary. Hence, disruption cassettes were always amplified several times and two PCR reactions were usually pooled to have sufficient material for several transformation experiments.

Disruption of *ERG5* by the linear cassette comprising *LEU2* marker worked out very well yielding about fifty transformants that grew on SD-leu plates. Some of these were re-streaked on new SD-leu plates to observe their growth behaviour and were then tested by Colony PCR as described (page 36). Just one of eleven transformants tested showed a positive result with primers annealing upstream of the *ERG5* gene, K1E5, and in the *LEU2* marker gene, K2E5 (Figure 23). This could be (i) due to unspecific integration of the disruption cassette yielding false positives growing on selective plates without a disruption in the *ERG5* gene, or (ii) due to problems with colony PCR, which is a very tricky and not fully reliable method to find positive transformants. The only positive transformant, the desired *erg5* knockout strain, was saved and analysed for sterol composition by GC/MS and used to create an *erg5erg6* double knockout strain.

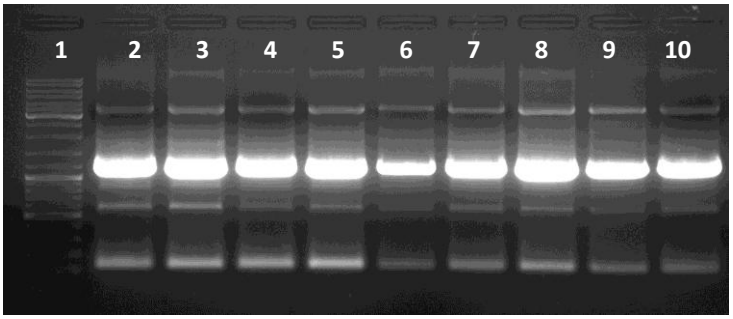

Figure 22: ERG5 disruptioncassette separated on an agarose gel

Table 14: Lane description of Figure 22

Sample ID	Description	Volume[µL]	Visible bands [bp]
1	Gene Ruler DNA Ladder Mix	10	-
2	*ERG5* disruption cassette 1	50	~1200
3	*ERG5* disruption cassette 2	50	~1200
4	*ERG5* disruption cassette 3	50	~1200
5	*ERG5* disruption cassette 4	50	~1200
6	*ERG5* disruption cassette 5	50	~1200
7	*ERG5* disruption cassette 6	50	~1200
8	*ERG5* disruption cassette 7	50	~1200
9	*ERG5* disruption cassette 8	50	~1200
10	*ERG5* disruption cassette 9	50	~1200

Colony PCR reaction mix:

~ 3 µL	Pellet *S. cerevisiae*
31.75 µL	deion. H_2O
5 µL	Dream Taq Buffer (10x)
5 µL	dNTP mix of 2 mM each
2.5 µL	primer K1E5 of 10 µM
2.5 µL	primer K2E5 of 10 µM
0.25 µL	DreamTaq DNA polymerase of 5 U/µL
50 µL	total volume

PCR cycling conditions:

95°C/3 min-(95°C/30 s-55°C/30 s-72°C/30 s) for 1000 bp) x35 -72°C/10 min -4°C/∞

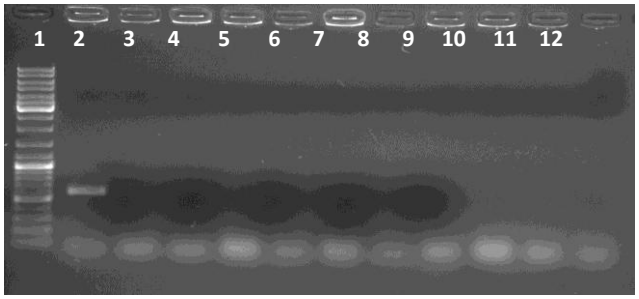

Figure 23: Colony PCR of *erg5::LEU2* transformants separated on an agarose gel

Table 15: lane description of Figure 23

Sample ID	Description	Volume [µL]	Visible bands [bp]
1	Gene Ruler DNA Ladder Mix	5	-
2	Transformant no. 1- *erg5*Δ::*LEU2*	10	600
3	Transformant no. 2- *erg5*Δ::*LEU2*	10	-
4	Transformant no. 3- *erg5*Δ::*LEU2*	10	-
5	Transformant no. 4- *erg5*Δ::*LEU2*	10	-
6	Transformant no. 5- *erg5*Δ::*LEU2*	10	-
7	Transformant no. 6- *erg5*Δ::*LEU2*	10	-
8	Transformant no. 7- *erg5*Δ::*LEU2*	10	-
9	Transformant no. 8- *erg5*Δ::*LEU2*	10	-
10	Transformant no. 9- *erg5*Δ::*LEU2*	10	-
11	Transformant no. 10- *erg5*Δ::*LEU2*	10	-
12	Transformant no. 11- *erg5*Δ::*LEU2*	10	-

The positive transformant no.1 was then verified by GC/MS analysis of sterols. Figure 24 shows a GC/MS chromatogram of a wild-type strain which was compared to the GC/MS chromatogram of the knockout strain which is shown in Figure 25.

Peaks labelled in the chromatograms were identified by their MS spectra and their relative retention time normalized for the internal cholesterol standard.

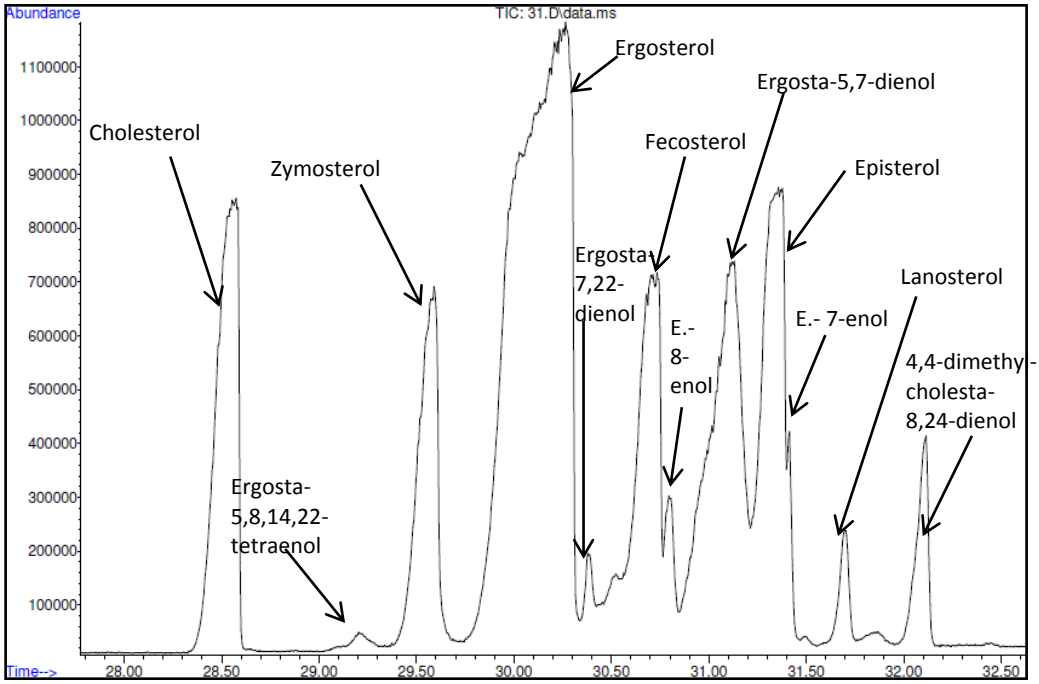

Figure 24: GC/MS chromatogram of the wild-type strain CEN.PK2.

Table 16: Relative amounts of main sterols of the wild-type GC/MS chromatogram

Sterol	Relative amount [%]
Zymosterol	10,4
Ergosterol	52,8
Fecosterol	8,3
Ergosta-5,7-dienol	12,3
Episterol	8,3
4,4-dimethyl-cholesta-8,24-dienol	3,6

GC/MS results of the wild-type looked exactly as expected. Ergosterol, the end product of the biosynthetic pathway is by far the most abundant of total sterols at more than fifty per cent. Additionally, a few ergosterol precursors were detected, i.e. zymosterol, ergosta-5,7-dienol, fecosterol and episterol, and make up between eight and twelve per cent. These sterols and a lot of other characterized peaks beside ergosterol, give a characteristic sterol pattern for a wild-type strain (Figure 24).

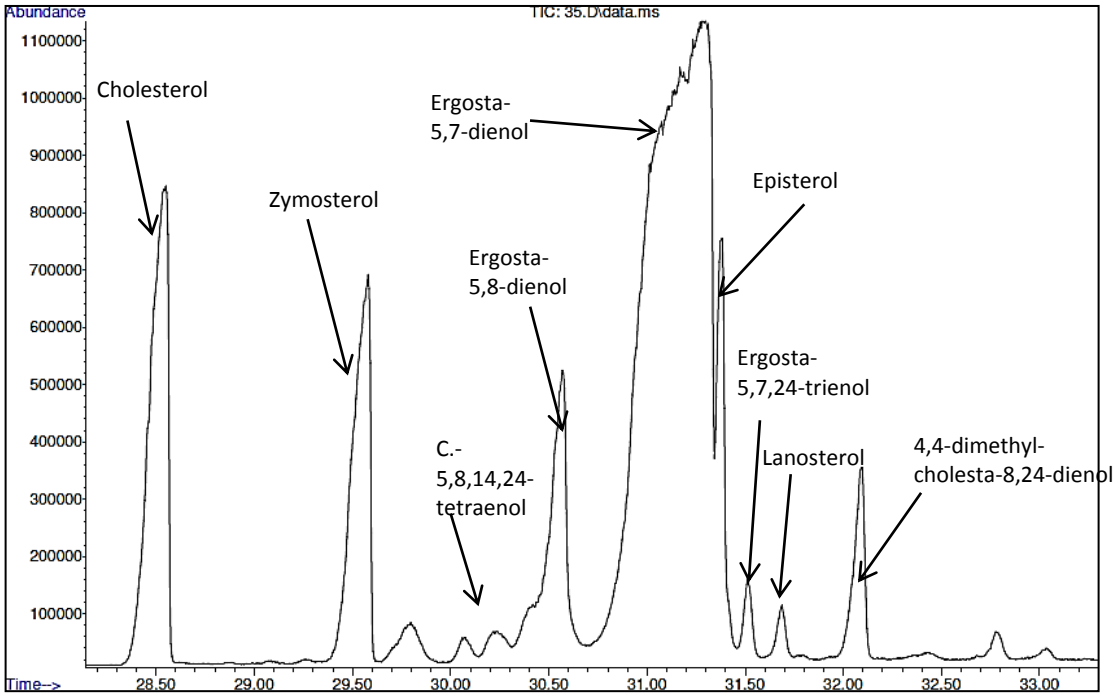

Figure 25: GC/MS chromatogram of the *erg5* knockout strain

Table 17: Relative amounts of main sterols of a GC/MS chromatogram of the *erg5* knockout strain

Sterol	Relative amount [%]
Zymosterol	33,4
Ergosta-5,8-dienol	5,0
Ergosta-5,7-dienol	53,1
Episterol	9,0

The *erg5* knockout strain on the other hand shows totally different GC/MS results with ergosta-5,7-dienol as main sterol which would be a substrate for Erg5p (Figure 25). However, as the C-22 desaturase is not expressed in an *erg5* knockout strain, the accumulation of ergosta-5,7-dienol as well as of earlier intermediates of the ergosterol pathway, such as zymosterol and episterol, confirms the genotype of the *erg5* knock-out strain.

4.2.2 Construction of the *erg5erg6*double-knockout strain

After amplification and purification of the *ERG6* disruption cassette (Figure 26), it was transformed into the verified *erg5* knockout strain. The transformation event did not work very efficiently and yielded only a few transformants to be re-streaked onto SD-trp plates. Ten transformants were tested by colony PCR with primers annealing upstream of the *ERG6* gene, K1E6, and in the *TRP1* marker gene, K2E6, respectively.

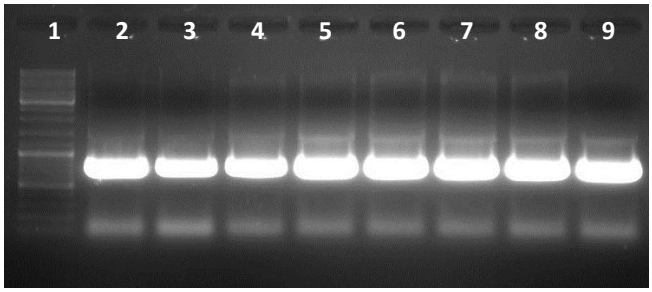

Figure 26: *ERG6* disruption cassettes, separated on an agarose gel

Table 18: lane description of Figure 26

Sample ID	Description	Volume[µL]	Visible bands [bp]
1	Gene Ruler DNA Ladder Mix	10	-
2	*ERG6* disruption cassette 1	50	~750
3	*ERG6* disruption cassette 2	50	~750
4	*ERG6* disruption cassette 3	50	~750
5	*ERG6* disruption cassette 4	50	~750
6	*ERG6* disruption cassette 5	50	~750
7	*ERG6* disruption cassette 6	50	~750
8	*ERG6* disruption cassette 7	50	~750
9	*ERG6* disruption cassette 8	50	~750
10	*ERG6* disruption cassette 9	50	~750

Colony PCR reaction mix:

~ 3 µL	Pellet *S. cerevisiae*
31.75 µL	deion. H_2O
5 µL	Dream Taq Buffer (10x)
5 µL	dNTP mix of 2 mM each
2.5 µL	primer K1E6of 10 µM
2.5 µL	primer K2E6 of 10 µM
0.25 µL	DreamTaq DNA polymerase of 5 U/µL
50 µL	total volume

PCR cycling conditions:

95°C/3 min-(95°C/30 s-55°C/30 s-72°C/30 s) x35 -72°C/10 min -4°C/∞

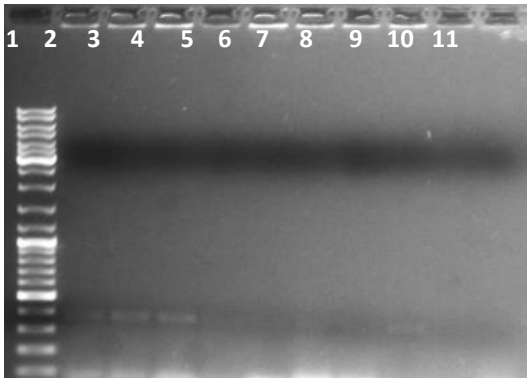

Figure 27: Colony PCR of putative *erg5erg6* transformants separated on an agarose gel

Table 19: Lane description of Figure 27

lane	Description	Volume [µL]	Visible bands [bp]
1	Gene Ruler DNA Ladder Mix	5	-
2	Transformant 1- *erg5erg6*	10	400
3	Transformant 2- *erg5erg6*	10	400
4	Transformant 3- *erg5erg6*	10	400
5	Transformant 4- *erg5erg6*	10	-
6	Transformant 5- *erg5erg6*	10	-
7	Transformant 6- *erg5erg6*	10	-
8	Transformant 7- *erg5erg6*	10	-
9	Transformant 8- *erg5erg6*	10	-
10	Transformant 9- *erg5erg6*	10	-
11	Transformant 10- *erg5erg6*	10	-

The transformants in lane 2, 3 and 4 (Figure 27) seemed to be positive *erg5erg6* double knockout strains because of the visible 400 bp fragment. The next step of verification was GC/MS analysis which was supposed to give an unambiguous sterol pattern. Putative *erg5erg6* transformant no.1 was prepared for GC/MS as described (page 40), and the chromatogram was interpreted as follows:

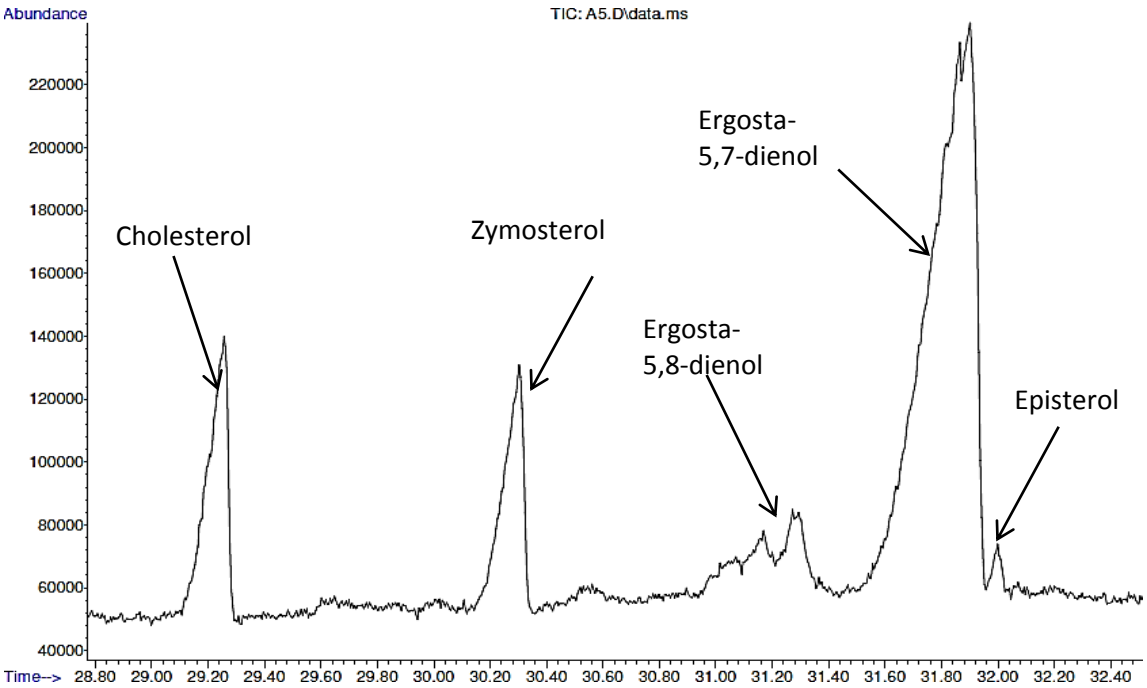

Figure 28: GC/MS chromatogram of false positive *erg5erg6* strain

This chromatogram closely resembled the results of the *erg5* knockout strain (compare Figure 25), particularly because of the abundance of ergosta-5,7-dienol. Thus, the desired *erg5erg6* double knockout strain despite growing on SD-leu-trp plates is most likable an *erg5* mutant strain with an ectopic integration of the *erg6*::*TRP1* disruption cassette. Therefore, the linear disruption cassette was transformed again and only very small transformant colonies were tested by colony PCR considering the possibility, that the *erg5erg6* double knock out strain might have a growth deficiency. Colony PCR was not only performed with the primers K1E6 and K2E6, but with three different primer combinations. The forward primer was unique, namely the already used K1E6 annealing upstream of the *ERG6* gene. Three different reverse primers were used. The first reverse primer annealed in the *TRP1* gene (K2E6), which should result in a 600 bp fragment. The second annealed in the middle of the *ERG6* gene (K2inE6), which should not give a DNA fragment when *ERG6* is correctly disrupted and the third annealed to the downstream region of *ERG6* (K2exE6) which should give a 1075 bp fragment when *ERG6* is correctly disrupted and a 1600 bp fragment when *ERG6* is still part of the genome (Figure 29).

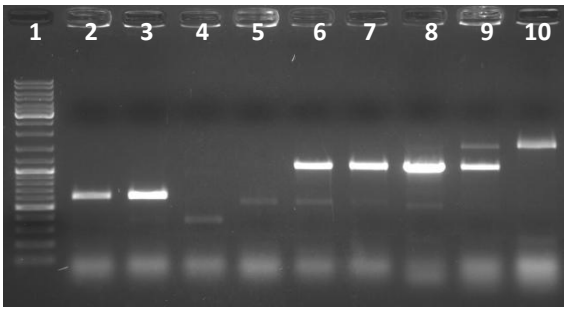

Figure 29: Colony PCR of second *erg5erg6* transformants with three different primer combinations (lane 2-4: K1E6+K2E6; lane 5-7: K1E6+ K2inE6); lane 8-10: K1E6+K2exE6)

Table 20: lane description of Figure 29

lane	Description	Volume [µL]	Expected bands [bp]	Visible bands [bp]
1	Gene Ruler DNA Ladder Mix	5	-	-
2	Transformant no. 4- *erg5erg6*	25	600	600
3	Transformant no. 5- *erg5erg6*	25	600	600
4	Transformant no. 7- *erg5erg6*	25	600	400
5	Transformant no. 4- *erg5erg6*	25	-	-
6	Transformant no. 5- *erg5erg6*	25	-	1080
7	Transformant no. 7- *erg5erg6*	25	-	1080
8	Transformant no. 4- *erg5erg6*	25	1075	1075
9	Transformant no. 5- *erg5erg6*	25	1075	1075+1600
10	Transformant no. 7- *erg5erg6*	25	1075	1600

Only “transformant no. 4“ showed the expected bands for all primer combinations and was therefore tested by GC/MS to prove that this was finally the *erg5erg6* double knockout strain. Figure 30 shows the chromatogram of the *erg5erg6* double knockout strain, indicating high amounts of cholesta-5,7,24-trienol, a lot of zymosterol and also some cholesta-7,24-dienol. Compared to a wild-type spectrum (Figure 24) it is striking that ergosta-sterols are not detectable in significant amounts, due to the disruption of Erg6p, the C-24 methyltransferase transforming the cholesta-structure to the ergosta-structure.

The three main sterols, account together for 96% of the total sterol content (Table 21).

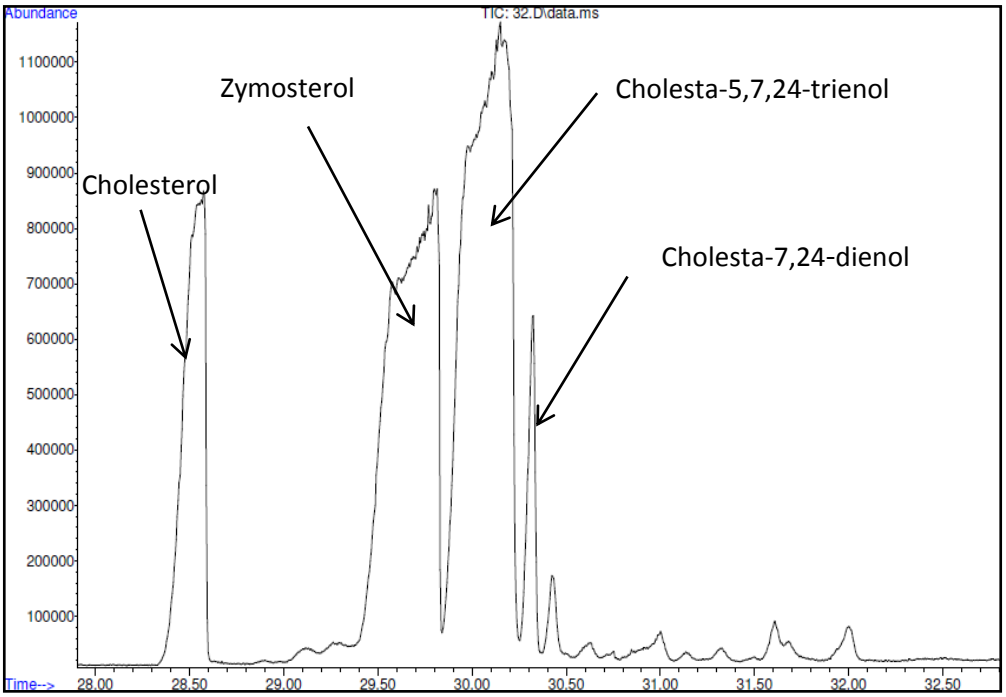

Figure 30: GC/MS analysis of the *erg5erg6* doubleknockout strain, only main peaks

Table 21: Relative amounts of the main sterols of the *erg5erg6* double knockout strain

Sterol	Relative amount [%]
Zymosterol	39,7
Cholesta-5,7,24-trienol	51,8
Cholesta-7,24-dienol	4,5

4.2.3 Further characterization of the *erg5erg6* double knockout strain

The verified *erg5erg6* strain was further characterized by ion analysis and tested for resistance to nystatin.

Ion analysis

The *erg5erg6* strain as well as the wild-type strain CEN.PK2 were cultivated in YPD medium and in SD-all medium to an OD of 1 and 4, respectively. Ion analysis was done in duplicate.

It turned out that ion accumulation first of all depends on the cultivation medium and the abundance of ions therein. The most obvious differences were observed between the copper and zinc content of the total cell extracts of the wild type. Copper accumulated in yeast cells about five times more in SD medium than in YPD. However, zinc was accumulated in wild-type about twice as much in YPD than in SD. Another remarkable result is that the *erg5erg6* strain does not show the same effect compared to the wild-type in both cultivation media. For example, the iron content of the *erg5erg6* strain increased about 77% in SD medium compared to the wild-type but just about 19% in YPD medium. The most striking result was that the magnesium concentration was much higher in the *erg5erg6* strain when cultivated in SD medium but practically unchanged when cultivated in YPD compared to the wild-type.

These results do not directly relate to the regulation of sterol biosynthesis at first glance, but they clearly show that sterols as membrane constituents have a tremendous impact on the whole complex cell system, even affecting ion accumulation or transport.

Table 22: Ion accumulation of the *erg5erg6* strain compared to the wild-type normalized for cell wet weight

Sample	Cu $_{324.754}$ [mg/kg]	Fe $_{238.204}$ [mg/kg]	Mg $_{280.270}$ [mg/kg]	Mn $_{259.373}$ [mg/kg]	Zn $_{213.856}$ [mg/kg]
CEN.PK2-SD	1.5	10.50	461.5	1.25	20.10
erg5erg6-SD	1.2	18.55	857.0	1.85	67.75
CEN.PK2-YPD	0.3	6.65	434.0	0.55	41.70
erg5erg6-YPD	0.4	7.90	413.5	0.60	72.60

Nystatin resistance

Nystatin is an inhibitor that specifically binds to sterols with an ergosta-like structure in the plasma membrane. It is rendering the membrane leaky and thus yeast is inviable. Because of the absence of Erg6p, the C-24 methyltransferase, the cholesta-structure is not modified to the ergosta-structure, meaning that nystatin should not bind and inhibit the growth of a strain when *ERG6* is deleted. The *erg5erg6* strain grew well on YPD plates supplemented with 5 µg/ mL nystatin, the wild-type strain did not grow at all. This was further proof of the successful deletion of *ERG6* and therefore, another verification of the *erg5erg6* double knockout strain. The *erg5* strain was also tested on nystatin plates and was found to be sensitive like the wild-type (data not shown).

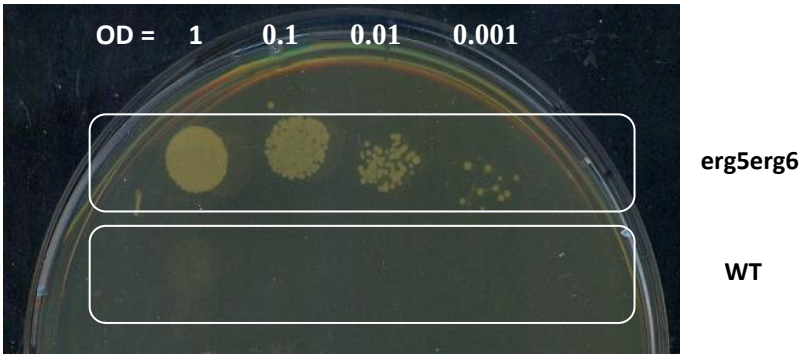

Figure 31: Wild-type, CEN.PK2 and *erg5erg6* knockout strains tested for nystatin sensitivity.

4.2.4 Construction of the *are2* strain

The yeast strain background CEN.PK2 has four selective markers: *leu2*, *trp1*, *his3* and *ura3*. Leucin and tryptophan were already used for the creation of the *ERG5* and *ERG6* disruption cassettes and histidin was reserved for the disruption of *ARE1*. To maintain the last marker, ura3, a *loxP-kanMX-loxP* disruption cassette (as described by Güldener, 1996) was used, combining the advantage of the dominant kan^r marker system and the *Cre-loxP* system. Yeast transformants become resistant to the aminoglycoside antibiotic G418 when expressing the *E. coli* kan^r gene (Webster, 1983). The primers used, FW_A2lox and RV_A2lox, were composed of about 20 bp homologous to the loxP-sites of the pUG6 plasmid at their 3' end and 40 bp homologous to sequences flanking the *ARE2* coding sequence at their 5'-end. The amplification of the disruption cassettes turned out to be more difficult than the amplifications of previous disruption cassettes, often yielding different sizes of the DNA fragments (Figure 32). For the transformation only disruption cassettes with exactly 1550 bp were used, as this was the number of bases calculated for the correct disruption cassette.

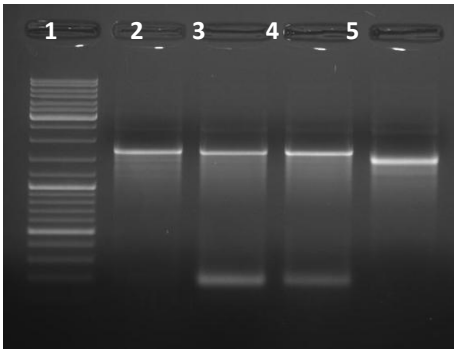

Figure 32: *ARE2* disruption cassettes separated over a standard agarose gel

Table 23: Lane description of Figure 32

Lane	Description	Volume [µL]	Visible bands [bp]
1	Gene Ruler DNA Ladder Mix	10	-
2	*ARE2* disruption cassette no.1	50	1550
3	*ARE2* disruption cassette no.2	50	1550
4	*ARE2* disruption cassette no.3	50	1550
5	*ARE2* disruption cassette no.4	50	1500

Transformation of this disruption cassette was repeated several times to get positive transformants. Transformation efficiency was very, very low in this case. The transformation plates, YPD+ G418 (200 mg/L), showed a lot of very small colonies that did not continue to

grow, upon re-streaking and gave only negative results when tested by Colony PCR. On average just one transformant per plate grew to a normal colony size. One transformant tested showed positive results when it was tested with primers annealing upstream of the *ARE2* gene, KA2up, and in the *kanMX* disruption cassette, Klox, but did not show a DNA fragment when using a reverse primer annealing in the *ARE2* gene, KA2rev, respectively.

Colony- PCR reaction mix:

~ 3 µL	Pellet *S. cerevisiae*
19 µL	deion. H_2O
25 µL	Maxima Green PCR Master Mix
2.5 µL	forward primer (K2up 10 µM)
2.5 µL	reverse primer (Klox 10 µM or K2rev)
52 µL	total volume

PCR cycling conditions:

95°C/4 min-(95°C/30 s-50°C/30 s-72°C/60 s) x40 -72°C/10 min -4°C/∞

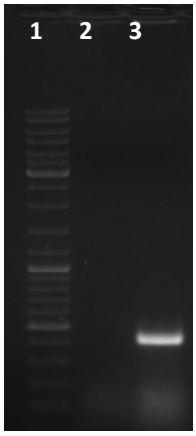

Figure 33: Colony PCR fragments of *are2* verification

Table 24: Lane description of Figure 33.

Lane	Description	Volume [µL]	Expected bands [bp]
1	Gene Ruler DNA Ladder Mix	5	-
2	Δ*are2* transformant 1: K2up + K2rev	15	0
3	Δ*are2* transformant 1: K2up+Klox	15	384

4.2.5 Construction of the *are1are2* strain

The *ARE1* disruption cassette was at first constructed as already described for all other disruption cassettes (see Figure 14) and the linear DNA fragment was then transformed into the verified *are2* strain. Several rounds of transformation yielded transformants that grew on selective SD-his plates without proper disruption of the *ARE1* gene, due to ectopic integration of the disruption cassette. This situation was confirmed by lipid extraction and analysis of those extracts by TLC (Figure 34 and Figure 35). Upon charring of lipids, the TLC plate still showed steryl esters which should not be detectable in a genuine *are1are2* double knockout strain (Zweytick, 2000).

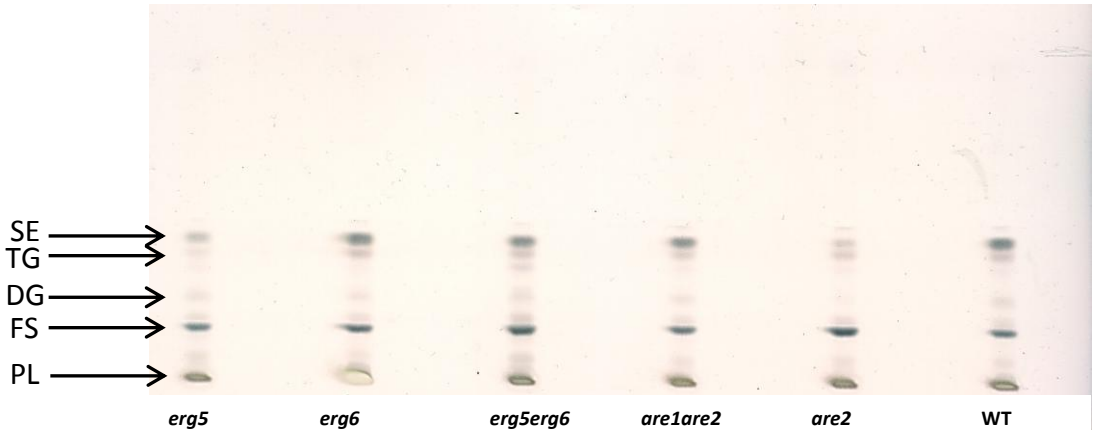

Figure 34: TLC analysis of lipid extracts of several strain constructs showing steryl esters (SE), triglycerides (TG), diglycerides (DG), free sterols (FS) and phospholipids (PL)

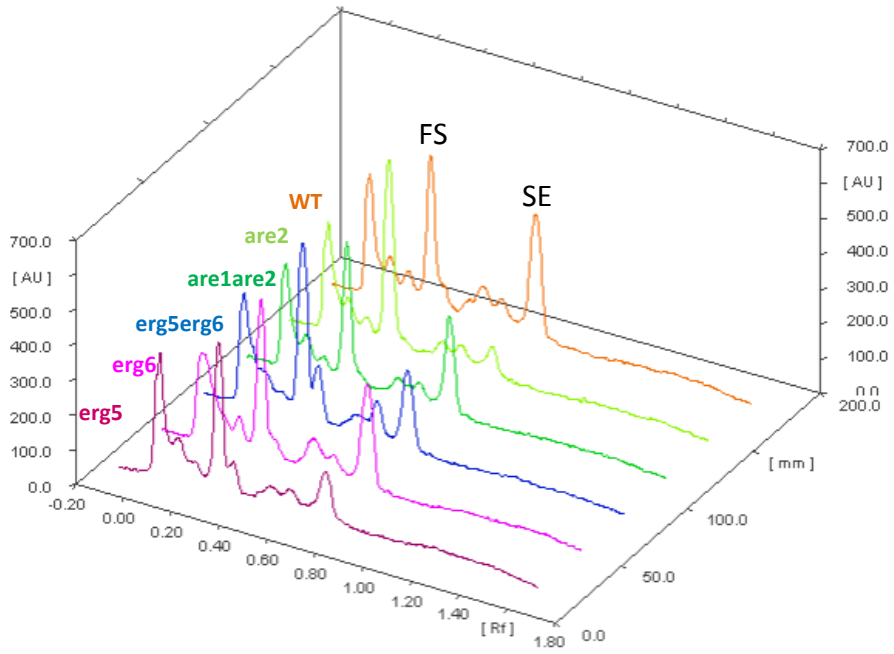

Figure 35: TLC scan of silica plate shown in Figure 34.

The reason for frequent unspecific integration of the *are1*::*HIS3* cassette were most likely gene conversions between the *HIS3* gene used as marker gene and the *his3Δ1* allele of the recipient yeast strain CEN.PK2-IC, which is not completely deleted for this particular marker gene, but carries only an internal deletion of 187 bp (Daniel, 2006).

Our suspicions were supported by colony PCR results with primers annealing upstream and downstream of the *erg5*, *erg6*, *are1* and *are2* locus in the corresponding double knockout strains. Already the size of those fragments told whether the genes *ERG5*, *ERG6*, *ARE1* and *ARE2* were disrupted with the desired selectable marker genes or were still intact. To be on the safe side about the nature of those DNA fragments, they were all sequenced. The sequences confirmed the colony PCR results.

Colony- PCR reaction mix:

~ 3 µL	Pellet *S. cerevisiae* (*erg5erg6* or *are1are2*)
19 µL	deion. H_2O
25 µL	Maxima Green PCR Master Mix
2.5 µL	forward primer (K1A1; KA2up; K1E5; K1E6)
2.5 µL	reverse primer (K2exA1; KA2down; K2exE5; K2exE6)
52 µL	total volume

PCR cycling conditions:

for DC check of *erg6* and *are1*:

95°C/4 min-(95°C/30 s-55°C/30 s-72°C/1.5 min) x40 -72°C/7 min -4°C/∞

for DC check of *erg5* and *are2*:

95°C/4 min-(95°C/30 s-50°C/30 s-72°C/60 s) x40 -72°C/10 min -4°C/∞

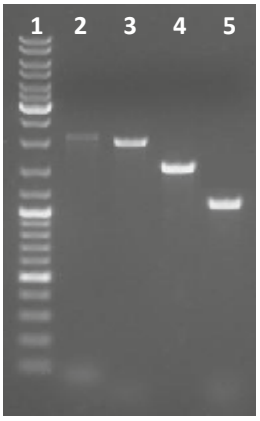

Figure 36: Disruption cassette check of all knockout strains

Table 25: Lane description of Figure 36

Lane	Description	Volume [µL]	Expected bands [bp]	Visible bands [bp]
1	Gene Ruler DNA Ladder Mix	5	-	
2	are1 DC check	20	952	2100
3	are2 DC check	20	1920	1920
4	erg5 DC check	20	1534	1534
5	erg6 DC check	20	1075	1075

The DNA fragments of the *are1::HIS3* and *are2::loxP-kanMX-loxP* loci were re-checked with two different primer combinations, the PCR mix was the same as mentioned above.

Primer combination 1: K1A1+ K2A1→ binding upstream and in the *ARE1* DC

Primer combination 2: K1A1+ K2exA1→ binding upstream and downstream of the *ARE1* DC

Primer combination 3: KA2up+ KA2down→ binding up- and downstream of the *ARE2* DC

Primer combination 4: KA2up+ Klox→ binding upstream and in the *ARE2* DC

PCR cycling conditions:

for primer combination 1 and 2:

95°C/4 min-(95°C/30 s-55°C/30 s-72°C/1.5 min) x40 -72°C/7 min -4°C/∞

for primer combination 3 and 4:

95°C/4 min-(95°C/30 s-50°C/30 s-72°C/1.5 min) x40 -72°C/7 min -4°C/∞

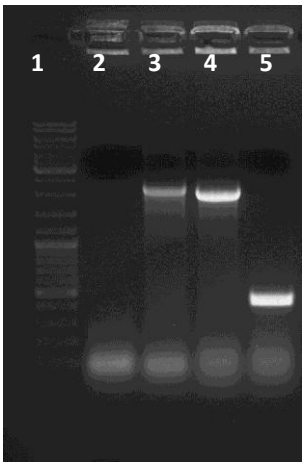

Figure 37: *are1* and *are2* disruption cassette check

Table 26: Lane description of Figure 37

Lane	Description	Volume [µL]	Expected bands [bp]	Visible bands [bp]
1	Gene Ruler DNA Ladder Mix	5	-	-
2	*are1* DC check primer comb. 1	20	400	-
3	*are1* DC check primer comb. 2	20	952	2100
4	*are2* DC check primer comb. 3	20	1920	1920
5	*are2* DC check primer comb. 4	20	384	384

The size of the DNA fragments already showed that the *HIS3* cassette was not correctly integrated at the *are1* locus and sequencing proved that the *ARE1* gene was still functional. In order to increase the chance for correct integration events at the *ARE1* locus, longer homologous fragments corresponding to the flanking regions of *ARE1* coding sequence were required (see page 31)

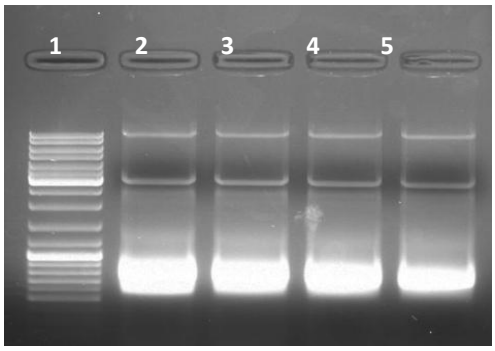

Figure 38: *Are1* disruption cassette separated over a standard agarose gel

Table 27: Lane description of Figure 32

Lane	Description	Volume [µL]	Expected bands [bp]
1	Gene Ruler DNA Ladder Mix	10	(not visible below 500 bp)
2	*ARE1* disruption cassette no.1	50	740
3	*ARE1* disruption cassette no.2	50	740
4	*ARE1* disruption cassette no.3	50	740
5	*ARE1* disruption cassette no.4	50	740

For the elongation of this disruption cassette, additional upstream- and downstream fragments of *ARE1* were amplified by colony PCR of a wild-type strain.

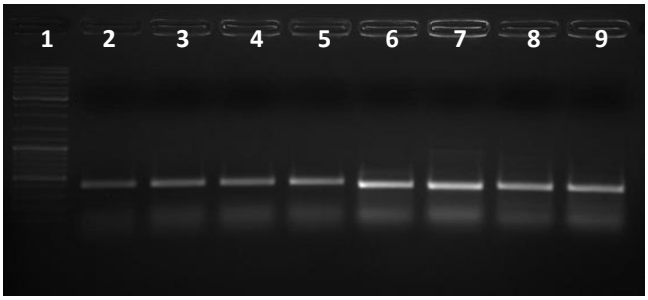

Figure 39: Upstream and downstream fragments of *ARE1* for the elongation of the *ARE1* disruption cassette

Table 28: Lane description of Figure 39

Lane	Description	Volume [µL]	Expected bands [bp]
1	Gene Ruler DNA Ladder Mix	10	-
2	*ARE1* upstream fragment	50	400
3	*ARE1* upstream fragment	50	400
4	*ARE1* upstream fragment	50	400
5	*ARE1* upstream fragment	50	400
6	*ARE1* downstream fragment	50	350
7	*ARE1* downstream fragment	50	350
8	*ARE1* downstream fragment	50	350
9	*ARE1* downstream fragment	50	350

Finally, the long disruption cassette was amplified as described in section 3.1.3.

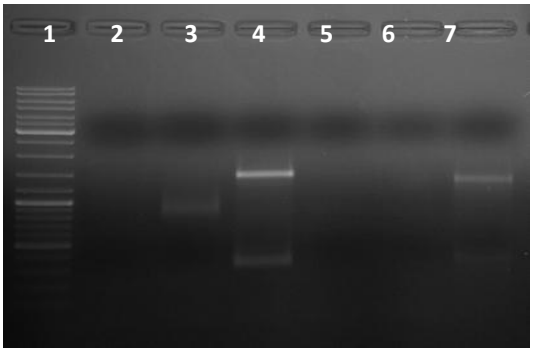

Figure 40: Elongated *ARE1*disruption cassette

Table 29: Lane description of Figure 40

Lane	Description	Volume [µL]	Expected bands [bp]	Visible bands [bp]
1	Gene Ruler DNA Ladder Mix	10	-	-
2	*ARE1* long disruption cassette	50	1483	-
3	*ARE1* long disruption cassette	50	1483	-
4	*ARE1* long disruption cassette	50	1483	1483
5	*ARE1* long disruption cassette	50	1483	-
6	*ARE1* long disruption cassette	50	1483	-
7	*ARE1* long disruption cassette	50	1483	1483

To obtain enough material for several transformation events, the elongated disruption cassette was eluted from a preparative gel with “Wizard” kit and used as a template for further amplifications with identical PCR conditions.

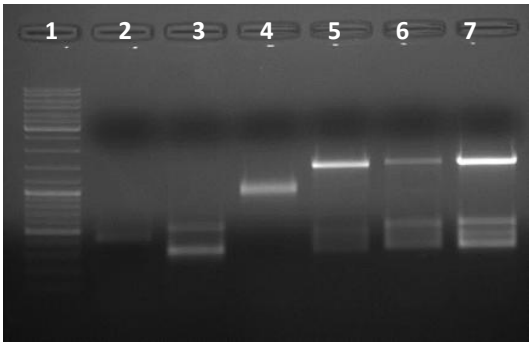

Figure 41: Amplification of elongated disruption cassette

Table 30: Lane description of Figure 41

Lane	Description	Volume [µL]	Expected bands [bp]	Visible bands [bp]
1	Gene Ruler DNA Ladder Mix	10	-	-
2	*ARE1* long disruption cassette	50	1483	400
3	*ARE1* long disruption cassette	50	1483	300+600
4	*ARE1* long disruption cassette	50	1483	1100
5	*ARE1* long disruption cassette	50	1483	1483
6	*ARE1* long disruption cassette	50	1483	1483
7	*ARE1* long disruption cassette	50	1483	1483

Disruption cassettes of 1483 bp, as calculated, were eluted and 750 ng were used for the transformation into the *are2* knockout strain.

Transformation efficiency was very low. Several transformations did not yield any transformants. One transformation yielded three transformants, which were streaked out onto YPD and tested by Colony PCR.

PCR reaction mix:

~ 3 µL	Pellet *S. cerevisiae*
19 µL	deion. H_2O
25 µL	Maxima Green PCR Master Mix
2.5 µL	forward primer (K1A1 10 µM)
2.5 µL	reverse primer (K2exA1 10 µM)
2.5 µL	dNTP mix of 2 mM each (K2exA1 10 µM)
52 µL	total volume

PCR cycling conditions:

95°C/4 min-(95°C/30 s-55°C/30 s-72°C/2 min) x30 -72°C/10 min -4°C/∞

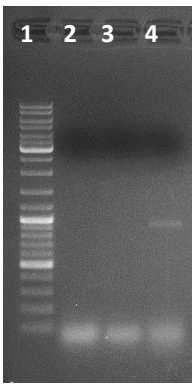

Figure 42: Colony PCR fragment of *are1are2* verification

Table 31: Lane description of Figure 42

Lane	Description	Volume [µL]	Visible bands [bp]
1	Gene Ruler DNA Ladder Mix	10	-
2	*Δare1Δare2* transformant 1	50	-
3	*Δare1Δare2* transformant 2	50	-
4	*Δare1Δare2* transformant 3	50	952

Transformant no.3 showed the expected band of 952 bp as calculated for a disrupted *ARE1* gene upon insertion of the *HIS3* marker. The next step was the verification of the *are1are2* double knockout by lipid analysis as this strain should not produce any steryl esters. Lipids were extracted by the method of Folch and the extracts were analysed by TLC and subsequent TLC scan at 275 nm, and finally charring of all lipids.

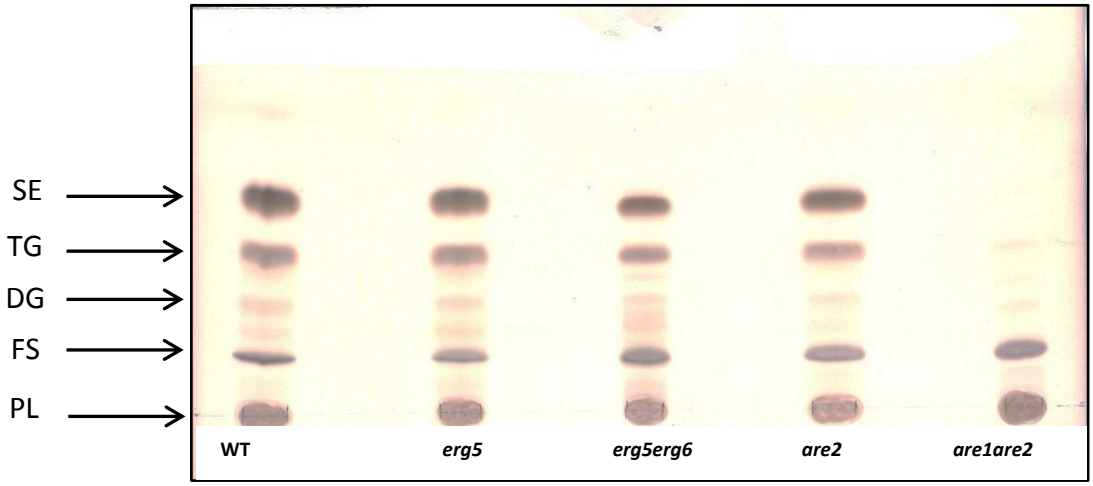

Figure 43: Charred TLC of all constructed strains compared to the wild-type (WT) showing steryl esters (SE), triglycerides (TG), diglycerides (DG), free sterols (FS) and phospholipids (PL)

The *are1are2* double knockout strain did not have any detectable steryl esters as shown by TLC (Figure 43) and had hardly any triglycerides either. Results were visualized by a TLC scan as well (Figure 44)

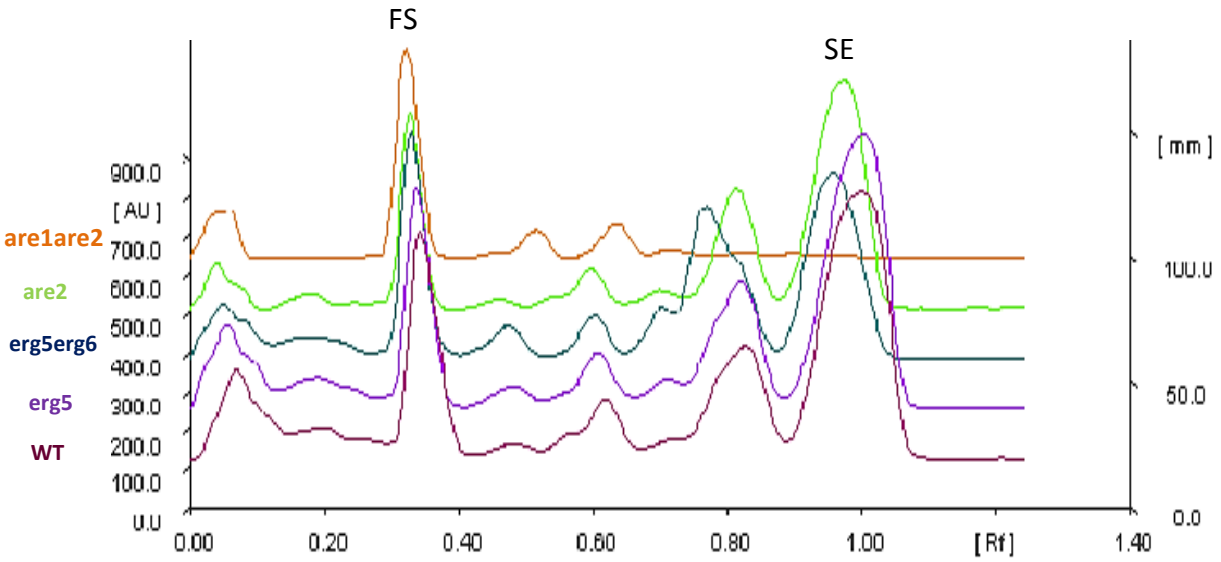

Figure 44: TLC scan of constructed strains compared to the wild-type

Therefore, TLC analysis confirmed the expected phenotype of a true *are1are2* double knockout strain. Therefore construction of *MATα erg5erg6* and *MATa are1are2* strains was supposed to be achieved.

4.2.6 Mating of *erg5erg6* x *are1are2*

The *MATα erg5erg6* double knockout strain was crossed with the *MATa are1are2* double knockout strain, to create the heterozygous diploid *erg5erg6are1are2* strain. The mating was regarded as successful because of growth of this quadruple mutant on SD-his-trp plates, the *HIS3* gene deriving from the *are1* disruption and the *TRP1* gene from the *erg6* disruption.

The diploid *erg5erg6are1are2* strain was sporulated for nearly two weeks before a few tetrads were detected. Compared to wild-type strains, which usually take about three to five days to sporulate, this was quite a long timespan.

The next logical step would have been the dissection of ascospores and the characterization of the desired haploid *erg5erg6are1are2* strain, but because of the result shown in the next section this would not have made any sense.

4.2.7 Growth of constructed strains and wild-types on selective plates

All strain constructions were tested on several selective plates to check the markers that were used for gene disruptions and also the markers that should still be available. For this purpose the strains *erg5*, *erg5erg6*, *are2*, *are1are2* as well as the diploid wild-type strain CEN.PK2 and the two haploid wild-type strains with opposite mating types, CEN.PK2-IC and CEN.PK2-ID, were streaked onto SD-trp, SD-his, SD-leu-trp, SD-ura and YPD+ G418 plates according to the template shown in Figure 45.

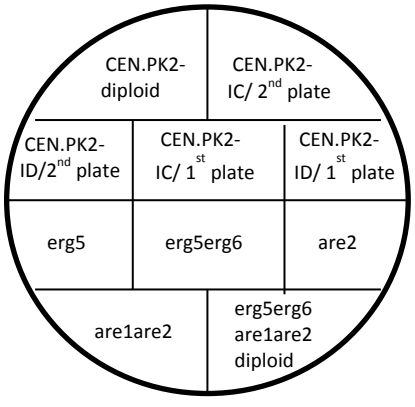

Figure 45: Template for selective plates

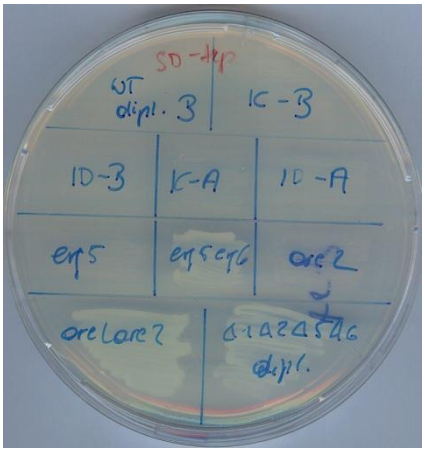

Figure 46: Test of strain constructions on SD-trp plate

It was expected that only the *erg5erg6* double knockout and the heterozygous diploid strains should be able to grow on SD-trp plates because of the disruption of *ERG6* with the selective marker tryptophan. But as can be seen in Figure 46, also the *are1are2* double knockout grew under this condition.

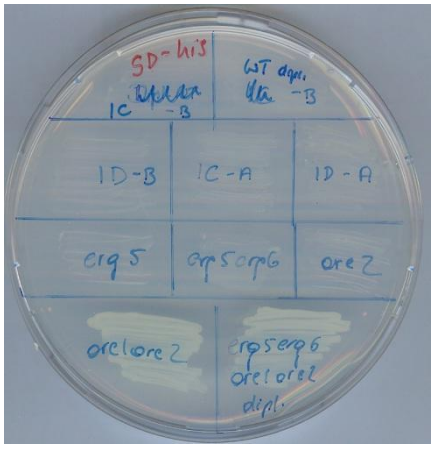

Figure 47:Test of strain constructions on SD-his plate

Only the *are1are2* strain carrying the *are1*::*HIS3* allele and the heterozygous diploid grew on SD-his plates (Figure 47). This was the expected result. As SD-his was the only selective plate necessarily used to test for disruption of *ARE1* in the *are2* knockout strain, it was believed until this series of growth tests that the *are1are2* strain would be useful for further work.

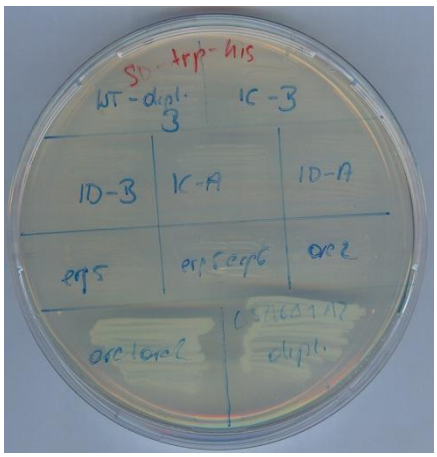

Figure 48: Test of strain constructions on SD-his-trp plate

As a functional *TRP1* gene should derive from *ERG6* disruption and a functional *HIS3* gene from *ARE1* disruption only, the combination of those two strains in the heterozygous diploid should be able to grow on SD-trp-his plates. But as Figure 48 shows, also the *are1are2* strain grew perfectly well on this selective plate supporting the results on the SD-trp plate.

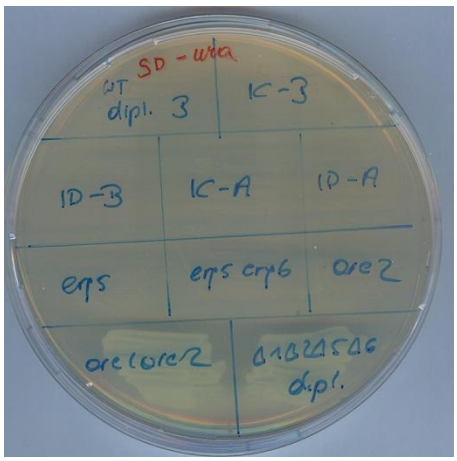

Figure 49: Test of strain constructions on SD-ura plate

The most surprising and unexplainable result of all was that the *are1are2* double knockout strain even grew on SD-ura plates even though the URA3 marker was not used for any transformation or any other experiment and is obviously still available in the *are2* knockout strain as well as in the initial wild-type strain CEN.PK2-IC (Figure 49).

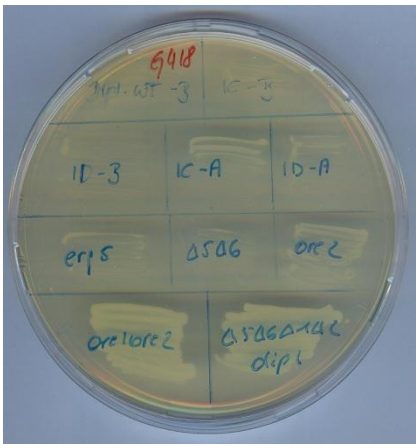

Figure 50: Test of strain constructs on YPD+ G418 plates.

The last selective plate, YPD+ G418, did not show any surprises. Only the *are2* and the *are1are2* strains and the heterozygous diploid grew as expected (Figure 50). Having a superficial look, it seems as if the haploid wild-type strain CEN.PK2-IC also grew on this plate. However, using too much cell material on a relatively small area of agar erroneously suggested growth. This becomes obvious when compared to the *are1are2* strain which grew indeed.

4.3 SITE SPECIFIC MUTAGENESIS

The complete deletion of *ERG6* in an *erg5* background was one strategy to create a strain that produces high amounts of cholesta-5,7,24-trienol. However, Erg6p is apparently part of a larger complex described by Mo et al. (2004). Therefore, it appeared to be an attractive idea to inactivate rather than delete *ERG6* to remain a functional Erg protein complex. The most obvious advantage of this strategy seemed to be that both enzymes, Erg2p and Erg3p, involved in the described complex and responsible for the conversion of zymosterol to cholesta-5,7,24-trienol, might have a better chance to sustain sterol flux toward cholesta-5,7,24-trienol when this complex is properly assembled.

Nine different *ERG6* mutants were created to see if this affects the activity of Erg6p and consequently the ratio of zymosterol to cholesta-5,7,24-trienol in total cellular sterols. Seven of these variants were single-point mutations in *ERG6* coding for the SAM (S-adenosylmethionine, Figure 52) binding domains which is distinguished by four conserved amino acids (shown in red in Figure 51). Two further mutations were introduced in the codon for aspartic acid at amino acid position 152, which is often a conserved amino acid involved in co- factor binding. SAM acts as methyl group donor for C-24-sterol methyl-transferase (Erg6p) and is therefore an essential cofactor for the functionality of this enzyme. The methyl group attached to the sulphur atom is chemically highly reactive, allowing transmethylation to an acceptor substrate.

Pos.	367	370	373	376	379	382	385	388	391	394	397	400
codons	GTT	CTC	GAC	GTT	GGT	TGT	GGT	GTT	GGG	GGC	CCA	G
aa	V	L	D	V	G	C	G	V	G	G	P	

Figure 51: Detail of the *ERG6* gene coding region for SAM binding; conserved amino acids shown in red

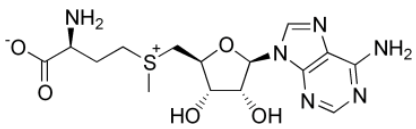

Figure 52: S-adenosylmethionine (Wikipedia)

Figure 51 shows the detail of the *ERG6* sequence fragment in which seven of nine mutations were introduced. Table 32 gives an overview of all mutations introduced. One approach was

to change the four amino acids to totally different ones, like exchanging glycine to tryptophan, i.e. a very small amino acid replaced by a bulky one. This might abrogate protein structure leading to dysfunctionality.

Another idea was to maintain the general structure of Erg6p by changing aminoacids to similar but slightly larger other ones, i.e. glycine to alanine or isoleucine, which should create variants that can still be embedded into the functional Erg complex but would not confer methyl-transferase activity any more. After transformation of the PCR products into electocompetent *E. coli* cells and isolation of plasmids possibly carrying the desired mutations, several plasmids of each transformation were sequenced by AGOWA. The results were interpreted using the software „seqman"of DNAStar. In all cases about five plasmids had to be sequenced to find a positive mutant. E6_4 could not be obtained even after several repetitions of the mutagenesis and transformation events, suggesting that it is not feasible to introduce four mutations concurrently within a reasonable number of testable plasmids. The sequencing results showed, however, that two deletions of nucleotides were introduced so that also this mutant was characterized.

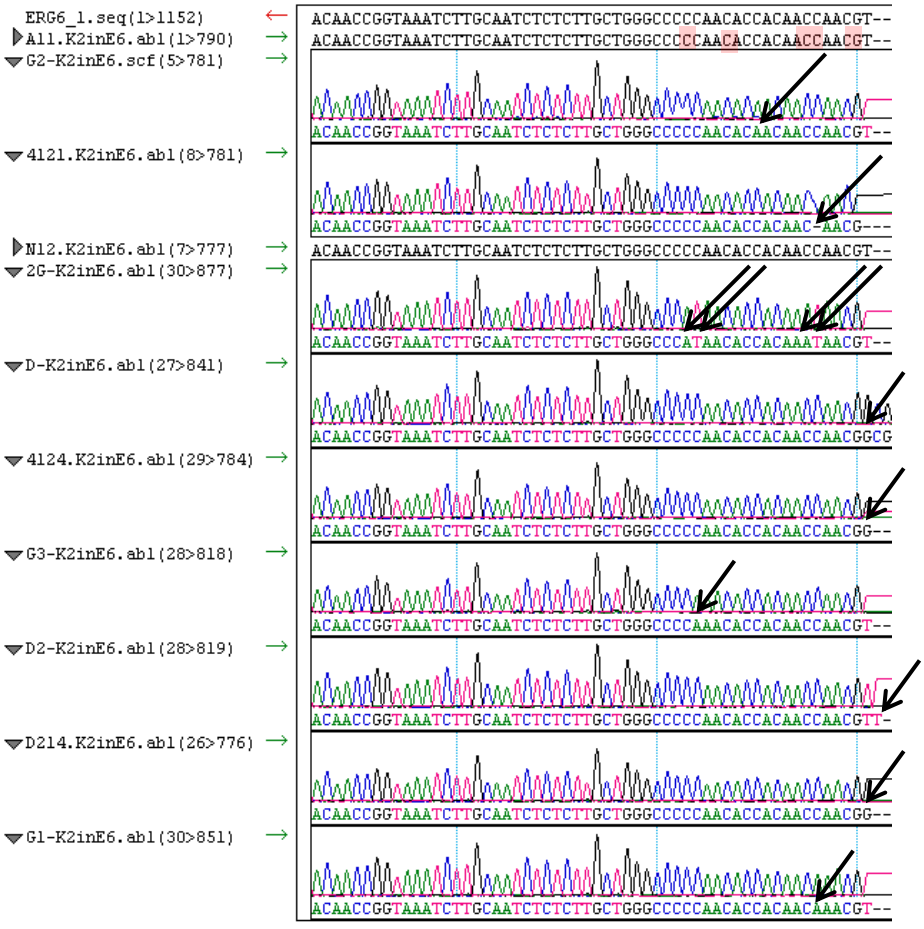

Figure 53: "Seqman" analysis of sequenced plasmids carrying the desired mutations in the SAM motif

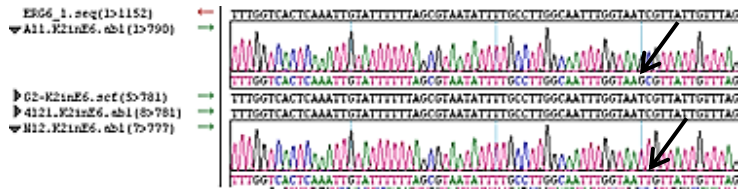

Figure 54: "seqman" analysis of sequenced plasmids carrying mutations at aa position 152

The plasmids carrying confirmed mutations were transformed into the *erg5erg6* double knockout strain. Transformants were selected on SD-ura plates, characterized by SDS-PAGE and Western Blot for Erg6p expression and stability. Subsequently, the strains were analysed by GC/MS regarding their sterol patterns to give evidence for Erg6p activity.

Table 32: Overview of Erg6 variants

Mutant name	Codon changed	aa changed	Nucleotide position in *ERG6*
E6_4 (variant not obtained)	GAC→ GCC GGT→ GCT GGT→ GCT GGG→ GCG	asp → ala gly→ ala gly→ ala gly → ala	374 380 386 392
E6_2G	GGT→ATT GGG→ATG	gly → ile gly→ ile	379, 380 391, 392
E6_D	GAC→ GCC	asp → ala	374
E6_D2	GAC→AAC	asp → asn	373
E6_G1	GGT→GTT	gly → cys	380
E6_G2	GGT→GTT	gly → cys	386
E6_G3	GGG→TGG	gly→ trp	391
E6_D152A	GAT→ GCT	asp → ala	455
E6_D152N	GAT→AAT	asp → asn	454

4.3.1 SDS-PAGE and Western Blot

Besides all Erg6 variants also the *erg5erg6* double knockout strain without and with one of two reference plasmids was analysed. LV denotes an empty expression vector only with the selective marker gene *URA3*, and pFL44-*ERG6* carries the functional *ERG6* gene. The latter vector was used for site-directed mutagenesis to generate the Erg6 variants.

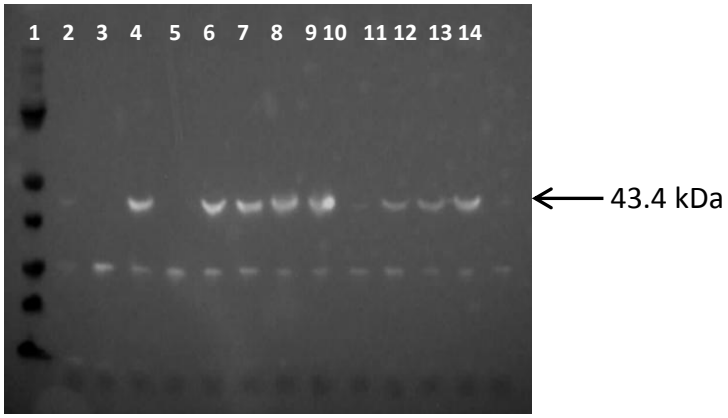

Figure 55: Western Blot of Erg6 variants

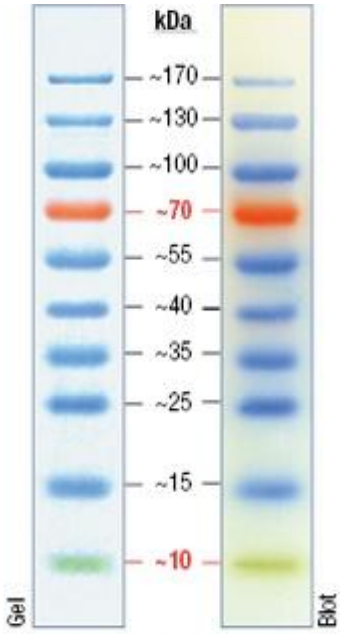

Figure 56: PageRuler ™ Prestained Protein Ladder

Table 33: Lane description of Figure 55

Lane	Sample
1	Prestained Protein Ladder 10 µL
2	WT
3	*erg5erg6*
4	*erg5erg6*+pFL44-*ERG6*
5	*erg5erg6*+LV
6	D152A
7	D152N
8	G1
9	G2
10	2G
11	G3
12	D
13	D2
14	4

As can be seen in Figure 55, all mutants express Erg6p but at different levels. Compared to the reference strain with a functional *ERG6* gene in lane 4, the variants from lane 6 to 9 show the best expression, and hardly any protein was detected for the mutants E6_G2 and E6_4. However, it has to be considered that the G:Box detection always exposes optimally

for the strongest signal (Figure 55), weak signals appear to be weaker than they actually are, which is especially obvious for the wild-type strain.

4.3.2 GC/MS measurements

All GC/MS experiments were performed three-fold at different time points. Several mutations successfully inactivated *ERG6.* Some variants were only partly inactive. Unfortunately, so far no variant had the desired effect of total inactivation of *Erg6* and a simultaneously shift in the zymosterol/ cholesta-5,7,24-trienol ratio toward the trienol. Zymosterol was still accumulating in high amounts in every Erg6 variant strain.

erg5erg6+ pFL44-*ERG6*

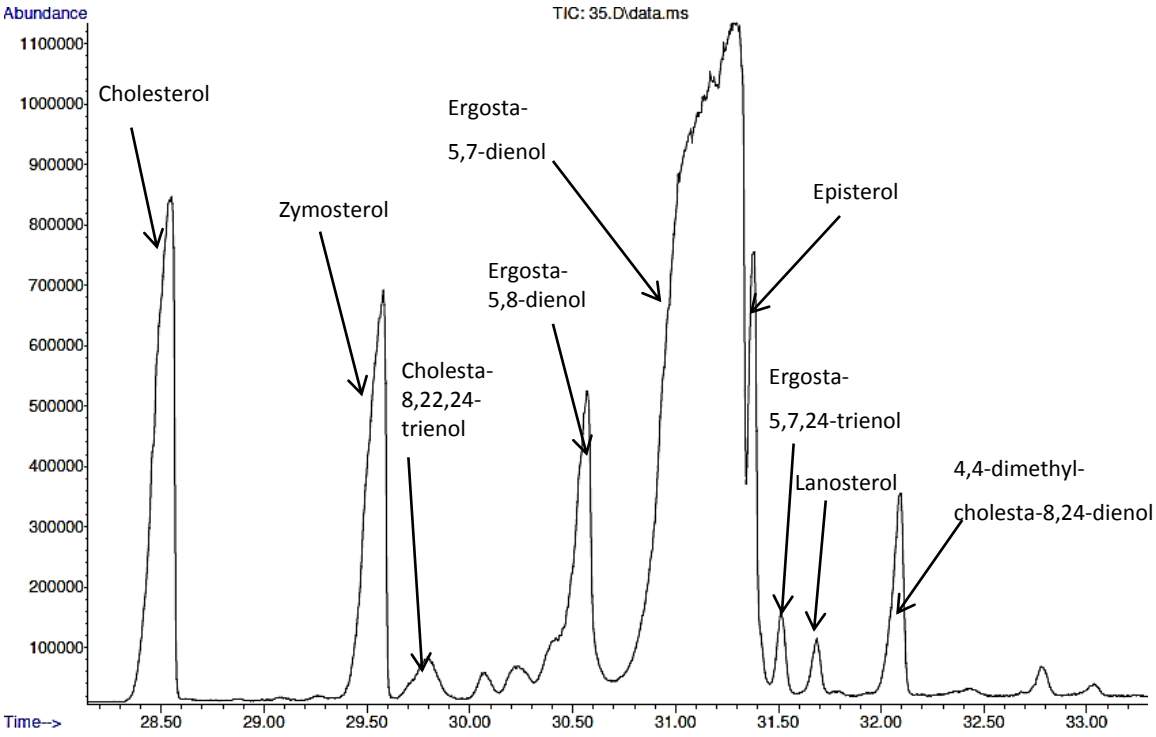

Figure 57**: GC/MS analysis of the reference strain erg5erg6+pFL44-ERG6**

Because of the functional *ERG6* gene on the plasmid that was transformed into the *erg5erg6* double knockout strain, this reference strain has a sterol pattern identical to the *erg5* knockout strain (Figure 25).

E6_LV

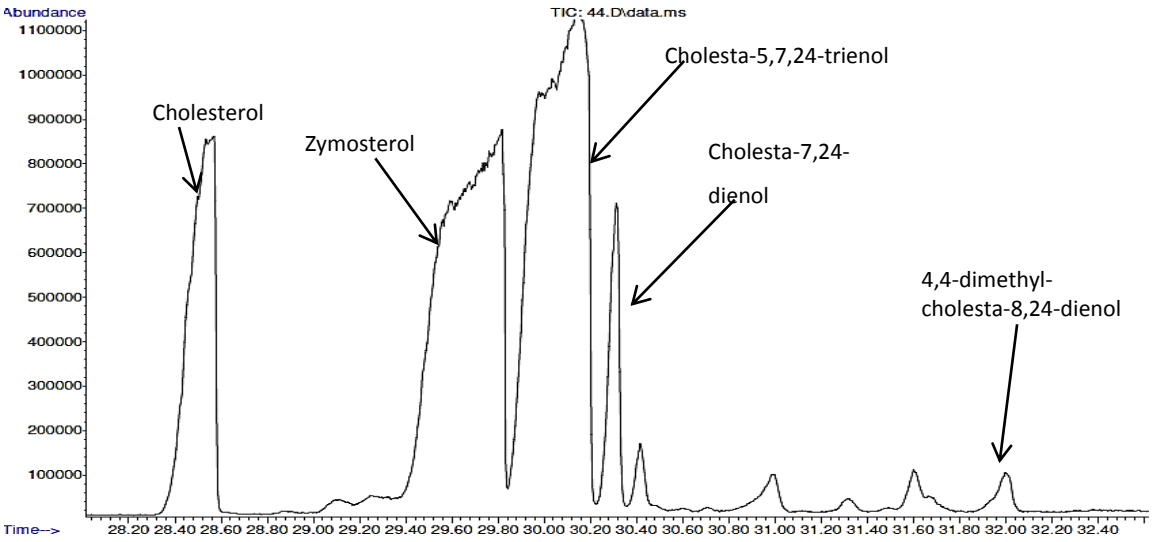

Figure 58: GC/MS analysis of the reference strain *erg5erg6*+LV

The reference strain *erg5erg6* with an empty plasmid just containing an *URA3* marker was expected to look exactly as the *erg5erg6* strain, which was confirmed by GC/MS analysis.

Variant E6_G3

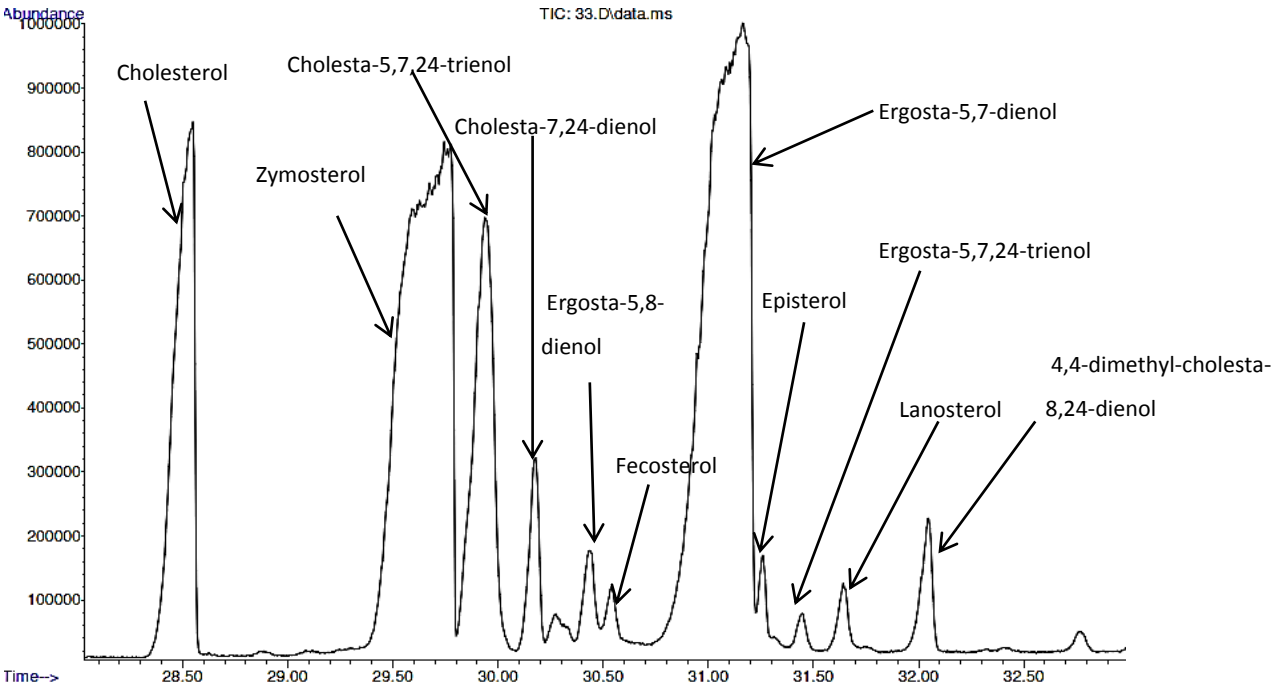

Figure 59: GC/MS analysis of Mutant E6_G3

The variant E6_G3 was created by exchanging the amino acid glycine for tryptophan at position 391 in the SAM motif. In general, glycine usually serves as a „turning point“for protein structures, so that the exchange of this small amino acid to a very big one might end

in the total destruction of the Erg6p structure. However, the chromatogram shows that ergosta-5,7-dienol is the main peak derived from the *erg5* knockout (Figure 25), followed by zymosterol and cholesta-5,7,24-trienol. The accumulation of the latter is typical of the *erg5erg6* double knockout strain (Figure 30) but ergosta-5,7-dienol would not be formed if ERG6p was inactivated, which leads to the conclusion that *ERG6* is still partly active.

E6_G2

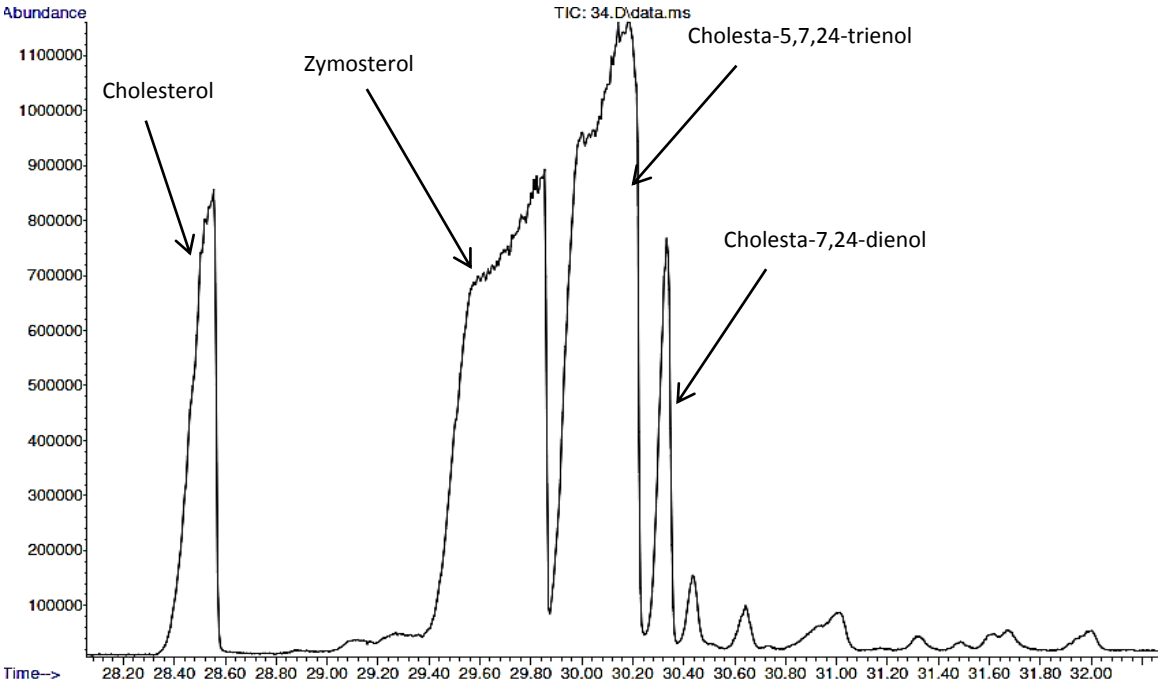

Figure 60: GC/MS analysis of variant E6_G2

This chromatogram represents the total inactivation of *ERG6* in this variant but without significant change of the sterol pattern compared to the deletion of *ERG6* (Figure 30).

E6_G1

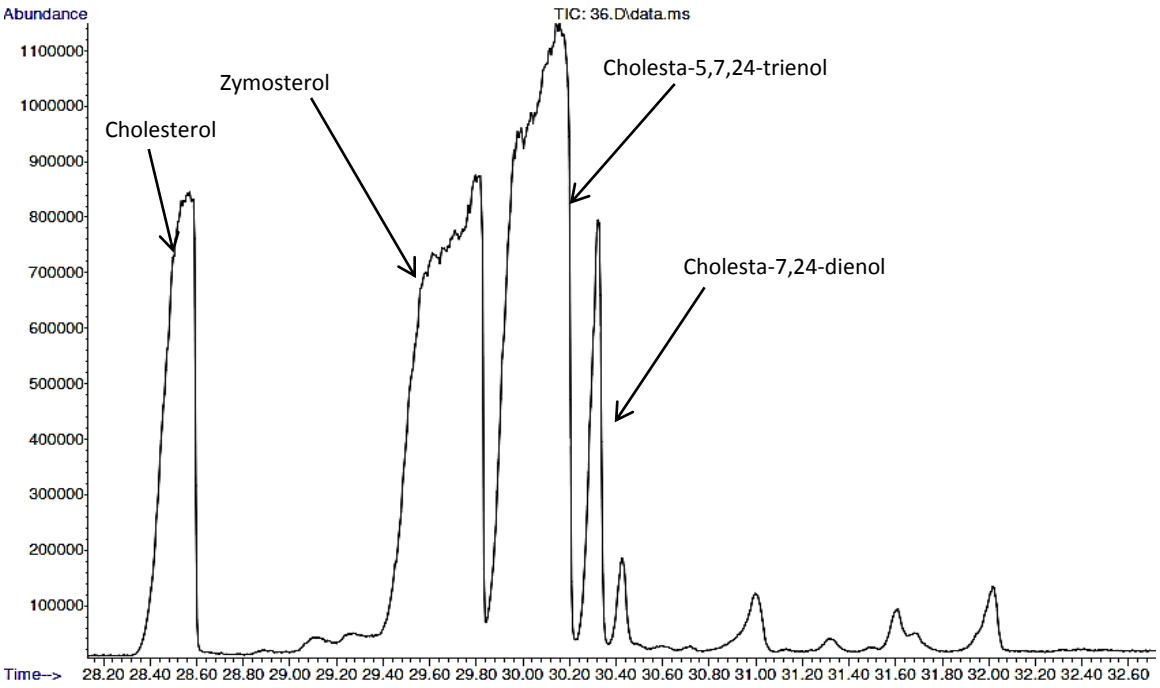

Figure 61: GC/MS analysis of the mutant E6_G1

This Erg6 variant yielded the same sterol pattern as mutant E6_G2, also without significant change of the zymosterol/ cholesta-5,7,24-trienol ratio despite successful inactivation of *ERG6*.

E6_D2

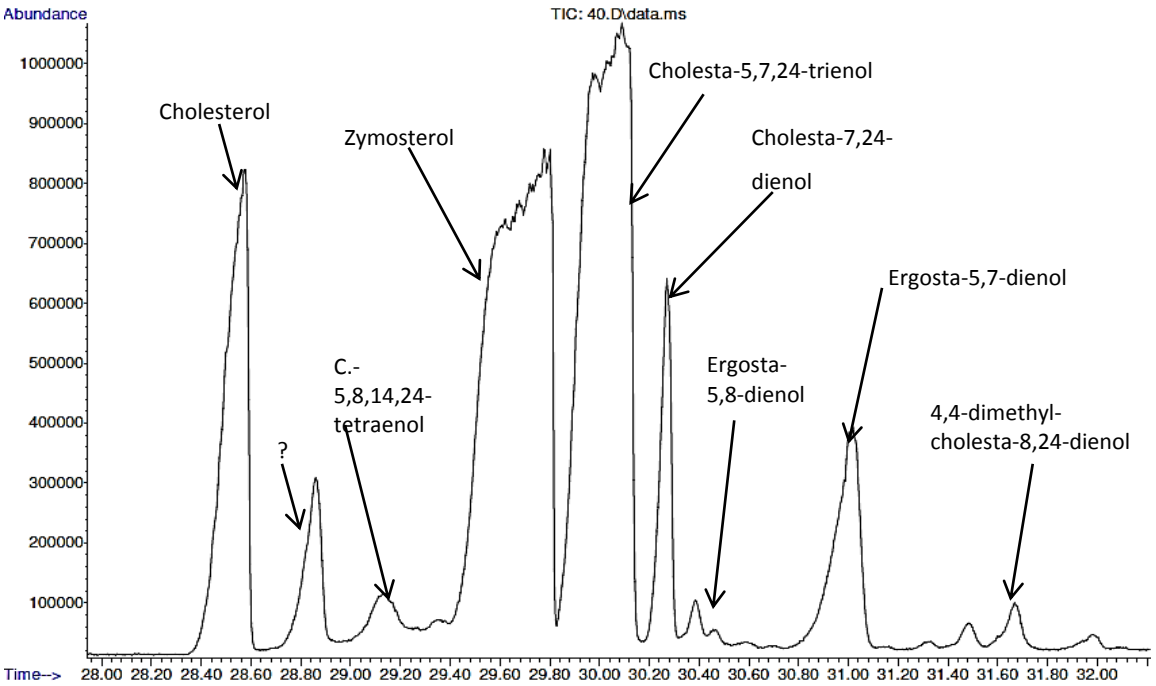

Figure 62: GC/MS analysis of the variant E6_D2

The sterol pattern indicated that there is Erg6p activity left because of the ergosta-5,7-dienol and ergosta-5,8-dienol peaks. This strain accumulated relevant amounts of cholesta-5,7,24-trienol and zymosterol, however at the same ratio as in the *erg5erg6* double knockout strain.

E6_D

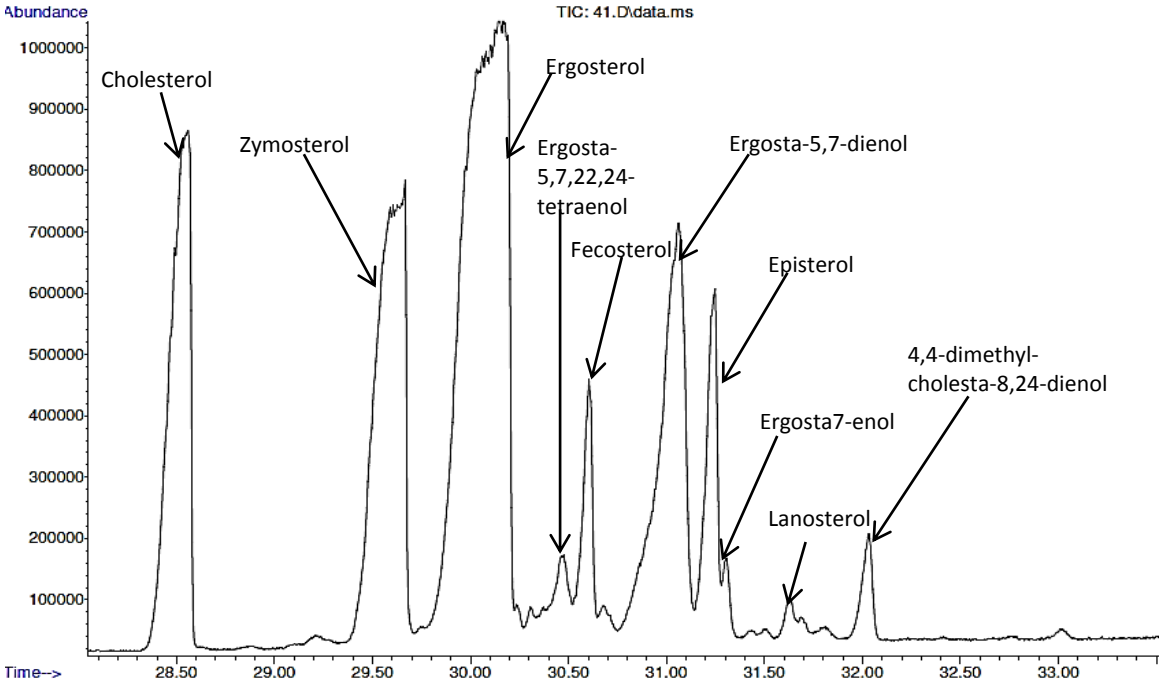

Figure 63: GC/MS analysis of the variant E6_D

There is no obvious explanation for the spectrum of E6_D with ergosterol as main sterol. Furthermore, the remaining sterol pattern looks like a wild-type spectrum with active *ERG5* and *ERG6* genes. Thus, a confusion of strains appears to be the most likeable explanation

E6_2G

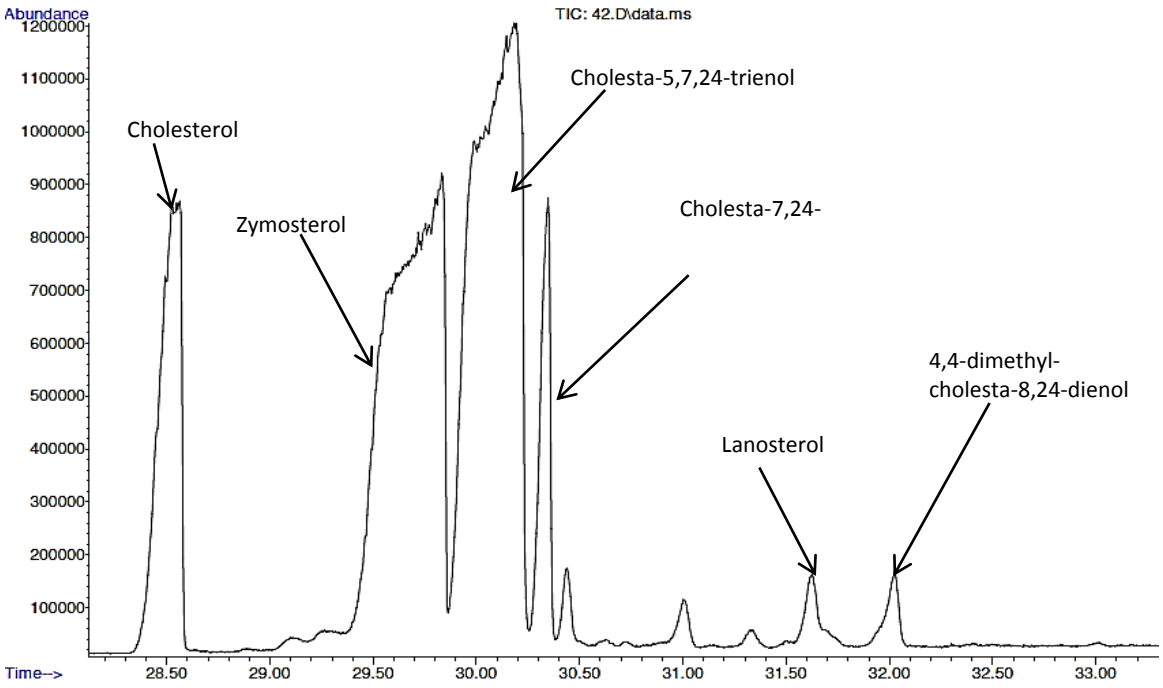

Figure 64: GC/MS analysis of the variant E6_2G.

This spectrum shows again high similarity to the spectrum of the *erg5erg6* double knockout strain suggesting that variant E6_2G is inactive.

E6_4

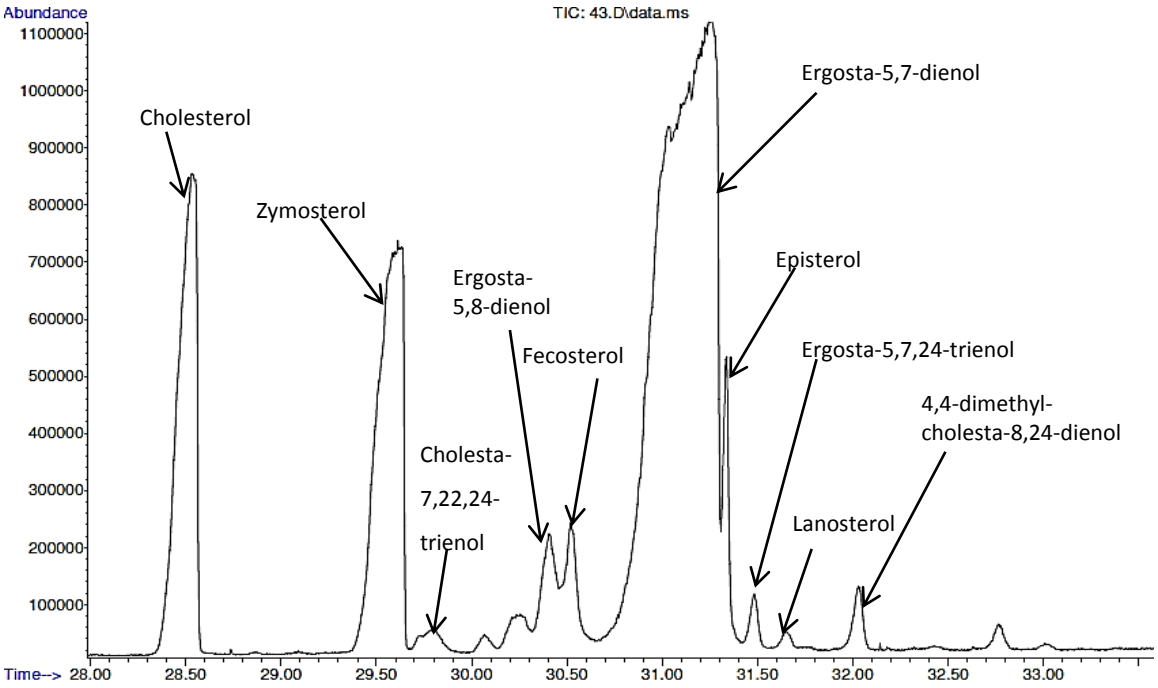

Figure 65: GC/MS analysis of the variant E6_4

This spectrum is similar to the *erg5* knockout strain (Figure 25) showing that Erg6p is fully functional even with an apparent nucleotide deletion that should normally lead to a frame shift and subsequently to an inactivation of *ERG6*. This phenomenon awaits a reasonable explanation

E6_D152N

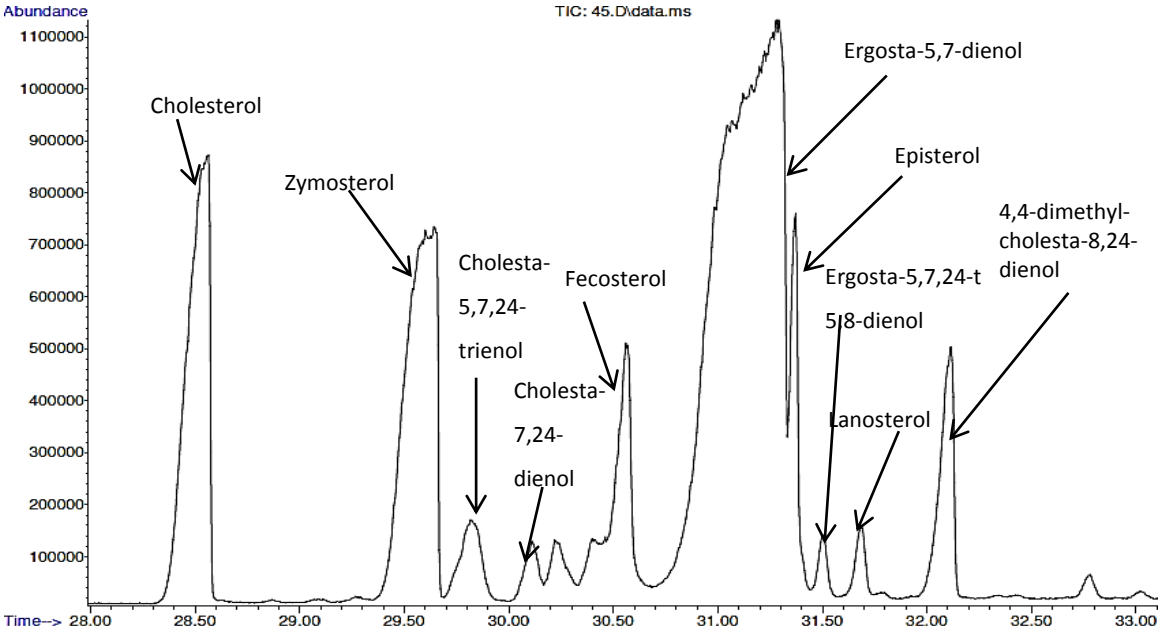

Figure 66: GC/MS analysis of the variant E6_D152N

The sterol pattern is comparable to the one of variant E6_G3 despite a lower amount of cholesta-5,7,24-trienol and zymosterol. This Erg6 variant is therefore only partially inactivated.

E6_D152A

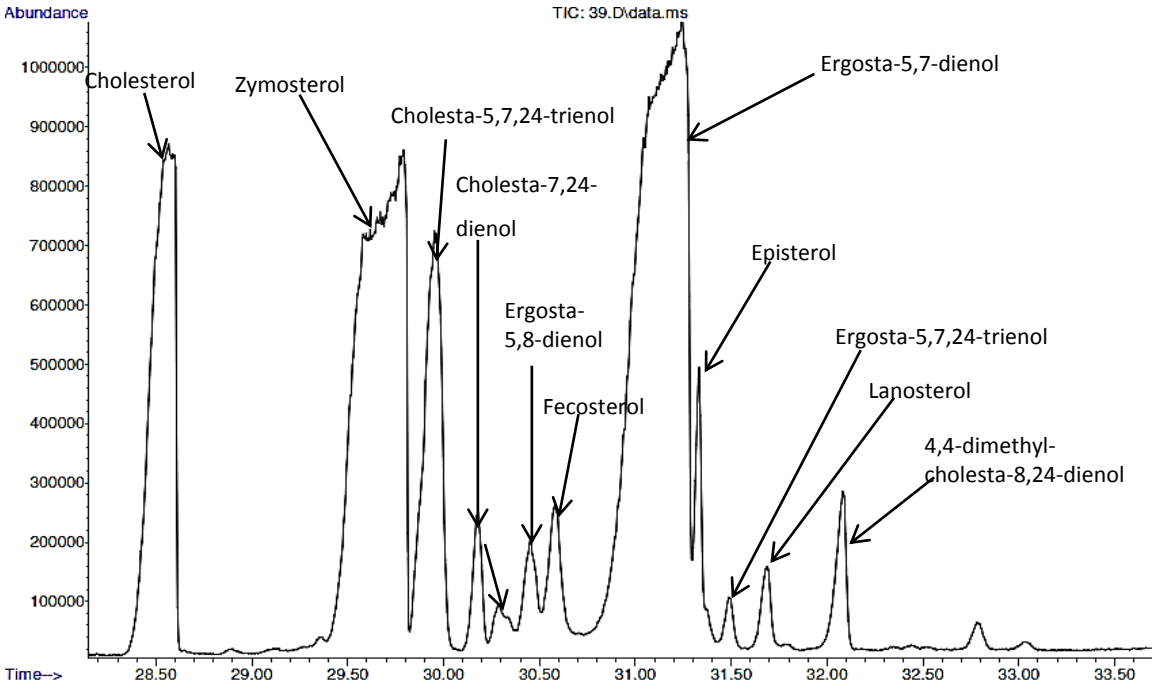

Figure 67: GC/MS analysis of variant E6_D152A

This is an interesting and promising mutant because of the high amount of zymosterol and cholesta-5,7,24-trienol although it is quite obvious that Erg6p is at least partly active, which can be seen by the dominant ergosta-5,7-dienol peak and several precursors that would not be detected if *ERG6* was inactive.

5 DISCUSSION

5.1 Check for *HAP1* mutations

The first part of my work was to check the CEN.PK2 strain background as well as a strain provided by DSM NP, SC0458 for an unwanted transposon insertion in the *HAP1* gene.

As Tamura et al. (2004) showed many wild-type strains contain a *Ty1* insertional mutation which leads to decreased expression of ergosterol-related genes. Given examples are the transcriptional regulation of *HMG1* and *ERG9* by *HAP1*. As one main target of the project is the high-level production of a certain sterol pathway intermediate it was important to avoid all yield-limiting influences.

The easiest way to find out whether the wild-type strains we wanted to use harbour the respective *Ty1* insertion or not was to amplify the *HAP1* locus. The expected fragment size was about 4500 base pairs without *Ty1* insertion, which was demonstrated for CEN.PK2 and SC0458. These strains clearly differed from BY4741, which is known to have the transposon insertion.

The first experiments were done according to colony PCR protocols but they did not yield a reliable picture of the amplified DNA fragments, which was probably due to the large size of the expected fragments of more than 10.000 bp. The more efficient method was to isolate genomic, which was then used as a template for the subsequent PCR.

The result of this investigation was that the wild-type strain CEN.PK2 does not have a *Ty1* insertion in the *HAP1* gene and, as Tamura et al. (2004) reported, this should be a qualification for proper expression of ergosterol-related genes, which was required for our work.

There is not much literature about the influences of *HAP1* mutations on other genes apart from the ergosterol pathway even though Brem et al. (2002) postulated that about 28 genes would be functionally linked to the *HAP1* gene.

During my work with the CEN.PK2 wild-type strain it showed some behaviour that was not known from other commonly used strain backgrounds, such as BY strains. Most strikingly,

CEN.PK2 strains grow hardly on SD medium as compared to other wild-type strains. This deficiency was compensated by a 5-fold increased supplementation of tryptophan in the medium. This probably indicates a close relationship between of the *HAP1* locus status and plasma membrane physiology in yeast.

Another phenomenon was revealed under the microscope. Cells of commonly used wild-types grown to the stationary phase normally show some clear lipid particles that can be seen as small black dots within the cell in phase contrast images. Much fewer lipid particles were observed in CEN.PK2 strains. To underscore the observation with more reliable fluorescence microscopy data a nile red staining may be performed.

On the whole, the influence of *HAP1* is probably just one example highlighting that it would definitely be an interesting research topic to find out more about the influence of different strain backgrounds on cell physiology.

5.2 Strain construction

The main part of this master thesis was the strain construction of the two double knockout strains *erg5erg6* and *are1are2*. The amplification of the disruption cassettes was done according to methods described by Lorenz, 1995; Longtine, 1998, and Güldener, 1996. After purification on agarose gels and elution of the disruption cassette fragments, several different transformation methods were tried for these strain constructions. Transformation of yeast was verified by growing the transformants on selective plates, subjecting them to colony PCR, and analysing their sterols and steryl esters by GC/MS and TLC

5.2.1 *erg5erg6* strain construction and characterization

The inactivation of the two genes, *ERG5* and *ERG6,* was the precondition to accumulate cholesta-5,7,24-trienol in yeast cells, which is not a naturally occurring intermediate of the ergosterol biosynthesis pathway in wild-type cells. For simplicity reasons *ERG5* and *ERG6* were deleted completely

The first gene deletion of *ERG5* could be done more or less without any problems following the scheme described in section3.1.1, yielding positive transformants right after the first transformation event and after incubation for four days at 30°C.

Disruption of ERG5 was verified by colony PCR (Figure 23) and by a sterol pattern corresponding to an *erg5* knockout strain. The most remarkable feature thereof is an

excessive accumulation of ergosta-5,7-dienol. Ergosta-5,7-dienol is a natural substrate of Erg5p and therefore accumulates in an *erg5* knockout strain. Erg5p converts ergosta-5,7-dienol into ergosterol. In a wild-type strain the pathway ends up with ergosterol, which is obviously the main peak in Figure 24, which shows the sterol pattern of the wild-type strain CEN.PK2.

The disruption of *ERG6* with the selective marker tryptophan turned out to be tricky. The first transformations did not yield any transformants at all, no matter which transformation method was applied, even electroporation was not successful. After reamplification of the disruption cassette the transformations were repeated. The elongation of the incubation time with carrier DNA turned out to be a good way to increase the transformation efficiency. The following transformation experiments yielded many false positives which all grew an SD-trp plates and even showed some distinct bands when checked by colony PCR. But only by GC/MS analysis it was realized that an already assumed *erg5erg6* double knockout was in fact just an *erg5* knockout strain with an unspecifically integrated disruption cassette conferring Trp heterotrophy. Figure 28 shows the chromatogram revealing the same sterol pattern as the *erg5* knockout strain. Hence, the transformation had to be repeated with a longer incubation time with carrier DNA and a higher concentration of the disruption cassette. Of each transformation plate, about eight transformants which grew more slowly than the transformants isolated during the first round were streaked onto new selective plates. This was done reasoning that the faster growing colonies might again be transformants with a functional *ERG6* gene, whereas colonies growing more slowly might be positive transformants.

Reliability of verifying transformants by Colony PCR was improved by using not only one primer combination, but by applying three different primer combinations that should trace out not only the integrated gene but also the gene which was meant to be deleted as well as the corresponding upstream and downstream regions.

In this case, we used a forward primer that annealed in the upstream region of *ERG6* and three different reverse primers, the first annealing inside the integrated *TRP1* gene, the second primer having sequence complementarity to the *ERG6* gene and the third binding to downstream regions of *ERG6*. These three combinations yielded an unambiguous signal to test transformants (Figure 29). The final proof for the successful deletion of *ERG6* came from

GC/MS analysis, which now gave a totally different picture compared to the spectra of the *erg5* strain and the wild-type strain (Figure 30).

In a wild-type strain, zymosterol acts as substrate for Erg6p. The most likely biosynthetic route would be that Erg6p converts zymosterol into fecosterol, which is isomerized by Erg2p, yielding episterol which is converted by Erg3p to ergosta-5,7,24(28)-trienol. In the case of strains lacking functional Erg6p, zymosterol is the substrate for Erg2p, and the resulting cholesta-7,24-dienol is further transformed into cholesta-5,7,24-trienol by Erg3p. This is the end product of the pathway when *ERG5* is deleted as well. These events are exactly represented in Figure 30, which shows the spectrum of the *erg5erg6* double knockout strain with cholesta-5,7,24-trienol as main peak, followed by zymosterol and cholesta-7,24-dienol.

To be sure that the haploid *erg5erg6* strain was produced with the original mating type of the wild-type in which the transformations have been made, mating type determination was done according to the method described in the section “materials and methods”. This test showed that the verified *erg5erg6* double knockout strain was haploid with mating type α.

The ion analysis of the *erg5erg6* strain as well as the growth test on nystatin plates were done in the course of a pre-screening of about forty strains which were all devoid of single genes supposedly involved in the regulation of sterol homeostasis. The data of this pre-screening, involving GC/MS analysis, lipid extraction, and analysis of the extracts by TLC as well as the already mentioned ion analysis and several phenotypic plate tests are not shown as part of this master thesis, but are available as raw data on the attached DVD. The only data of those tests that are interpreted in this present master thesis are the ones that concern the strains *erg5erg6* and the corresponding wild-type CEN.PK2.

The first striking result of the analysis of the ion contents of Cu, Mn, Zn, Mg and Fe of whole cell lysates showed that there are clear differences in the composition between cells cultivated in YPD and in SD medium, respectively. This could have been foreseen because of the totally different composition of the media.

Nevertheless, the most surprising result was that YPD and SD measurements show different effects of nearly all ions tested. For example, the *erg5erg6* strain seemed to have much more magnesium in SD medium but less in YPD medium, compared to the wild-type. These measurements can’t give a real connection to the ergosterol pathway regulation but they clearly show that the deletion of two genes of this important pathway changes much more

than just the sterol pattern and that different membrane compositions obviously have a tremendous impact on the ion accumulation and depletion capacity.

The growth test on nystatin plates was just one of many phenotypic tests that were done with different supplements to YPD plates. *erg5erg6* is resistant to nystatin. Because of the specificity of nystatin for the ergosterol structure and its related sterols this is a verification of the successful deletion of *ERG6* and is therefore an important and relevant result for this thesis. The *erg5* strain is sensitive to nystatin because their main sterols still have an ergosta-based structure. Upon inactivation of *ERG6* cholesta-structures arise, and therefore such strains are no targets for the inhibition by nystatin.

5.2.2 *are1are2* strain construction

The deletion of the two genes coding for the acyltransferases Are1p and Are2p was a very complex and time consuming work.

The *ARE2* gene was deleted with a *loxP-kanMX-loxP* disruption cassette, to maintain the last selective marker of the wild-type strain CEN.PK2, *ura3*. The amplification of the disruption cassette was successful from the beginning, although the amplified DNA fragments showed slightly different sizes, which made a very careful calculation and size estimation necessary to be sure to extract disruption cassettes of correct size.

The transformation efficiency of the *ARE2* disruption cassette into CEN.PK2-IC was extremely low. Eight rounds of transformations were made before a positive transformant was discovered. All transformations showed very small colonies after three days which did not continue to grow, neither did they grow upon re-streaking. Even the adjustment of the genetic in concentration did not improve transformation success. Only a single transformant grew to a big and smeary dot. It was re-streaked onto a new YPD+ G418 plate for further investigations.

This transformant grew very well on G418 plates and the verification by Colony PCR revealed that this transformant was a positive *are2* knockout strain with a functional kanamycin resistance gene. The analysis of lipid extracts by GC/MS also showed that the amount of steryl esters was remarkably decreased which was taken as further proof for the inactivation of Are2p.

The deletion of the *ARE1* gene was characterized by many wrong integration events, and simple repetitions of the transformation events were not successful. According to Daniel (2005), that might have happened because of internal gene conversion of the *his3Δ1* allele of the recipient strain with the *HIS3* marker gene that was introduced. The likelihood for this internal gene conversion was much higher than for the disruption of the *ARE1* gene. The best strategy to avoid this problem, while still using the *HIS3* marker, seemed to create a disruption cassette with much longer homologous fragments that are corresponding to the flanking regions of the *ARE1* coding sequence.

The elongation of the disruption cassette was done by amplifying additional upstream and downstream regions in separate PCR reactions and pouring those to the standard disruption cassettes by overlap-extension PCR.

The next round of transformations yielded three transformants that were tested by Colony PCR. One transformant turned out to be a genuine *are1are2* double mutant and was further investigated by the analysis of Folch lipid extracts on TLC. As expected this strain did not harbour any steryl esters (Figure 43 and Figure 44). Surprisingly, there were also hardly any triglycerides that could be detected, which raises the question how the two enzymes Are1p and Are2p might be involved in the formation of triglycerides.

MATα erg5erg6 and *MATa are1are2* were mated to obtain a heterozygous diploid *erg5erg6are1are2* on SD-his-trp plates. The diploid strain was treated for sporulation.

While waiting for detectable tetrads and writing to write this master thesis, the results took a turn by the incidental observation that the *are1are2* double knockout strain was able to grow on all selective plates tested (Figure 46- Figure 50), which cannot be explained. It seems as if the whole strain background changed just while transforming the *are1* disruption cassette into *are2*.

The present result of the *are1are2* strain construction can be summed up as successful and verified construction of the *are1are2* strain. However, it cannot be used for future work as it does not have the appropriate markers to transform *URA3* based cassettes. There are two strategies to obtain the desired strains.

- Mating of *erg5erg6* with *are2* before transforming the *are1* disruption cassette.

This would have the advantage that the mating and subsequent transformation should be more straight forward than generating a new *are1are2* double knockout and crossing it with

the *erg5erg6* double mutant. The tetrads of the diploid *erg5erg6are1are2* strain will then be dissected and the haploid strain will be found by testing several tetrads on appropriate selective plates.

Another possibility, however much more time consuming would be would be:

- Back-crossing of the *are1are2* mutant with a wild-type strain to yield an are1are2 strain with appropriate markers.

Finally, the *erg5erg6* strain would be mated with the adjusted *are1are2* strain.

5.3 Site specific mutagenesis: *ERG6* mutants

The Erg6 variants were created reasoning that inactivation instead of deleting *ERG6* might change the ratio of zymosterol to cholesta-5,7,24-trienol in favour of the latter, the desired product.

For this purpose, nine different Erg6 variants were generated, seven single point mutations in the area of *ERG6* coding for SAM binding domains (S-adenosylmethionine, Figure 52) and two further alterations at the amino acid position 152. Both areas were regarded as important for the functionality of Erg6p.

Nearly all variants were expressed in an *erg5erg6* double mutant. Some variants did not show any Erg6p activity, others were interpreted as partly inactivated. The overall goal, however, to reduce the amount of zymosterol in favour of cholesta-5,7,24-trienol, could not be reached.

The most interesting variants were D2 and D152A which showed a sterol pattern that was partly typical of an *erg5* knockout strain but did also show accumulation of cholesta-5,7,24-trienol, which normally does not occur in an *erg5* strain. Considering that zymosterol can be detected in an erg5 strain as well as in an *erg5erg6* strain, these variants might be interesting regarding the cholesta-5,7,24-trienol to zymosterol ratio if Erg6p, D2 or D152A could be further inactivated.

A promising approach could be the combination of mutations of D152A, D2 and also G3 variants.

5.4 Prospect

This master thesis laid the foundation for future work to reach the final project target of creating a yeast strain that produces mainly cholesta-5,7,24-trienol and hardly any by-products, such as zymosterol.

Future work in the project will aim creating a haploid *erg5erg6are1are2* quadruple mutant that does not show any strain background nebulosities as explained on previous pages. Therefore, additional mating, sporulation and dissection of ascospores as well as new transformation experiments will be necessary.

Once this improved strain is verified by TLC analysis of lipid extracts and proper growth on selective plates, the next stage will be to introduce a plasmid carrying the truncated version of HMG-CoA reductase to increase the total sterol content.

Another main part of the project will be to express sterol acyltransferases of other eukaryotes and variants thereof in *are1are2* strains to see if an acyltransferase with selectivity for cholesta-5,7,24-trienol over zymosterol can be found or developed. Therefore, a screening system for sterol selectivities of sterol acyltransferases will be developed.

As far as the strategy to inactivate Erg6p will be pursued, it might be a good idea to create variants with combinations of alterations within the SAM binding region and the amino acid position 152.

6 SUMMARY

The content of my master thesis can be divided into four main topics. The analysis of the *HAP1* locus of the CEN.PK2 strain background, the construction of the *erg5erg6* double knockout strain as well as the construction of the *are1are2* double knockout strain, and the creation of nine different Erg6 variants with the aim to inactivate Erg6p, but concomitantly boost cholesta-5,7,24-trienol formation.

My work showed that the CEN.PK2 strain does not have an insertional mutation caused by the *Ty1* transposon as many other commonly used laboratory strains. Therefore this strain provides an ideal background for efficiently producing ergosterol-related compounds.

The PCR mediated deletion of the two genes *ERG5* and *ERG6* was done to create a strain that produces very high amounts of cholesta-5,7,24-trienol, an industrial precursor of vitamin D3. Another, undesired, sterol accumulating with this genetic setup is the precursor zymosterol. The conversion of accumulating zymosterol to the desired product cholesta-5,7,24-trienol is the subject of the project this master thesis is part of.

The construction of the *are1are2* double knockout strain was a necessary to test different acyltransferases for sterol substrate specificity. This strain did not produce any steryl esters, which can be seen as proof of successful strain construction. Unfortunately, the constructed strain seems to lack *ura3* and *trp1* markers which cannot be explained at the moment. Thus, the double mutant will have to be reconstructed.

The inactivation instead of the deletion of *ERG6* might be one possibility to change the ratio between zymosterol and cholesta-5,7,24-trienol in favour of the latter. The inactivation was successfully done by amino acid changes within the SAM binding region of Erg6p at amino acid position 152. The aim to specifically change the sterol pattern was reached with the mutants created, but these may be the knowledge basis to generate more promising variants.

7 INDICES

7.1 References

References that are not quoted in the present master thesis should be seen as further reading.

Adams, A., Gottschling, D. E., Kaiser, C., Stearns, T.: Methods in Yeast Genetics. *Cold Spring Harbor Laboratory Press***(1997)**

Athenstaedt, K., Zweytick, D., Jandrositz, A., Kohlwein, S.D., and Daum, G.: Identification and Characterization of Major Lipid Particle Proteins of the Yeast Saccharomyces cerevisiae. *Journal of Bacteriology* 181 (20), 6441-6448 **(1999)**

Bailey, R.B., and Parks, L.W.: Yeast sterol esters and their relationship to growth. *Journal of Bacteriology* 124, 606-612 **(1975)**

Bard, M., Downing, J.F.: Genetic and biochemical aspects of yeast sterol regulation involving 3-hydroxy-3-methylglutaryl coenzyme A reductase. *Journal of general microbiology* 125 (2), 415-20 **(1981)**

Brem, R.B., Yvert, G., Clinton, R., and Kruglyak, L.: Genetic dissection of transcriptional regulation in buddying yeast. *Science* 296, 752-755 **(2002)**

Chang, T.-Y., Chang, C.C.Y., Ohgami, N., Yamauchi, Y.: Cholesterol sensing, trafficking, and esterification. *Annual Review of Cell and Developmental Biology* 22, 129-157 **(2006)**

Connerth, M., Czabany, T., Wagner, A., Zellnig, G., Leitner, E., Steyrer, E. and Daum, G. : Oleate Inhibits Steryl Ester Synthesis and Causes Liposensitivity in theYeast. *JBC Papers***?? (2010)**

Czabany, T., Wagner, A., Zweytick, D., Lohner, K., Leitner, E., Ingolic, E., and Daum, G.: Structural and Biochemical Properties of Lipid Particles from the Yeast Saccharomyces cerevisiae. *The Journal of Biological Chemistry* 283(25), 17065-17074 **(2008)**

Daniel, J.A., Yoo, Jiyoun, Bettinger, B.T., Amberg, D.C. and Burke, D.J.: Eliminating Gene Conversion Improves High- Throughput Genetics in Saccharomyces cerevisiae. *Genetics* 172: 709-711 **(2006)**

Daum, G., Lees, N. D., Bard, M., Dickson, R.: Biochemistry, Cell Biology and Molecular Biology of Lipids of Saccharomyces cerevisae. *Yeast* 14, 1471-1510 **(1998)**

Elble, R.: A Simple and Efficient Procedure for Transformation of Yeasts. *BioTechniques* 13 (1), 18-20 **(1992)**

Folch J., Lees M., Stanley G.H.S.: A simple method for the isolation and purification of total lipids from animal tissues. *Journal of Biological Chemistry*, 226, 497- 506 **(1957)**

Güldener, U., Heck, S., Fiedler, T., Beinhauer, J. and Hegemann, J. H.: A new efficient gene disruption cassette for repeated use in budding yeast. *Nucleic Acid Research* 24(13), 2519-2524 **(1996)**

Guo, Z., Cromey, D., Billheimer, J. T., Sturley, S. L.: Identification of potential substrate-binding sites in yeast and human acyl- CoA sterol acyltransferases by mutagenesis of conserved sequences. *Journal of Lipid Research* 42, 1282-1291 **(2001)**

Heese- Peck, A., Pichler, H., Zanolar, B., Watanabe, R., Daum, G., and Riezman, H.: Multiple Functions of Sterols in Yeast Endocytosis. *Molecular Biology of the Cell* 13, 2664-2680 **(2002)**

Harju, S., Fedosyuk, H.and Peterson, K.R.: Rapid isolation of yeast genomic DNA: Bust n'Grab. *BMC Biotechnology* 4, 8 **(2004)**

Launhardt, H., Hinnen, A. and Munder, T.: Drug- induced Phenotypes Provide a Tool for the Funcional Analysis of Yeast Genes. *Yeast* 14, 935-942 **(1998)**

Leber, R., Landl, K., Zinser, E., Ahorn, H., Spök, A., Kohlwein, S., Turnowsky, F. and Daum, G.: Dual Localization of Squalene Epoxidase, Erg1p, in Yeast Reflects a Relationship between the Endoplasmic Reticulum and Lipid Particles. *Molecular Biology of the Cell* 9, 375-386 **(1998)**

Leber, R., Zinser, E., Hrastnik, C., Paltauf, F., Daum, G.: Export of steryl esters from lipid particles and release of free sterols in the yeast Saccharomyces cerevisiae. *Biochimica et Biophysica Acta* 1234, 119-126 **(1994)**

Leber, R., Zinser, E., Zellnig, G., Paltauf, F. and Daum, G.: Characterization of Lipid Particles of the Yeast Saccharomyces cerevisiae. *Yeast*10, 1421-1428 **(1994)**

Lewis, T. A., Rodriguez, R. J. and Parks, L. W.: Relationship between intracellular sterol content and sterol esterification and hydrolysis in Saccharomyces cerevisiae. *Biochimica et Biophysica Acta* 921, 205-212 **(1987)**

Longtine, M. S., McKenzie, A., Demarini, D. J., Shah, N. G., Wach, A., Brachat, A., Philippsen, P. and Pringle, J. R.: Additional Modules for Versatile and Economical PCR- based Gene Deletion and Modification in Saccharomyces cerevisiae. *Yeast* 14, 953-961 **(1998)**

Maczek, J.: Metabolic Modelling: Vergleichende Regulationsanalyse der Sterolbiosynthese. Dissertation. Technische Universität Berlin. **(2009)**

Mo, C. and Bard, M.: Erg28p is a key protein in the yeast sterol biosynthetic enzyme complex. *Journal of Lipid Research* 46, 1991-1998 **(2005)**

Mo, C., Valachovic, M., Bard, M.: The ERG 28- encoded protein, Erg28p, interacts with both the sterol C-4 demethylation enzyme complex as well as the late biosynthetic protein, the C-24 sterol methyltransferase (Erg6p). *Biochimica et Biophysica Acta* 1686, 30-36 **(2004)**

Müllner, H. and Daum, G.: Dynamics of neutral lipid storage in yeast. *Acta Biochimica Polonica* 51 (2), 323-347 **(2004)**

Müllner, H., Deutsch, G., Leitner, E., Ingolic, E. and Daum, G.: YEH2/YLR020c Encodes a Novel Steryl Ester Hydrolase of the Yeast Saccharomyces cerevisiae. *The Journal of Biological Chemistry* 280 (14), 13321-13328 **(2005)**

Müllner, H., Zweytick, D., Leber, R., Turnowsky, F. and Daum, G.: Targeting of proteins involved in sterol biosynthesis to lipid particles of the yeast Saccharomyces cerevisiae. *Biochimica et Biophysica Acta* 1663, 9-13 **(2004)**

Ott, R. G., Athenstaedt, K., Hrastnik, C., Leitner, E., Bergler, H., Daum, G.: Flux of sterol intermediates in a yeast strain deleted of the lanosterol C-14-demethylase Erg11p. *Biocimica et Biophysica Acta* 1735(2), 111-118 **(2005)**

Pagani, M.A., Casamayor, R.S., Atrian, S. and Ariño J.: Disruption of iron homeostasis in Saccharomyces cereivisiae by high zinc levels: a genome-wide study. *Molecular Microbiology* 65(2), 521-537 **(2007)**

Pichler, H.: Modulating membrane properties-sterol cell biology in yeast. *Cell Biology and Dynamics of Yeast Lipids,* 179-199 **(2005)**

Polakowski, T., Bastl, R., Stahl, U., Lang, C.: Enhanced sterol-acyl transferase activity promotes sterol accumulation in Saccharomyces cerevisiae. *Appl Microbiol Biotechnol* 53, 30-35 **(1999)**

Rieger, K.-J., Kaniak, A., Coppée, J.-Y., Aljinovic, G., Baudin- Baillieu, A., Orlowska, G., Gromadka, R., Groudinsky, O., Di Rago, J.-P., and Slonimski, P. P.: Large- Scale Phenotypic Analysis- the Pilot Project on Yeast Chromosome III. *Yeast* 13, 1547-1562 **(1997)**

Rosenfeld, L., Reddi, A.R., Leung, E., Aranda, K., Jensen, L.T., Culotta, V.C.: The effect of phosphate accumulation on metal ion homeostasis in Saccharomyces cerevisiae. *J Biol Inorg Chem* 15(7), 1051-1062 **(2010)**

Schimmoeller, F., Singer- Krueger, B., Schroeder, S., Krueger, U., Barlowa, C. and Riezman, H.: The absence of Emp24p, a component of ER- derived COPII-coated vesicles, caused a defect in transport of selected proteins to the golgi. *EMBO journal*, 14 (7), 1329-1339, **(1995)**

Sorger, D., Athenstaedt, K., Hrastnik, C., and Daum, G.: A Yeast Strain Lacking Lipid Particles Bears a Defect in Ergosterol Formation. *The Journal of Biological Chemistry*279(30), 31190-31196 **(2004)**

Tamura, K., Gu, Y., Wang, Q., Yamada, T., Ito, K. and Shimoi, H.: A *hap1* Mutation in a Laboratory Strain of Saccharomyces cerevisiae Results in Decreased Expression of Ergosterol- Related Genes and Cellular Ergosterol Content Compared to Sake Yeast. *Journal of Bioscience and Bioengineering* 98(3), 159-166 **(2004)**

Taramino, S., Valachovic, M., Oliaro- Bosso, S., Viola, F., Teske, B., Bard, M., Balliano, G.: Interactions of oxidosqualene cyclase (Erg7p) with 3-keto reductase (Erg27p) and other enzymes of sterol biosynthesis in yeast. *Biochimica et Biophysica Acta*1801,156-162 **(2010)**

Tiwari, R., Köffel, R. and Schneiter, R.: An acetylation/ deacetylation cycle controls the export of sterols and steroids from S. cerevisiae. *The EMBO Journal*26, 5109-5119 **(2007)**

Veen, M., Lang, C.: Interaction of the ergosterol biosynthetic pathway with other lipid pathways. *Biochemical Society Transactions* 33, 1178-1181 **(2005)**

Volland, C., Urban- Grimal, D., Geraud, G., Haguenauer- Tsapis, R.: Endocytosis and degradation of the yeast uracil permease under adverse conditions. *Journal of Biological Chemsitry*, 269 (13), 9833-9841 **(1994)**

Wagner, A. and Daum, G.: Formation and mobilization of neutral lipids in the yeast Saccharomyces cerevisiae. *Biochemical Society Transactions* 33, 1174-1177 **(2005)**

Wagner, A., Grillitsch, K., Leitner, E., Daum, G.: Mobilization of steryl esters from lipid particles of the yeast Saccharomyces cerevisae. *Biochimica et Biophysica Acta*1791, 118-124 **(2009)**

Webster, T. D., Dickson, R. C.: Direct selection of Saccharomyces cerevisiae resistant to the antibiotic G418 following transformation with a DNA vector carrying the kanamycin-resistance gene of Tn903. *Gene* 26 (2-3), 243-52 **(1983)**

Yang, H., Bard, M., Bruner, D. A., Gleeson, A., Deckelbaum, R. J., Aljinovic, G., Pohl, T. M., Rothstein, R., Sturley, S.L.: Sterol Esterification in Yeast: A two-gene process. *Science* 272, 1353-1356 **(1996)**

Yu, C., Kennedy, N. J., Chang, C. C. Y. and Rothblatt, J. A.: Molecular Cloning and Characterization of Two Isoforms of Saccharomyces cerevisiae Acyl- CoA:Sterol Acyltransferase. *The Journal of Biological Chemistry* 271 (39), 24157-24163 **(1996)**

Zinser, E., Paltauf, F., and Daum, G.: Sterol Composition of Yeast Organelle Membranes and Subcellular Distribution of Enzymes Involved in Sterol Metabolism. *Journal of Bacteriology* 175(10): 2853-2858 **(1993)**

Zweytick, D., Hrastnik, C., Kohlwein, S. D., Daum, G.: Biochemical characterization and subcellular localization of the sterol C-24(28) reductase, Erg4p, from the yeast Saccharomyces cerevisiae. *FEBS Letters* 470, 83-87 **(2000)**

Zweytick, D., Leitner, E., Kohlwein, S.D., Yu, Chunjiang, Rothblatt, J., Daum, G.:Contribution of Are1p and Are2p to steryl ester synthesis in the yeast Saccharomyces cerevisiae. *Eur. J. Biochem.*267, 1075-1082 **(2000)**

7.2 List of figures

7.3 List of tables

Synopsis – Zusammenfassung in deutscher Sprache

Die Biosynthese von Ergosterol in Hefe ist ein komplexer biochemischer Mechanismus mit beinahe dreißig Reaktionen. Durch Deletion der daran beteiligten Gene *ERG5* und *ERG6*reichern sich die Zwischenstufen Cholesta-5,7,24-trienol und dessen Vorstufe Zymosterol vermehrt an. Diese werden anschließend durch die beiden Acyltransferasen Are1p und Are2p verestert und in Lipidpartikel gespeichert, wo sie für weitere Umwandlungen nicht direkt verfügbar sind. Cholesta-5,7,24-trienol ist eine Vorstufe von Vitamin D3 und daher von industrieller Bedeutung. Um es in großen Mengen gewinnen zu können, muss jedoch die Umwandlung von Zymosterol zu Cholesta-5,7,24-trienol durch Erg2p und Erg3p effizienter erfolgen, bevor dieses verestert wird. Dies könnte einerseits mit modifizierten Acyltransferasen erreicht werden, die selektiv nur Zymosterol verestern, oder indem ein in der Literatur beschriebener Komplex mehrerer Erg-Proteine, in den auch Erg2p und Erg3p involviert sind, erhalten wird, indem *ERG6* nur inaktiviert statt deletiert wird. Ein Ziel dieser Arbeit war es, die beiden doppel-knockout Stämme *erg5erg6* und *are1are2*, sowie in weiterer Folge die quadruple Mutante *erg5erg6are1are2* herzustellen, um in Zukunft Acyltransferasen aus verschiedenen Organsismen testen zu können. Ein weiteres Ziel war es, mehrere *ERG6*-Mutanten zu erstellen und diese bezüglich einesveränderten Cholesta-5,7,24-trienol-Anteils zu charakterisieren.

Synopsis

The ergosterol biosynthesis pathway in yeast is a very complex mechanism with nearly thirty reactions. Upon deletion of the two involved genes *ERG5* and *ERG6*, yeast cell acquire the capacity of producing high amounts of cholesta-5,7,24-trienol and its precursor zymosterol, which are esterified by the two acyltransferases Are1p and Are2p and stored in lipid droplets where they are not directly available for further conversions anymore. Cholesta-5,7,24-trienol is a precursor of vitamin D3 and therefore of industrial interest. To increase yield, it is necessary that zymosterol is converted efficiently by Erg2p and Erg3p. One way would be to engineer acyltransferases towards selective recognition of cholesta-5,7,24-trienol. Another way would be to maintain an Erg-complex, in which also Erg2p and Erg3p are involved, by inactivating rather than deleting *ERG6*.One aim of this work was to construct two double knockout strains: *erg5erg6* and *are1are2* and the quadruple mutant*erg5erg6are1are2* to test acyltransferases of other organisms. Another aim was to create several *ERG6* mutants and to characterize them with respect to their cholesta-5-7-24-trienol to zymosterol ratio.

8 APPENDIX

8.1 The standard genetic code

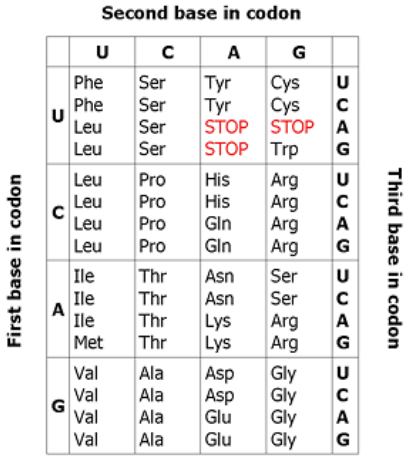

First base in codon	Second base in codon: U	C	A	G	Third base in codon
U	Phe	Ser	Tyr	Cys	U
	Phe	Ser	Tyr	Cys	C
	Leu	Ser	STOP	STOP	A
	Leu	Ser	STOP	Trp	G
C	Leu	Pro	His	Arg	U
	Leu	Pro	His	Arg	C
	Leu	Pro	Gln	Arg	A
	Leu	Pro	Gln	Arg	G
A	Ile	Thr	Asn	Ser	U
	Ile	Thr	Asn	Ser	C
	Ile	Thr	Lys	Arg	A
	Met	Thr	Lys	Arg	G
G	Val	Ala	Asp	Gly	U
	Val	Ala	Asp	Gly	C
	Val	Ala	Glu	Gly	A
	Val	Ala	Glu	Gly	G

8.2 Single-letter and three-letter amino acid codes

Amino acid	Three letter code	One letter code
Alanine	ala	A
Arginine	arg	R
Asparagine	asn	N
Aspartic acid	asp	D
Cysteine	cys	C
Glutamic acid	glu	E
Glutamine	gln	Q
Glycine	gly	G
Histidine	his	H
Isoleucine	ile	I
Leucine	leu	L
Lysine	lys	K
Methionine	met	M
Phenylalanine	phe	F
Proline	pro	P
Serine	ser	S
Threonine	thr	T
Tryptophan	try	W
Tyrosine	tyr	Y
Valine	val	V